

Spring 2015

Investigation of Pulse Detonation Engines: the Effect of Variable Blockage Ratio on the Deflagration to Detonation Transition

Christopher Tate
Embry-Riddle Aeronautical University

Follow this and additional works at: <https://commons.erau.edu/edt>



Part of the [Aerospace Engineering Commons](#)

Scholarly Commons Citation

Tate, Christopher, "Investigation of Pulse Detonation Engines: the Effect of Variable Blockage Ratio on the Deflagration to Detonation Transition" (2015). *Doctoral Dissertations and Master's Theses*. 252.
<https://commons.erau.edu/edt/252>

This Thesis - Open Access is brought to you for free and open access by Scholarly Commons. It has been accepted for inclusion in Doctoral Dissertations and Master's Theses by an authorized administrator of Scholarly Commons. For more information, please contact commons@erau.edu.

**INVESTIGATION OF PULSE DETONATION ENGINES; THE EFFECT OF
VARIABLE BLOCKAGE RATIO ON THE DEFLAGRATION TO
DETONATION TRANSITION.**

By

Christopher Tate

A Thesis Submitted to the Graduate Studies Office in Partial Fulfillment of the Requirements for
the Degree of Master of Science in Aerospace Engineering

Embry-Riddle Aeronautical University

Daytona Beach, FL

Spring, 2015

Investigation of Pulse Detonation Engines; the Effect of Variable Blockage Ratio on the Deflagration to Detonation Transition.

By Christopher

This thesis was prepared under the direction of the candidate's thesis committee chair, Dr. Magdy S Attia, Department of Aerospace Engineering, and has been approved by the members of his thesis committee. It was submitted to the Aerospace Engineering Department and was accepted in partial fulfillment of the requirements for the degree of Master of Science in Aerospace Engineering.

THESIS COMMITTEE



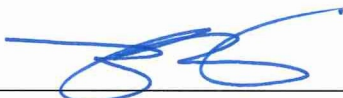
Dr. Magdy Attia
Chairman



Dr. Eric Perrell
Member



Dr. Mark Ricklick
Member



Department Chair, Dr. Anastasios Lyrintzis
or Graduate Program Coordinator, Dr. Yi Zhao

4/14/2015

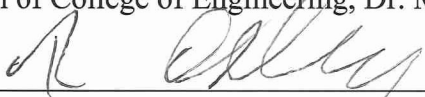
Date



Dean of College of Engineering, Dr. Maj Mirmirani

4/20/15

Date



Associate VP for Academics, Dr. Robert Oxley

4-20-2015

Date

ACKNOWLEDGEMENTS

I would like to thank Dr. Magdy Attia for all the support, guidance, and education provided through our interactions. Additionally I would like to extend my gratitude to Jeff Vizcaino, Darrell Stevens, and Bill Russo for their assistance and all my coworkers in the Embry-Riddle Gas Turbine Lab.

ABSTRACT

Author: Christopher Tate

Title: Investigation of Pulse Detonation Engines; the Effect of Variable Blockage Ratio on the Deflagration to Detonation Transition.

Institution: Embry-Riddle Aeronautical University

Degree: Master of Science in Aerospace Engineering

Year: 2015

Detonation and constant volume combustion is well known to be thermodynamically more efficient than the typically utilized constant pressure. There have been numerous approaches of achieving detonation through deflagration-to-detonation transition most of which use evenly spaced obstacles with a specified constant blockage ratio to generate turbulence and pressure fluctuations. There have been few efforts to study effects of varying blockage ratio as a function of axial distance. This research analyzes the effect of variable blockage ratio on deflagration-to-detonation transition in ethylene-air mixtures. The experiments show that with certain blockage ratio functions detonation is more repeatable and produces a smaller variation in both peak pressure and wave velocity representative of consistently stable detonations.

TABLE OF CONTENTS

TITLE	1
ACKNOWLEDGEMENTS.....	3
ABSTRACT	4
TABLE OF CONTENTS	5
LIST OF FIGURES	8
LIST OF TABLES.....	12
NOMENCLATURE	13
1. PROBLEM STATEMENT	14
2. DETONATION THEORY.....	15
2.1. Deflagration	15
2.2. Detonation.....	16
Chapman-Jouguet Condition.....	17
ZND Model	20
2.3. Thermodynamic Cycles	21
Humphrey Cycle.....	21
Fickett-Jacobs Cycle.....	23
2.4. Detonation Waves	25
2.5. Detonation Wave Formation	26
2.6. Detonation Transition	27
2.7. Methods of Flame Acceleration	28
2.8. Performance Impact of DDT Enhancing Obstacles	29
3. TEST EQUIPMENT AND METHODOLOGY.....	31
3.1. Experimental Hardware	31
Detonation Tube	35
Obstacles	36
Flanges.....	36

Flange gaskets	36
Bolts and Nuts	36
Check valves.....	36
Injection block and Fuel Manifold	36
3.2. Sensors and Instrumentation	37
Pressure Transducers:.....	37
Combustion (Ion) Sensors	37
Signal Conditioner:.....	37
Data Acquisition Board	37
Power Supply.....	37
Injector Solenoids.....	38
Injector Driver	38
Ignition coil and Igniter	38
3.3. Control System and Data Acquisition	38
LabView Control Panel	38
LabView Injector and Spark Control	42
3.4. Experimental Method.....	47
Firing Cycle 1	47
Firing Cycle 2	48
Blockage Ratio Configurations	49
4. EXPERIMENTAL RESULTS	52
4.1. Theoretical Results.....	52
4.2. Results.....	53
4.3. Firing Cycle 1.....	55
4.4. Firing Cycle 2.....	58

Pressure Trends	60
Velocity Trends	67
5. CONCLUSIONS.....	74
5.1. Summary	74
5.2. Recommendations	74
Monitoring Onset of Detonation Transition.....	74
Filling	75
Mixing	76
Future Studies	76
REFERENCES	78
APPENDIX A: CALCULATION OF FILLING PARAMETERS	83
APPENDIX B: DRAWINGS AND DIAGRAMS	88
APPENDIX C: RAW DATA & RESULTS	110
Firing Cycle 1 Data	111
Firing Cycle 2 Data	130

LIST OF FIGURES

Figure 2.1 Control volume used in CJ Model	18
Figure 2.2. Huginot Curve	19
Figure 2.3 Variation of physical parameters through a typical detonation wave	21
Figure 2.4 P-v diagrams of Brayton and Humphrey Cycles	22
Figure 2.5 T-s diagrams of Brayton and Humphrey Cycles	22
Figure 2.6 Physical steps that make up the Fickett-Jacobs cycle.	24
Figure 2.7 P-v diagram of Fickett-Jacobs cycle compared with Humphrey and Brayton	25
Figure 2.8 Numerical soot foil pattern for a stable detonation wave	26
Figure 2.9 Experimental soot foil pattern for an unstable detonation wave	26
Figure 2.10 Schematic of detonation tube using Shchelkin spiral.	29
Figure 3.1 Ethylene Cell Size vs. Equivalence Ratio	32
Figure 3.2 Detonation Tube Overview	33
Figure 3.3 Experimental Set-up	33
Figure 3.4 Ignition section of detonation tube	33
Figure 3.5 Measurement section of detonation tube	34
Figure 3.6 Various obstacles and spacer for internal geometry	34
Figure 3.7 Interior obstacle configuration	35
Figure 3.8 Injector plate	35
Figure 3.9 LabView VI	39
Figure 3.10 Input Control for LabView VI	39
Figure 3.11 Data Logging and Timing Panel for LabView VI	41
Figure 3.12 Graph Output Control	41

Figure 3.13 Fuel Control System	44
Figure 3.14: Spark Plug Ignition Control System	44
Figure 3.15 Calculation Node for LabView VI	45
Figure 3.16 Ignition Wiring	46
Figure 3.17 Injector Wiring	46
Figure 3.18 Digital signals for firing cycle 1	48
Figure 3.19 Digital signals for firing cycle 2	48
Figure 3.20 Constant blockage ratios	49
Figure 3.21 Converging blockage ratios	50
Figure 3.22 Diverging blockage ratios	50
Figure 3.23 Converging-diverging blockage ratios	50
Figure 3.24 Alternating blockage ratios at 50% of tube length	51
Figure 3.25 Alternating blockage ratios at 25% of tube length	51
Figure 3.26 Alternating blockage ratios at every obstacle	51
Figure 4.1 Detonation Velocity and Pressure vs. Equivalence Ratio	52
Figure 4.2 Typical deflagration sensor traces	54
Figure 4.3 Typical detonation sensor traces	54
Figure 4.4 Distribution of peak pressures for firing cycle 1	56
Figure 4.5 Distribution of wave velocities for firing cycle 1	57
Figure 4.6 Firing number vs. Velocity	58
Figure 4.7 Average peak pressures for Firing Cycle 2	62
Figure 4.8 Measured peak pressures for each run of Case 1	62
Figure 4.9 Measured peak pressures for each run of Case 2	63

Figure 4.10 Measured peak pressures for each run of Case 3	63
Figure 4.11 Measured peak pressures for each run of Case 4	63
Figure 4.12 Measured peak pressures for each run of Case 5	64
Figure 4.13 Measured peak pressures for each run of Case 6	64
Figure 4.14 Measured peak pressures for each run of Case 7	64
Figure 4.15 Measured peak pressures for each run of Case 8	65
Figure 4.16 Measured peak pressures for each run of Case 9	65
Figure 4.17 Measured peak pressures for each run of Case 10	66
Figure 4.18 Measured peak pressures for each run of Case 11	66
Figure 4.19 Measured peak pressures for each run of Case 12	66
Figure 4.20 Measured peak pressures for each run of Case 13	67
Figure 4.21 Average wave velocities for Firing Cycle 2	69
Figure 4.22 Measured wave velocities for each run of Case 1	69
Figure 4.23 Measured wave velocities for each run of Case 2	70
Figure 4.24 Measured wave velocities for each run of Case 3	70
Figure 4.25 Measured wave velocities for each run of Case 4	70
Figure 4.26 Measured wave velocities for each run of Case 5	71
Figure 4.27 Measured wave velocities for each run of Case 6	71
Figure 4.28 Measured wave velocities for each run of Case 7	71
Figure 4.29 Measured wave velocities for each run of Case 8	72
Figure 4.30 Measured wave velocities for each run of Case 9	72
Figure 4.31 Measured wave velocities for each run of Case 10	72
Figure 4.32 Measured wave velocities for each run of Case 11	73

Figure 4.33 Measured wave velocities for each run of Case 12	73
Figure 4.34 Measured wave velocities for each run of Case 13	73
Figure 7.1: Mass vs. Pulse Width curves for Propane	86
Figure 7.2 Mass vs. Pulse Width curves for Methane	86
Figure 7.3: Mass vs. Pulse Width curves for Air	87

LIST OF TABLES

Table 2.1 Detonation vs. Deflagration properties products/reactants	17
Table 2.2 Sample Hydrocarbon Chapman-Jouguet Parameters (100kPa, 298K)	20
Table 3.1 Detonation Tube Details	36
Table 4.1 Velocity and Peak Pressure Overview for Firing Cycle 1	56
Table 4.2 Detonation Velocity and Peak Pressure overview for Firing Cycle 2	59
Table 4.3 Deflagration Velocity and Peak Pressure overview for Firing Cycle 2	60

NOMENCLATURE

γ	Ratio of specific heats
η_{th}	Thermal efficiency
ρ	Density
P	Pressure
T	Temperature
R	Gas constant
M	Mach number
V	Volume
C_p	Heat capacity at constant pressure
q_c	Specific heat of combustion
u	velocity
BR	Blockage Ratio

Subscripts

CJ	Denotes Chapman-Jouguet conditions
FJ	Denotes Fickett-Jacobs Cycle
0	Denotes stagnation condition
1	State 1, before detonation wave
2	State 2, after detonation wave

1. PROBLEM STATEMENT

Detonation reliability and performance are of interest in modern research of deflagration to detonation transition (DDT) enhancing obstacles. Much of the research has examined internal geometry and many different researchers have found that there are several competing effects of obstacles. This is due to obstacles having different influences on flames and shock waves. Larger obstacles promote the flow and flame acceleration at the price of weakening shocks through diffraction and adding losses in pressure. The observed mechanism of flame acceleration in studies suggests that the run-up time and distance to DDT can be minimized using variable blockage ratio. The intent of this research is to identify a higher performing blockage ratio function and empirical correlations between variable blockage ratio and detonation performance characteristics through testing a variety of configurations.

2. DETONATION THEORY

Combustion is broken down into two types. Deflagration is the most common type and is found daily such as in internal combustion engines. It occurs at subsonic speeds and at constant pressure and releases energy at a relatively low rate. Detonation on the other hand releases a high amount of energy in a short period of time. Detonation is commonly known as knocking in internal combustion engines where it can cause severe damage. It also has a tendency of occurring in pipelines running long distances which can lead to explosions which will shut down productivity. Where in these circumstances detonation is undesirable, there is potential for this explosive energy in aerospace when the rapid energy released can be harnessed for either thrust production or creating shaft power. There are however some design challenges that still have to be overcome such as noise levels and managing the cyclic nature of the methods to produce detonations.

2.1. Deflagration

The subsonic combustion of reactants is referred to as deflagration. In non-enclosed volumes this reaction process usually results in a small pressure drop and a large increase in temperature.

Usually the pressure loss is insignificant and it is useful to model the process as isobaric.

Deflagration is most frequently observed when igniting fuel and oxidizer. It is typical in internal combustion engines representing the Otto and Diesel thermodynamic cycles as well as in turbine engines representing the Brayton cycle. In the case of a tube open at both ends, the combustion wave for most hydrocarbon-air mixtures usually propagates in the range of 0.2-2 m/s (Glassman & Yetter, 2008). In a tube where combustion is initiated at one end that is closed and the tube is sufficiently long enough, the propagating combustion wave will undergo the transition from deflagration to detonation as sometimes seen in pipelines.

2.2. Detonation

Detonation is a shock wave that is sustained by an exothermic reaction in a highly compressed region of fuel and oxidizer mixture existing in the wave. Where deflagrations happen around 1m/s, detonations occur at speeds in the range of 2000 m/s. Unlike in deflagrations, the velocity is not controlled by heat conduction and radical diffusion; rather, the shock wave structure of the supersonic wave raises the temperature and pressure enough to cause explosives reactions and energy release to sustain the wave propagation (Glassman & Yetter, 2008). This formation and propagation of a detonation wave compresses the gas upstream causing the extreme pressure and temperature following combustion when compared to deflagrations. This process is described by the one dimensional Chapman-Jouguet theory and the Zel'dovich-von Neumann-Döring model. Detonations are modeled as a constant volume combustion as in the Humphrey and Fickett-Jacobs thermodynamic cycles. The efficiency in these cycles and method of combustion produces an efficiency of 1.3-1.5 times that of an isobaric combustion cycle at an equivalent pressure ratio. If mechanical efficiencies can be preserved, this could lead to a similar increase in fuel efficiencies (Bussing & Pappas, 1994). Shown in Table 2.1 are the differences between detonations and deflagrations. The subscript “r” designates reactants and “p” designates the reaction products. It is clear that the Mach number of the wave front is much higher for detonations and the same can be said about the pressure, temperature and density ratios.

Table 2.1 Detonation vs. Deflagration properties products/reactants

	Usual magnitude of Ratio	
Ratio	Detonation	Deflagration
U_r/C_r^a	5 to 10	0.0001 to 0.03
U_p/u_r	0.4 to 0.7	4 to 16
P_p/P_r	13 to 55	0.98 to 0.976
T_p/T_r	8 to 21	4 to 16
ρ_p/ρ_r	1.4 to 2.6	0.06 to 0.25
^a C_r is the acoustic velocity in the unburned gasses. U_r/C_r is the Mach number of the wave.		

Chapman-Jouguet Condition

The formulation of the Chapman-Jouguet (CJ) condition is done by assuming that the detonation wave is a steady, planar and one dimensional. It states that the flow behind the detonation wave travels at sonic speed in reference to the combusted products. The four primary assumptions of the CJ condition are as follows (Davis, Craig, & Ramsay, 1965):

- Detonation approaches steady-state
- Flow is laminar and one dimensional
- Detonation products approach state of equilibrium at some distance behind the detonation front.
- Detonation velocity is the minimum permitted by the conservation conditions

These assumptions were required to obtain a detonation velocity using the Hugonot relations. To obtain the velocity, there exist four integrated conservation and state equations and five unknowns (Glassman & Yetter, 2008). This CJ condition requires no knowledge of the structure of the detonation wave and thermodynamic equilibrium calculations but still results in detonation velocities that closely agree with experimental results. This makes the process of finding the CJ detonation velocity relatively simple.

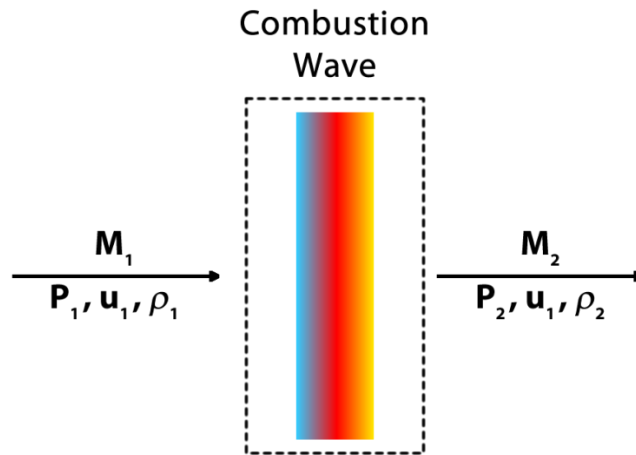


Figure 2.1 Control volume used in CJ Model

The CJ condition model uses a control volume around a planar shock as shown in Figure 2.1. Since this model does not consider the shock structure, the final state of the flow downstream of the wave can be determined from those upstream while satisfying the Rankine-Hugiot relations. In solving the Rankine Hugiot relations iteratively, there exists a minimum value that satisfies the conservation equations known as the CJ condition. In Figure 2.2 the $P - \nu$ diagram known as the Hugiot curve shows possible solutions to the Rankine-Hugiot relations. The dashed lines that are tangent to the Hugiot curve represent Rayleigh lines where the horizontal and vertical dashed lines represent lines of constant P and $1/\rho$. These lines divide the Hugiot curve into five regions. Where these tangent Rayleigh lines intersect the Hugiot curve is called the CJ point. The upper CJ point represents the region of detonations and the lower represents that of deflagrations. The upper CJ point is where the burned gas velocity is sonic relative to the detonation wave. Region I from the figure represents strong detonations, region II represents weak detonations, region III is eliminated because it gives non-real intersections with Rayleigh lines, regions IV and V represent weak and strong deflagrations respectively.

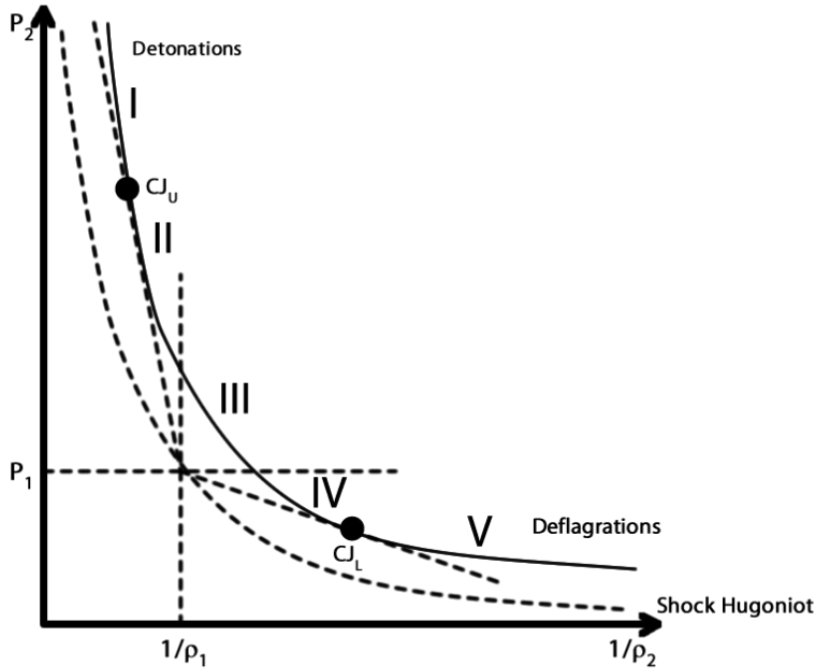


Figure 2.2. Hugonot Curve

NASA Glen Research Center developed a Chemical Equilibrium with Applications(CEA) program with a detonation function that allows one to easily calculate the detonation parameters. Some common hydrocarbons with both air and oxygen are analyzed using CEA and shown in Table 2.2.

Table 2.2 Sample Hydrocarbon Chapman-Jouguet Parameters (100kPa, 298K)

Mixture	P/P ₁	T/T ₁	ρ/ρ_1	M _{CJ}	U _{CJ} (m/s)
Methane-Air (CH ₄)	17.4	9.4	1.8	5.1	1800
Propane-Air (C ₃ H ₈)	18.4	9.6	1.8	5.3	1796
Ethylene-Air (C ₂ H ₄)	18.5	9.6	1.8	5.3	1821
Acetylene-Air (C ₂ H ₂)	19.3	10.6	1.8	5.4	1864
Methane-O ₂ (CH ₄)	29.6	12.6	1.9	6.8	2390
Ethylene-O ₂ (C ₂ H ₄)	33.8	13.3	1.9	7.3	2374
Acetylene-O ₂ (C ₂ H ₂)	34.2	14.3	1.8	7.4	2426
Propane-O ₂ (C ₃ H ₈)	36.6	13	1.9	7.7	2357

ZND Model

In the early 1940's Zeldovich, von Neumann, and Döring independently developed a theory for the structure of detonation waves and is known as the ZND theory. Similarly to the CJ condition the ZND model assumes one dimensional flow but models the shock wave as a discontinuity neglecting transport effects as well as accounting for chemical kinetics and mechanisms of reactions. The ZND theory breaks down a detonation wave into three regions. The first is a planar shock traveling at the CJ velocity that heats and compresses the reactants by introducing a large amount of energy. This is known as the von Neumann, or post shock state. The next region is referred to as the induction zone and here the chemical reaction rates are negligible as there is only a small fraction of reactants burning. The physical properties remain roughly constant in the induction zone. The third region is the reaction zone where the reaction rates increase exponentially. Temperature increases drastically as the pressure and density decrease until the reaction reaches equilibrium. The pressure, density and temperature profiles observed in the ZND model are typical of hydrocarbon oxidation as this type of reaction follows an Arrhenius law and has a large activation energy.

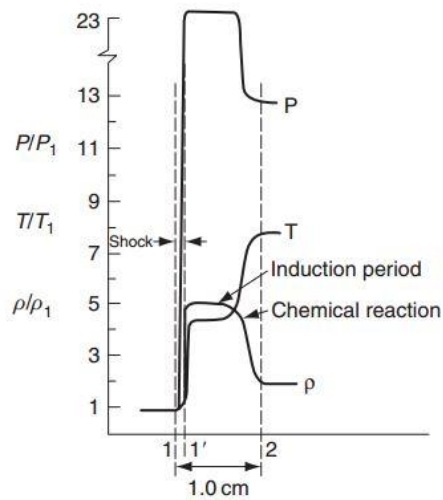


Figure 2.3 Variation of physical parameters through a typical detonation wave

2.3. Thermodynamic Cycles

Pulse detonation engines and detonations are categorized as a mechanism for constant volume combustion or pressure gain combustion. This can be modeled closely by the Humphrey and Fickett-Jacobs cycles but the two differ in overall efficiency and theoretical work output.

Humphrey Cycle

The Humphrey cycle, also known as the Atkinson cycle is commonly used for evaluating efficiency of detonations. The P-v diagram and T-s diagram in Figure 2.4 and Figure 2.5 show the Humphrey compared to the Brayton cycle. The Humphrey consists of isentropic compression (1-2), constant-volume heat addition (2-3), isentropic expansion (3-4), and constant pressure heat rejection (4-1). It closely resembles the Brayton cycle and is often compared to it regarding efficiency. The main advantage of the Humphrey cycle over the Brayton cycle is that the heat addition includes an increase in pressure due to a constant volume. This leads to the Humphrey cycle having a much greater expansion ratio than compression ratio, therefore engines utilizing the Humphrey cycle are able to produce more power than those with the Brayton cycle given the

same inlet conditions of the combustor. This also leads to efficiency advantages of the Humphrey cycle as it creates less entropy with constant volume heat addition.

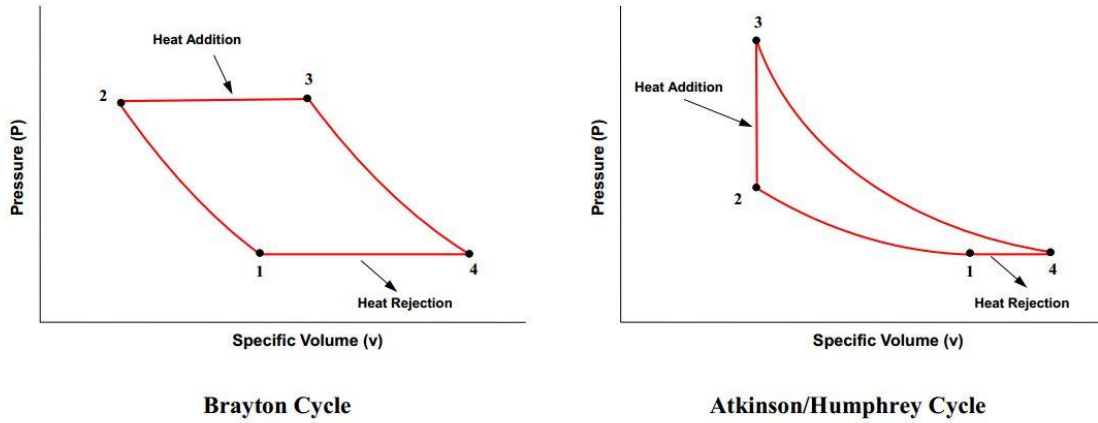


Figure 2.4 P-v diagrams of Brayton and Humphrey Cycles

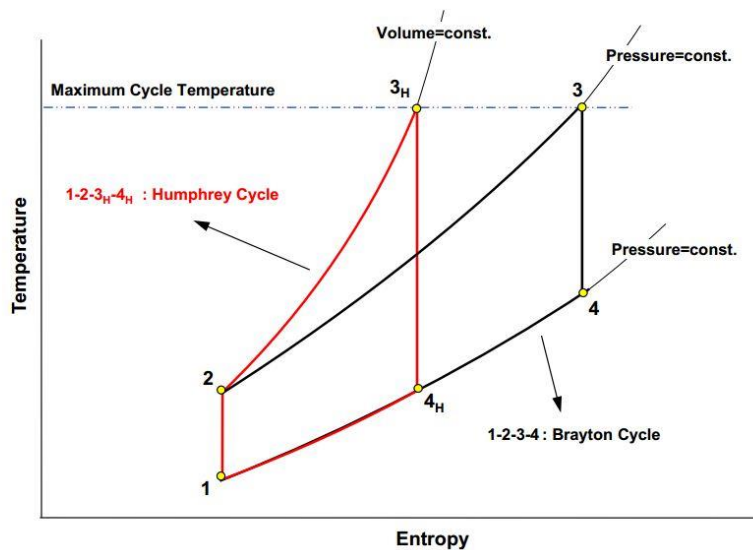


Figure 2.5 T-s diagrams of Brayton and Humphrey Cycles

The efficiency of the Humphrey cycle is defined below based on the work of (Bussing & Pappas, 1994). When compared to the Brayton cycle, one can see that the Humphrey cycle has an extra term that will always be less than one. Therefore, given the same temperature ratios and specific heat, the Humphrey cycle will in fact have a higher efficiency.

Humphrey Cycle Thermal Efficiency $\eta_{th,Humphrey} = 1 - \left(\frac{T_0}{T_1}\right) * \gamma \left[\frac{\left(\frac{T_2}{T_1}\right)^{\frac{1}{\gamma}-1}}{\left(\frac{T_2}{T_1}\right) - 1} \right]$

Brayton Cycle Thermal Efficiency $\eta_{th,Brayton} = 1 - \left(\frac{T_0}{T_1}\right)$

Fickett-Jacobs Cycle

The Fickett-Jacobs (FJ) cycle is a conceptual thermodynamic cycle used to calculate the maximum amount of work that can be extracted from detonating a given mass (Wintenberger & Shepherd, Thermodynamic Cycle Analysis for Propagating Detonations, 2005). The FJ cycle is based on a piston cylinder arrangement shown in Figure 2.6 below.

The physical steps of this conceptual cycle are as follows:

- a) Reactants are in their initial state.
- b) Reactants are isentropically compressed.
- c) External work applied to left piston initiates detonation.
- d) Detonation propagates through cylinder leaving post detonation product moving with piston at v_p .
- e) Detonation products adiabatically and reversibly come to rest by converting energy of mechanical motion to external work.
- f) Products are isentropically expanded to initial pressure.
- g) Heat is extracted by reversibly cooling products at constant pressure until the initial temperature is reached.
- h) Completing the cycle is converting products back to products.

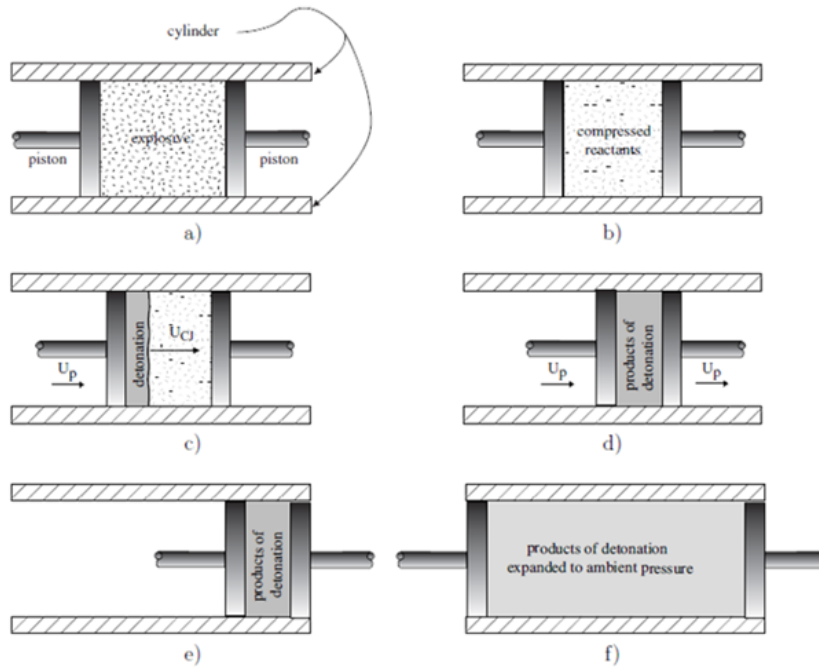


Figure 2.6 Physical steps that make up the Fickett-Jacobs cycle.

The cycle can be seen compared to the Brayton and Humphrey cycle in Figure 2.7 below. The values for thermal efficiency for a perfect gas model by using the one- γ model of detonation which related the CJ Mach number to the specific heat of combustion (Wintenberger & Shepherd, Thermodynamic Cycle Analysis for Propagating Detonations, 2005). The FJ cycle thermal efficiency is defined as

$$\eta_{th,FJ} = 1 - \frac{C_P T_1}{q_c} \left[\frac{1}{M_{CJ}^2} \left(\frac{1 + \gamma M_{CJ}^2}{1 + \gamma} \right)^{\frac{\gamma+1}{\gamma}} \right]$$

Where:

$$M_{CJ} = \sqrt{\mathcal{H} + 1} + \sqrt{\mathcal{H}}$$

$$\mathcal{H} = \frac{(\gamma^2 - 1)q_c}{2\gamma RT_2}$$

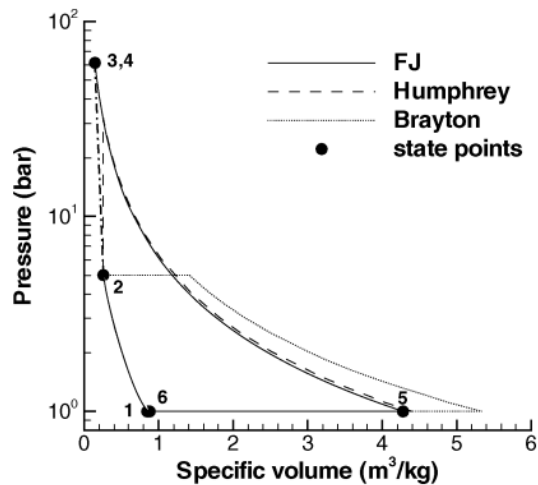


Figure 2.7 P-v diagram of Fickett-Jacobs cycle compared with Humphrey and Brayton

2.4. Detonation Waves

The CJ and ZND detonation theory both assume the structure of a detonation wave is one dimensional and give results that closely match experimental results but what occurs in reality is far from one dimensional. Aft of the leading shock exists transverse shocks. These transverse shocks intersect with the leading shock and create localized regions of elevated pressure and temperature known as triple points. These triple points accelerate the local reaction rates and aid in stabilization of the detonation wave.

In a stable detonation, the traces of these triple points create a “fish scale” pattern as can be seen in Figure 2.8 **Error! Reference source not found.** However, there are also unstable detonations that can create irregular soot foil patterns as shown in Figure 2.9 from (Khokhlov, Austin, Pintgen, & Shepherd, 2004). In the work of Khokhlov, Ausin, Pintgen, and Shepherd, numerical analyses were completed with experimental validation on the detonation wave structure of stoichiometric ethylene-air mixtures with varying dilution using argon and nitrogen. This

effectively changed the ratio of specific heats (1.15-1.35) which drastically changed to stability of the detonation wave. Planar laser-induced fluorescence images from experiments showed features of the unstable detonation waves that include wrinkles in the shock front, pronounced filaments of unburned reactants on the front, pockets of unreacted material behind the front, secondary detonation cell structure, as well as strong localized explosions originating at the intersections of transverse waves.

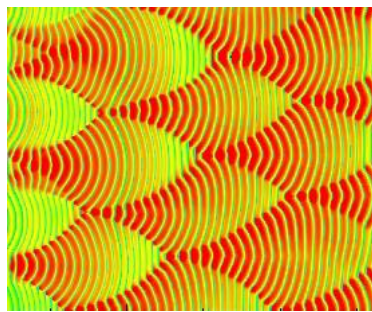


Figure 2.8 Numerical soot foil pattern for a stable detonation wave



Figure 2.9 Experimental soot foil pattern for an unstable detonation wave

2.5. Detonation Wave Formation

Burned gas products from the initial deflagration have a specific volume that is on the order of 5-15 times that of the unburned gas ahead of the flame. Consider a tube or pipe with a single closed end filled with a flammable gas mixture. With ignition at the closed end this will lead to

acceleration. Since each preceding compression wave that results from this expansion heats the unburned gas mixture, sound velocity increases and the succeeding waves catch up with the initial one. This preheating tends to increase the flame speed and rates of reaction which accelerates the unburned reactants to the point where turbulence is produced. The turbulence creates ripples and eddies in the flame front and increases the burning surface area. This further increases the velocity and acceleration of the unburned gases and strong compression waves are formed. This leads to the formation of a detonation kernel, or small explosion that accelerates the local reaction rates further leading to a shock strong enough to auto ignite the reactants behind the front. This auto ignition transitions an unstable detonation wave to a stable one. At this point, the energy from the chemical reactions initiated by shock compression and heating are enough to sustain the detonation (Glassman & Yetter, 2008).

The transition to detonation will occur in a smooth walled tube of sufficient length; however, this transition can be shortened both in length and time. With the addition of turbulence, using mechanisms as simple as rough walls, the deflagration to detonation time can be drastically shortened making applications to harness the benefits of constant volume combustion in a detonation tube more feasible.

2.6. Detonation Transition

Detonation initiation can be divided into two categories; direct initiation and detonation transition. Direct initiation is caused by a blast created by rapid energy addition. This is typically done with a high energy spark discharge, exploding wires, or with solid or gaseous explosives. Detonation transition is achieved through flame acceleration. Direct initiation has rather large power requirements with energy requirements ranging from tens of kilojoules to thousands of kilojoules. For applications in a pulse detonation where a high frequency is desired it makes the

required power impractical especially in aerospace applications where weight is of concern. Therefore, focus in pulse detonation revolves around detonation transition through obstacle-shock wave interaction.

Deflagration to detonation transition (DDT) is a commonly used method to achieve detonation using a fractional amount of energy than direct initiation. DDT consists of a subsonic combustion wave that is accelerated to a supersonic combustion wave. First deflagration is initiated usually with a relatively low energy spark to create a flame. The flame is accelerated and increases the energy release rate forming strong shock waves. One or more localized explosions reach the critical ignition energy creating small blast waves. These blast waves interact with the shocks from the flame acceleration and join to form a self-sustaining detonation.

2.7. Methods of Flame Acceleration

Obstacles placed in the detonation tube will shorten both the time and distance required to achieve detonation transition. These obstacles introduce turbulence and pressure fluctuations into the flow. This can lead to wrinkles in the flame front leading to an increased burning surface area. Pressure perturbations are also caused that aid in triggering the transition to detonation. The Shchelkin spiral is the most common method used to partially block the combustion chamber to accelerate DDT. The Shchelkin spiral was originally described by Kirill Ivanovich Shchelkin in his 1965 book *Gas Dynamics of Combustion*. The most important parameter for the spiral is the blockage ratio (BR). Blockage ratio is shown in Figure 2.10 and is defined as the percentage of the detonation tube passage area that is blocked by the obstacle. Similarly orifice plates have the same definition of blockage ratio but instead of a spiral, they are simply washers spaced within the detonation tube.

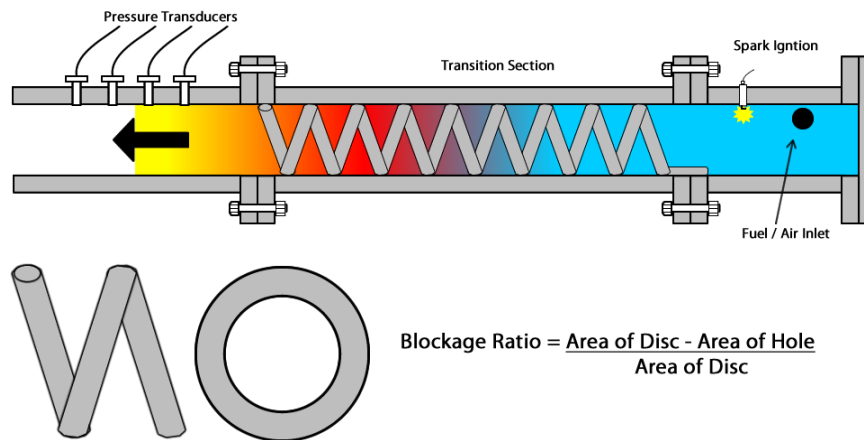


Figure 2.10 Schematic of detonation tube using Shchelkin spiral.

2.8. Performance Impact of DDT Enhancing Obstacles

The performance effects of the obstacles to enhance DDT are currently being studied extensively. One study of the effect of blockage ratio by (Gamezo, Ogawa, & Oran, 2009) shows obstacles have competing effects of blockage ratio on DDT. This is due to different shape and size obstacles having different influences on flames and shock waves (Frolov, Aksenov, & Skripnik, Detonation Initiation in a Natural Gas -Air Mixture in a Tube with a Focusing Nozzle, 2011) (Vasil'ev, Roy, Frolov, Santoro, & Tsyganov, 2003). On one side, larger obstacles create a more non-uniform flow which leads to faster flow and flame acceleration promoting DDT. The accelerating flow generates shocks that reflect from obstacles and interact with the flame and eventually become strong enough to ignite detonation. On the other side, larger obstacles have been numerically shown to inhibit DDT by weakening shocks through the diffraction process (Gamezo, Ogawa, & Oran, 2009). Another numerical study out of NASA Glen with experimental validation from Air Force Research Lab analyzed the performance of obstacles

including both drag and heat transfer (Paxon, Schauer, & Hopper, 2009). It was found that DDT obstacles can reduce specific impulse by 10%.

The Shchelkin spiral and orifice plates were the only obstacles used until recently. The Naval Post Graduate School has studied improvements on detonation initiation using swept-ramp obstacles similar to vortex generators. Interestingly enough, simulations and tests using evenly spaced sets of two swept ramp obstacles at each axial location that were rotated 180 degrees gave pressure losses of 50% less than those using the spiral and was able to consistently achieve detonation (Brophy, Dvorak, Dausen, & Myers, 2012). There was a study completed that used hybrid obstacles consisting of vortex generators in conjunction with orifice plates. This configuration was able to achieve reliable and repeatable DDT with an L/D of 15.

3. TEST EQUIPMENT AND METHODOLOGY

3.1. Experimental Hardware

The detonation tube used in this experiment was designed to use Ethylene-Air mixtures to achieve detonation through detonation transition using orifice plates. It was developed by a past researcher for studies into the effects that fill percentage, frequency, and equivalence ratio had on pressure and wave speed. These findings can be found in *Investigation of Pulse Detonation Engines; Theory, Design, and Analysis* (Vizcaino, 2013).

The cell width of Ethylene-Air mixtures is around 1 inch at stoichiometric conditions which led to a 2 inch diameter detonation tube. In former investigations, a blockage ratio of 45% proved to be optimal giving an inside diameter of 1.5 inches. This gave a wide band of operating conditions to achieve stable detonations as can be seen in Figure 3.1. While this was good for past research, to study the effect of variable blockage ratio several sized orifice plates were machined and the blockage ratios were 30, 35, 45, 50, and 55%. The largest blockage ratio of 55% results in an inside diameter of 1.09 inches which drastically narrows the band of operation when used.

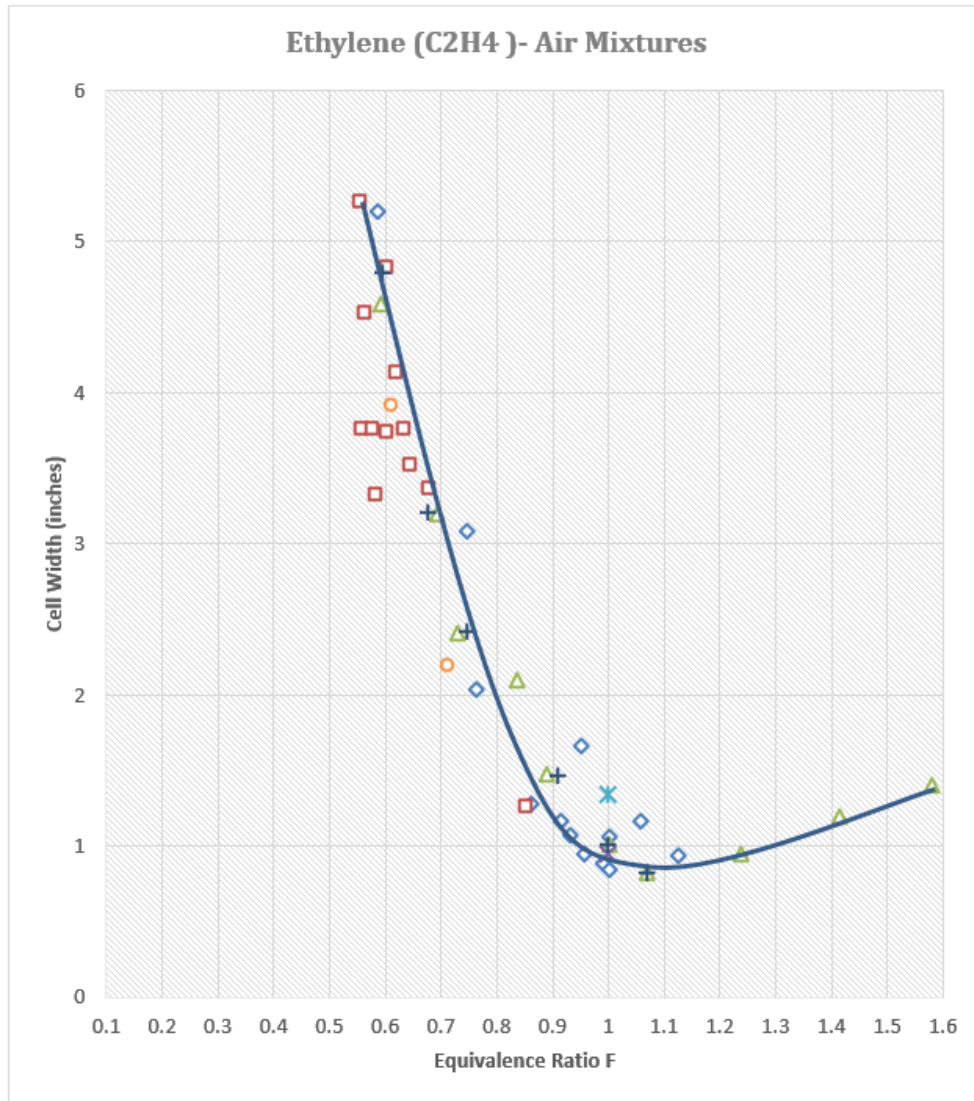


Figure 3.1 Ethylene Cell Size vs. Equivalence Ratio

The detonation tube is modular and consists of three sections; ignition, detonation transition, and measurement. Between each section an injector plates where both fuel and air are injected tangential to the tube. These injector plates were designed to promote mixing of the fuel and air upon injection. The obstacles are machined stainless steel thin washers and are spaced by thin wall pipe which allows for easy reconfiguration. The thickness of the thin wall pipe was accounted for in the calculation of blockage ratios.

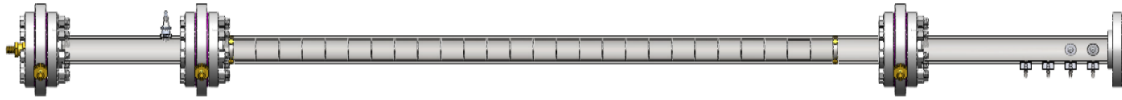


Figure 3.2 Detonation Tube Overview



Figure 3.3 Experimental Set-up

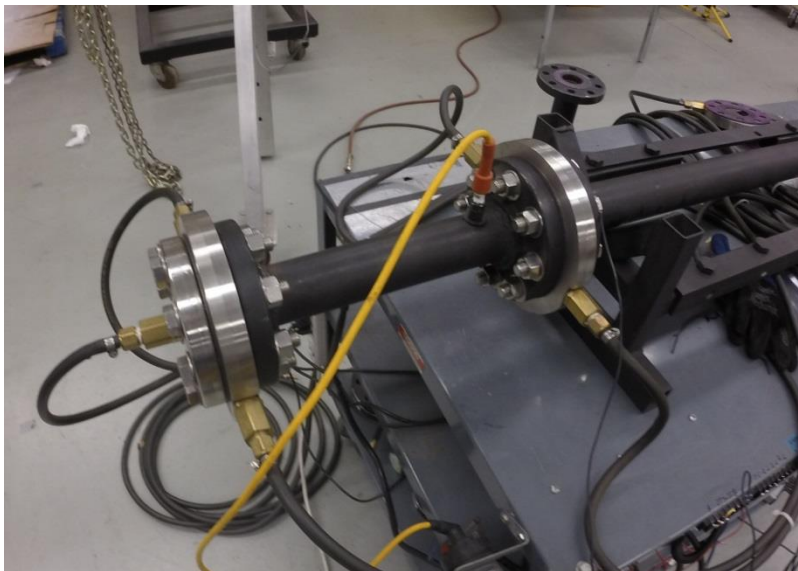


Figure 3.4 Ignition section of detonation tube

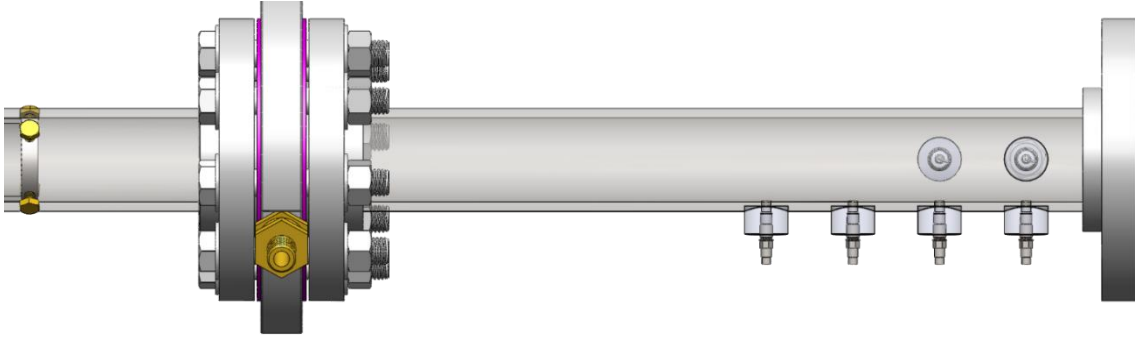


Figure 3.5 Measurement section of detonation tube

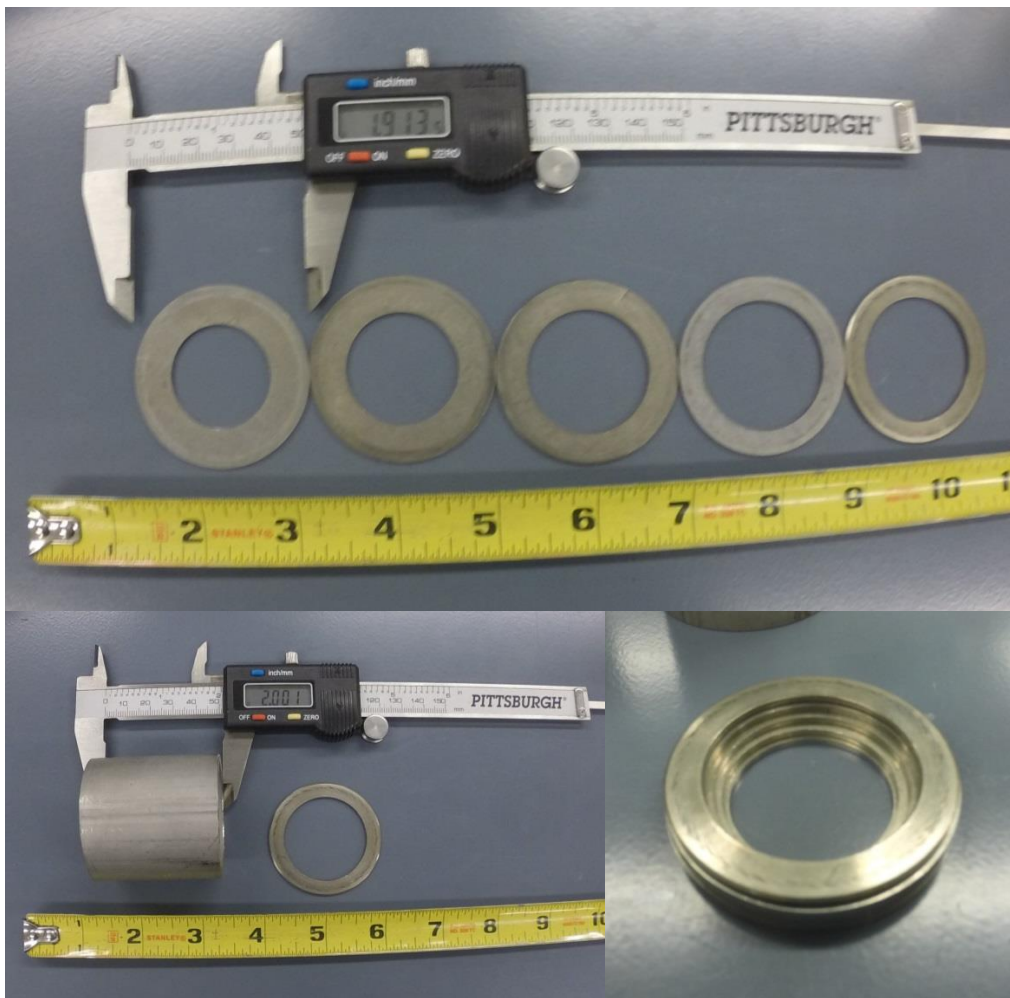


Figure 3.6 Various obstacles and spacer for internal geometry

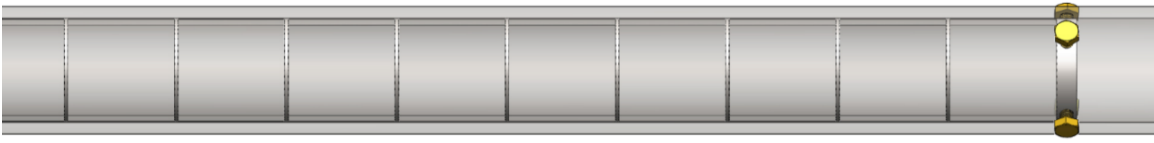


Figure 3.7 Interior obstacle configuration

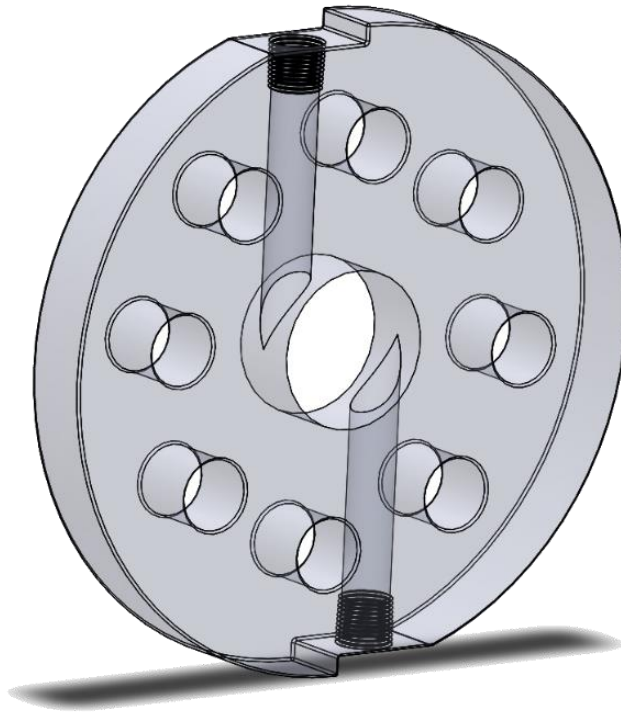


Figure 3.8 Injector plate

Detonation Tube

The detonation tube was constructed from schedule 80 stainless steel 304 with a nominal diameter of 2" and meets ASTM standard A312. Strength and temperature response of the material is shown below.

Table 3.1 Detonation Tube Details

Nom. ID, inches	2.0	Outer Diameter, inches	2.375
Wall thickness, min., inches	0.189	Wall thickness, nominal, inches	0.216
Working Pressure PSI (ambient T)	3,411	Yield strength, min, PSI	30,000
Burst pressure PSI (ambient T)	13,642	Tensile strength, min, PSI	75,000
Melting Point	2550-2640		
Maximum Service Temperature	1380-1700		

Obstacles

The obstacles were made from stainless steel 304 washers and manufactured to the specified dimensions.

Flanges

The flanges were socket-weld, class 300, conforming to MSS SP-6, SP-25, ASTM A182, and ANSI/ASME B16.5 standards.

Flange gaskets

The flange gaskets were chosen to be full face class 300 gaskets conforming to ASME B16.20 standards and manufactured from NOVATEC engineered graphite and able to withstand continuous temperatures of 925 degrees Fahrenheit

Bolts and Nuts

Bolts were chosen to be grade 2 stainless steel bolts with a minimum tensile strength of 70 kpsi.

Check valves

Check valves were of the Fluorelastomer seal type with a maximum pressure rating of 1000 psi at 70 degrees Fahrenheit and have and can operate at temperatures of up to 400 degrees Fahrenheit.

Injection block and Fuel Manifold

The injection blocks and fuel manifold delivery systems were machined from 6061 aluminum.

3.2. Sensors and Instrumentation

Pressure Transducers:

The pressure transducers used were the PCB Piezotronic model 111A24. They have a maximum measurement range of 2000 psi at 5.0mv per psi with a NIST calibration certificate. They can resolve down to 20 mpsi and have a rise time of less than 1.5 microseconds. They can withstand flash temperatures of 3000F and static pressures of 10,000 psi but steady state operating temperature is limited to 275F.

Combustion (Ion) Sensors

The Ion sensors were constructed from Autolite brand number 26 spark plugs unaltered and connected to a PCB signal conditioner to provide a constant voltage potential across the electrodes. The post was connected to the positive supply voltage of the signal conditioner and the body was grounded to the common system ground and the signal conditioner ground.

Signal Conditioner:

The signal conditioner is a PCB 482C15 unit for signal conditioning which supports up to 4-channels and individually adjustable voltage gain settings. The signal conditioner provides a constant current source needed for the pressure transducers. The default current is set to 4mA and the conditioner output is AC coupled.

Data Acquisition Board

A National Instruments USB-6351 DAQ was used for the experiments. Out of all the unit's features, only the analog inputs and timers were used for testing. The analog inputs are capable of sampling at a rate of up to 1.25 MHz (multichannel aggregate) with 16-bit resolution and range of ± 10 V. They were used to record the pressure signals. The 32-bit counter/timers were used as control lines to trigger the injection solenoids and ignition system.

Power Supply

An adjustable 3-15 VDC 40A B&K Precision 1692 switching power supply was used to power the igniter, coil, and the injector driver box. The unit has a fixed-voltage mode (at 13.8 VDC),

used for testing. A digital display on the unit's front panel shows the output voltage and instant current draw.

Injector Solenoids

The injector valves are manufactured by AFS, model GS-series. They are 'peak-and-hold' type valves. In order for them to have a fast response (opening/closing time), a high current must be initially applied. Once the valve is open, a lower 'hold' current is sufficient to keep them open. This avoids overheating the units. The manufacturer published mass flow vs. time curves were obtained by using an AFS injector driver box. Therefore, to be able to properly correlate injector opening time with mass flow, an AFS injector driver box was used.

Injector Driver

The injector driver box is an AFS 8-channel unit. It was powered by 13.8 VDC from the power supply. It automatically provided the peak-and-hold output needed to trigger the injectors, based on logic-level input signals from the DAQ.

Ignition coil and Igniter

The ignition module and coil were BOSCH units, fitted to several European cars. They were powered by the 13.8VDC power supply, using heavy wire as described before. The ignition module is of the 'dumb' type: i.e. coil charge time was directly controlled by the DAQ. A wire wound noise suppression cable was used to connect the coil to the spark plug. The spark plug used for all experiments is a standard Autolite 26 spark plug.

3.3. Control System and Data Acquisition

The LabView virtual instrument was designed by the former researcher (Vizcaino, 2013) but some modifications were necessary due to software changes.

LabView Control Panel

The control panel which controls the fuel, air, and spark timing as well as data measurement was created using NI LabView 2011 and interfaces with the NI USB-6351 digital acquisition system

used in analog to digital conversion (ADC). The virtual instrument (VI) is designed to control all the parameters that govern the filling and detonation of the fuel / air mixture save for the fuel and air pressures which must be manually set at their respective regulators.

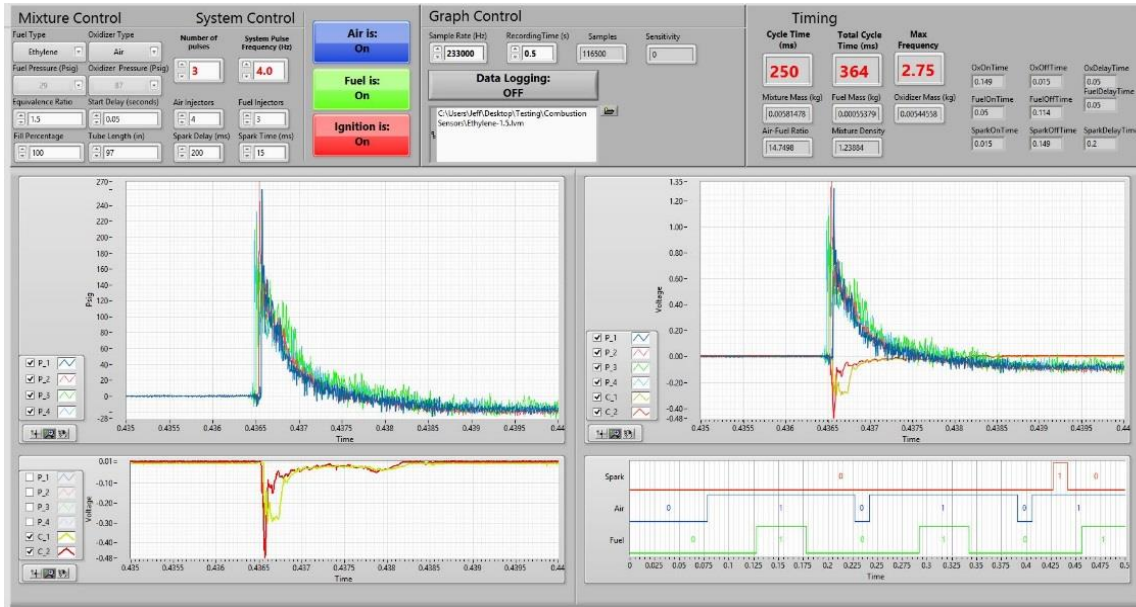


Figure 3.9 LabView VI

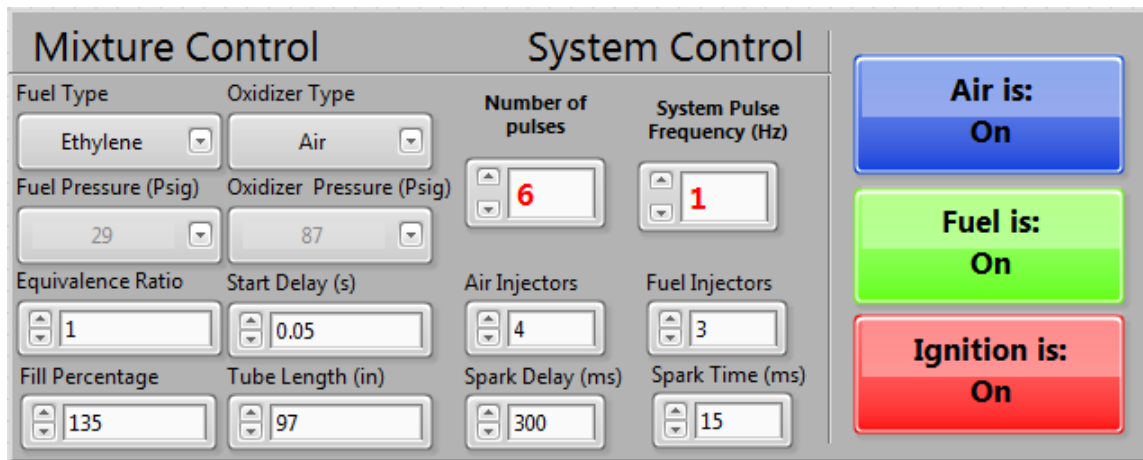


Figure 3.10 Input Control for LabView VI

The input control panel shown above in Figure 3.10 controls all the filling parameters for the fuel and air as well as the spark timing. The fuel and oxidizer types control the values used to

calculate the stoichiometric air to fuel ratio and the proper injector curve fit. Fuel and oxidizer pressures are also used for injector curve fitting the injected mass vs. pulse width. Equivalence ratio, fill percentage, and tube length control the injected mass of fuel and air. Modifying the equivalence ratio directly adjust the amount of fuel delivered to the detonation tube while keeping the amount of air constant. Modifying the fill percentage and tube length controls the overall volume used to calculate the mass of fuel and air needed. Increasing the fill percentage multiplies the volume by the appropriate constant whereas modifying the tube length will modify the volume by a ratio of L/L_o as governed by the equation $V = \pi R^2 L$. Modifying the pulse number directly changes the number of fuel, air, and spark On/Off pulse while System pulse frequency will determine how close those pulses are to each other. The system pulse frequency effectively controls the time between one pulse and the next. Injector numbers tell the VI code how to divide the total pulse time, if 2 oxygen injectors are used instead of 4 the total required fill time for air will double and likewise with the fuel. Start delay and spark delay control the time between when the user presses the run button and the appropriate signal is generated. In the current implementation all timing is triggered by the air high pulse (the digital on signal) which means that the initial delay is actually the air delay and the spark delay is the time between when the air injectors are closed and when the spark is ignited. Spark time controls how long the spark plug is firing which directly controls the energy deposition rate. The air, fuel, and ignition toggle buttons control whether or not the digital pulses are sent to the injector and spark devices. By default these buttons are set to off.

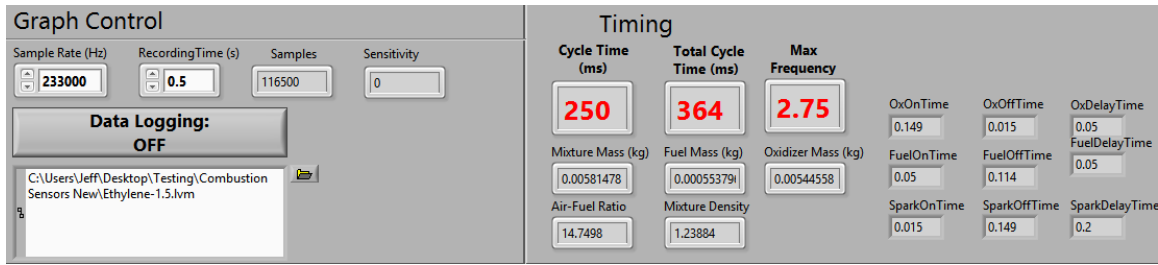


Figure 3.11 Data Logging and Timing Panel for LabView VI

The logging and timing panel control the data logging features of the VI. It allows for controlling the sampling rate, recording time, and whether or not to log data to a file. The timing panel displays the calculated data from the given inputs such as estimated fuel and air mass delivered and pulse widths. It is important to note however that the sample rate of the DAQ is limited to 1.4 million samples per second total across all ports which means that if six sensors are connected and recorded then the maximum sample rate is $1.4\text{MS}/6$ or 233.33 KHz. To remove sensors from being recorded one needs to remove it from the DAQMX node in the LabView backend.

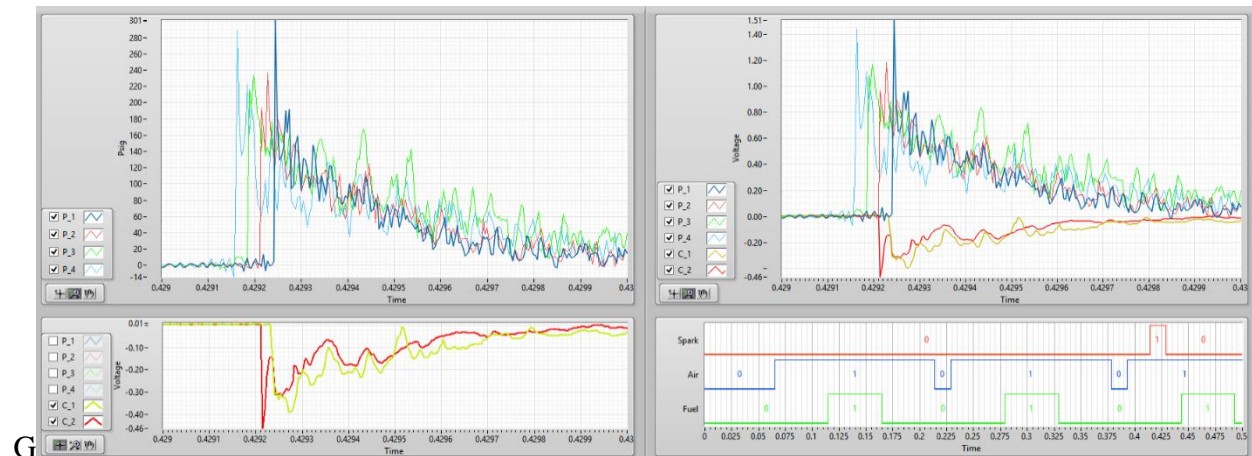


Figure 3.12 Graph Output Control

The graph output panels show all the current sensors traces being used during the run. Recording is started when the simulation is started although it can be changed to start when any of the injector control pulses are fired or turned off. The top left corner shows just the scaled pressure

sensor traces, bottom left shows just ion sensor traces, top right shows the combined raw data from both pressure and ion sensors and bottom left shows the digital pulses sent to the injectors and spark plugs.

LabView Injector and Spark Control

The VI employed in the experimental setup employs the use of pulse width modulation (PWM) to deliver the precise amount of fuel desired for the inputs in the LabView control panel. Each pulse time is calculated by the process outlined in

APPENDIX A: CALCULATION OF FILLING PARAMETERS, and then controlled by three independent hardware counters supplied by the NI DAQ. The VI uses the inputs from the control panel to determine the required filling time for both the fuel and air injectors. Adjusting the equivalence ratio, fill percentage, volume, and number of injectors controls modify the width of the pulses (the “on times”) while pulse number and frequency modify the spaces between pulses or the “off times”. Spark delay time will modify the distance between the last fuel / air pulse and the ignition pulse. Start delay will modify the time between when the user presses the run button and the first pulse starts.

The LabView code following the calculation node is necessary to convert the desired pulse times into digital on off signals and is created in three parts. First a pulse generator node is created which tells the DAQ a digital pulse needs to be generated and on what channel. After the pulse is generated the DAQ is then informed of how many pulses need to be generated and in what mode to run them. Lastly the signal is when to start whether is triggered on run, external signal, or from internal digital signal. The pulse is then generated based on the rising or falling action of the signal, i.e. on or off. If the triggering is set on rising then the pulse is simultaneous with the trigger start and if set to falling it simultaneous with the end of a trigger.

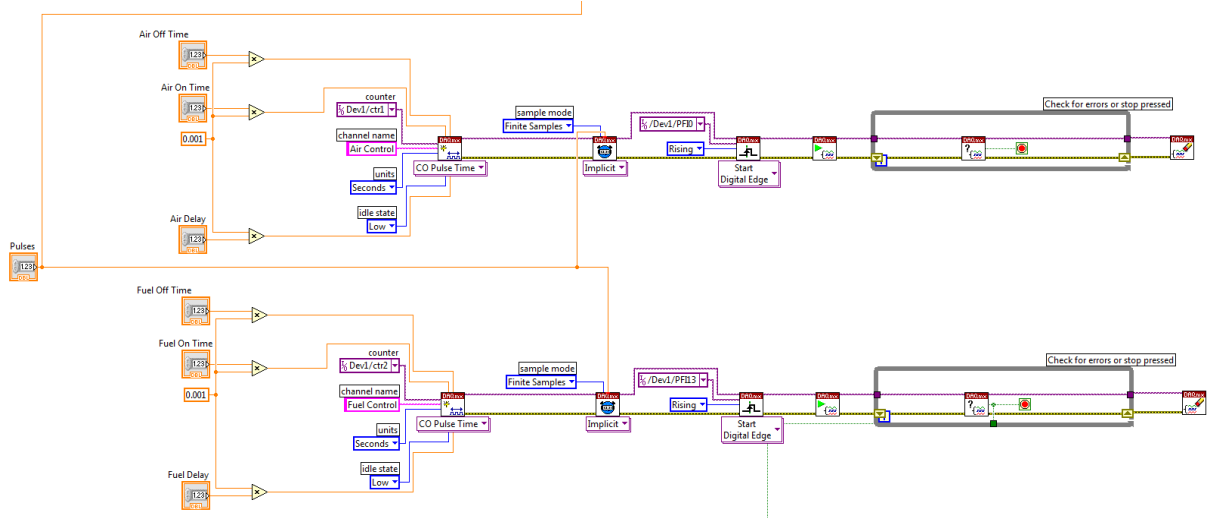


Figure 3.13 Fuel Control System

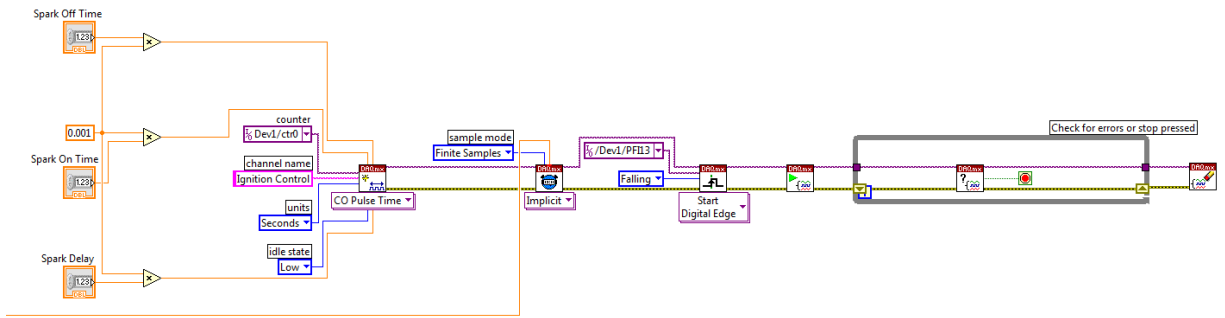


Figure 3.14: Spark Plug Ignition Control System

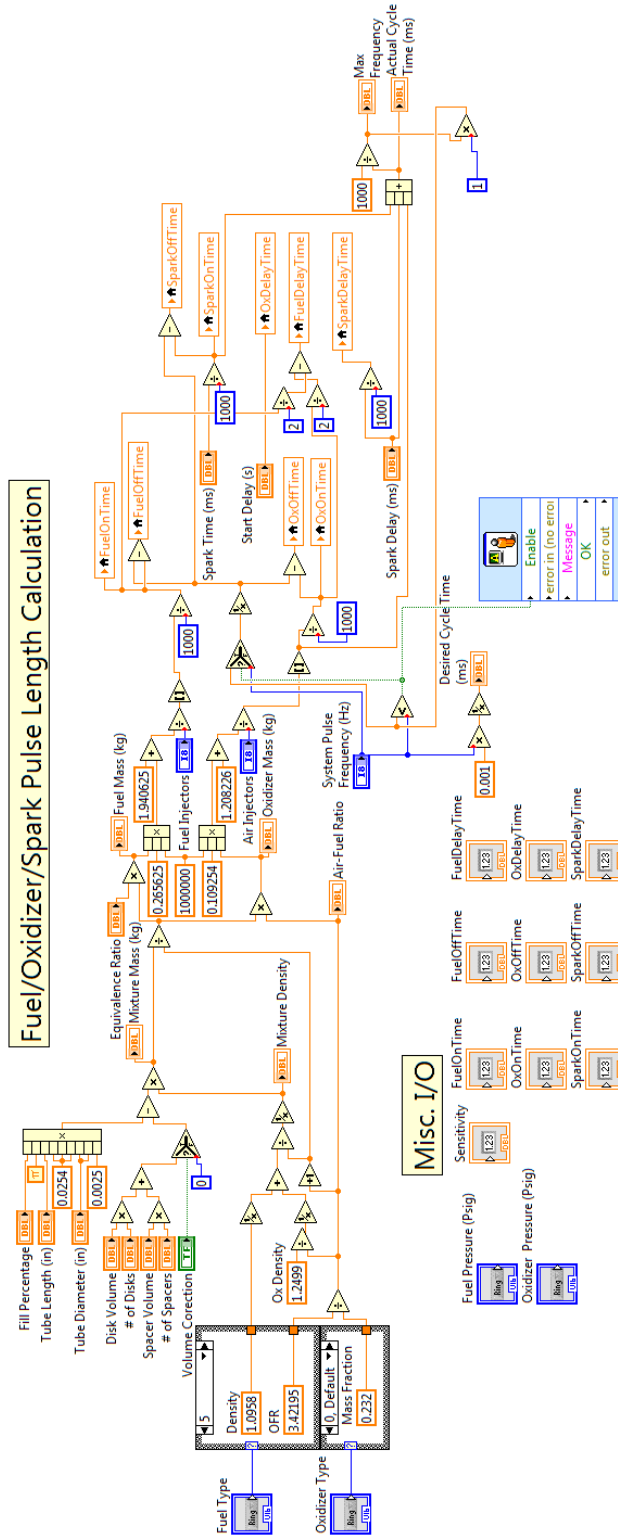


Figure 3.15 Calculation Node for LabView VI

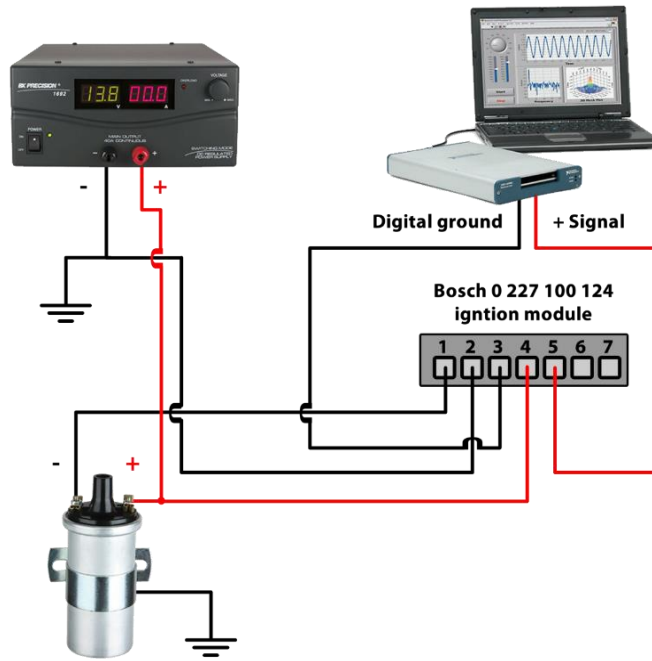


Figure 3.16 Ignition Wiring

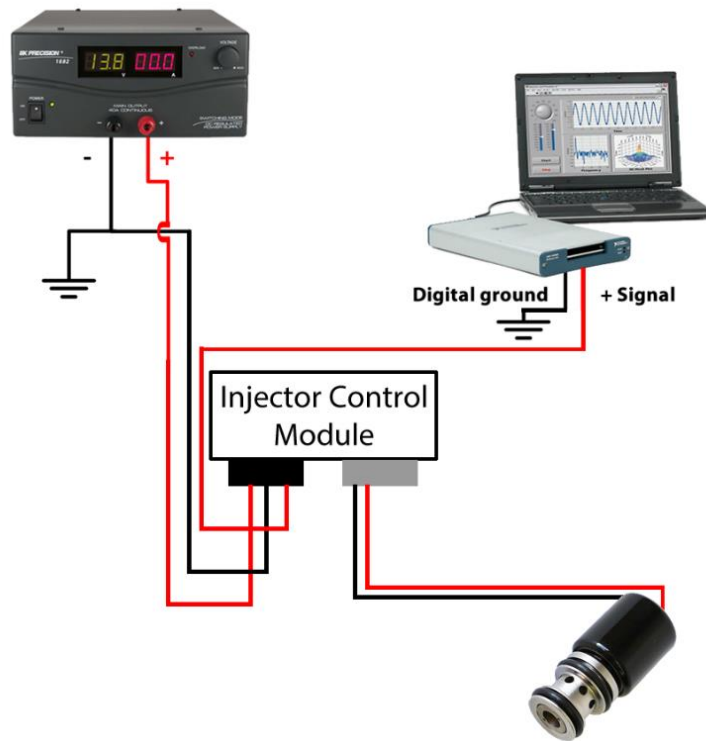


Figure 3.17 Injector Wiring

3.4. Experimental Method

Experimental tests were conducted to establish a baseline performance with constant blockage ratios. The test configuration was then changed to test the effects of variable blockage ratio on detonation performance. All tests were run with the same equivalence ratio of 1.3, fill percentage (130% for cycle 1, 100% for cycle 2), and frequency (1Hz for cycle 1 and 6Hz for cycle 2) when compared to the baseline constant blockage ratio tests. There were two different filling and firing cycles tested. One cycle consisted of overfilling the detonation tube by 30% with no additional purge cycle and firing. From this point forward this will be considered firing cycle 1. The second cycle consisted of two filling pulses each at 100% fill. This was found to be optimal in obtaining successful ignitions.

Firing Cycle 1

Firing cycle 1 consisted of filling and firing with no purge cycle included. This was done to test six consecutive pulses at the maximum cycle frequency as limited by the time for air injection and the spark delay time required to get adequate mixing to ensure successful ignition. The digital signals that define this cycle can be seen below in Figure 3.18. The cycle begins after a specified delay time and the cycle period begins with the air pulse and ends with the spark. The LabVIEW virtual instrument was designed to calculate the air and fuel pulse widths. It was noticed that 130% fill produced the highest percentage of successful ignitions. It was noted after testing was completed for this report that with or without the last injector manifold there was no impact on performance of ignitions and successful detonations. This would explain why there was a need to overfill the detonation tube by 30%. These injectors amounted to 33% of the fuel and 25% of the air being injected.

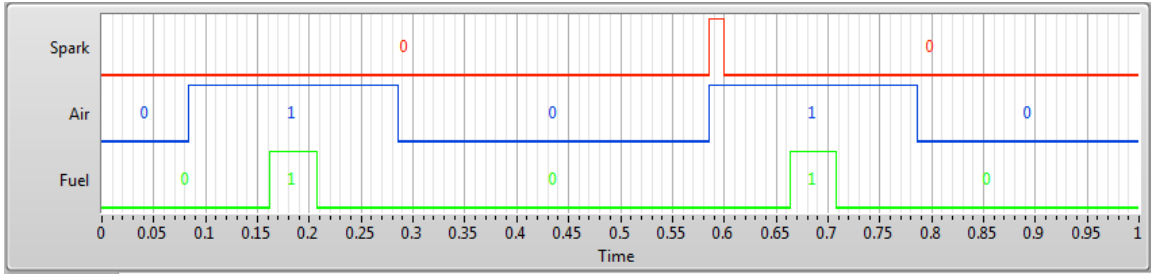


Figure 3.18 Digital signals for firing cycle 1

Firing Cycle 2

Firing cycle 2 was used to give results that will not have dependency on filling and mixing issues that arise using firing cycle 1 that will be discussed later. This cycle ensures that the full extent of the detonation tube is properly filled with a fuel/air mixture. The digital signals for this cycle can be seen in Figure 3.19 below. The cycle consists of two air and fuel pulses at 6 Hz each of which inject enough fuel and oxidizer to fill the detonation tube. The gas mixture is ignited 20ms after the second pulse. This pulse configuration was found by trial and error to ignite 100% of the time showing that the fuel and air were mixed adequately enough. Other cycles were tested as well including filling 200% in one pulse but the performance was inferior. This is likely due to the impulse of the second pulse promoting turbulent mixing. Another cycle was attempted that consisted of two pulses at 50% fill each but this also produced inferior performance. This is likely due to the later noticed lack of contribution from the last fuel and oxidizer injectors resulting in an effectively lower fill percentage.

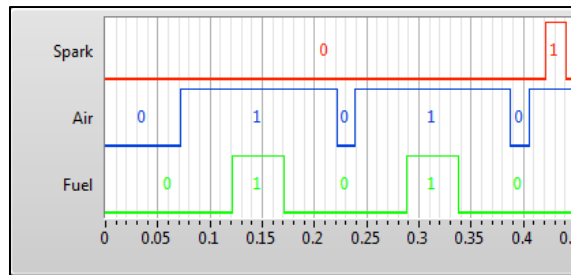


Figure 3.19 Digital signals for firing cycle 2

Blockage Ratio Configurations

A wide variety of variable blockage ratio configurations were tested for detonation performance totaling thirteen configurations. They can be categorized into a different categories including constant, converging (increasing), diverging (decreasing), converging-diverging, and alternating at various percentages of the detonation tube length. The configurations can be understood from Figure 3.20 to Figure 3.26 where the blockage ratios are shown as a function of the detonation tube length. It is expected that configurations that reduce in blockage ratio will result in superior performance. The theory is that the larger blockage ratio earlier on will help accelerated the flow rapidly while the reduced blockage ratio will have less impedance on the shock wave. Tests were completed on converging sections with the expectation of inferior results. The alternating blockage ratio configurations were tested to investigate if changes in the strength of pressure perturbations would affect the performance warranting further numerical investigations.

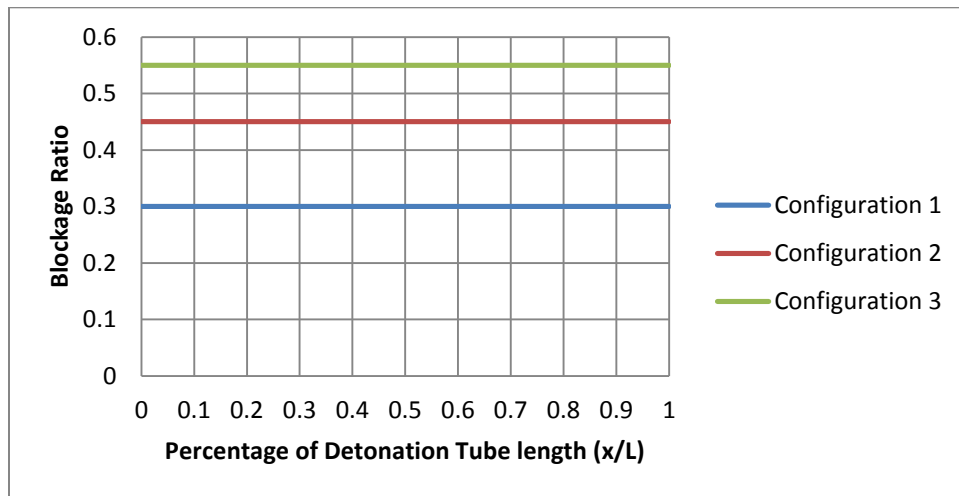


Figure 3.20 Constant blockage ratios

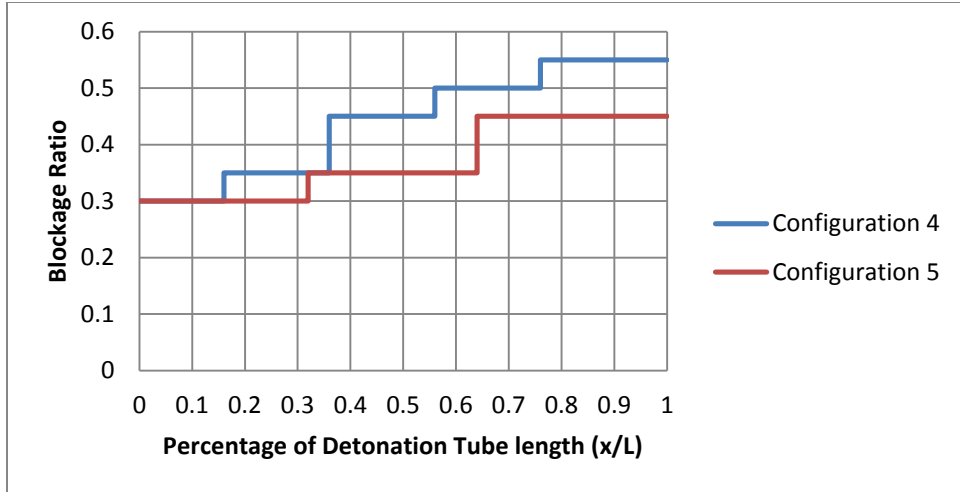


Figure 3.21 Converging blockage ratios

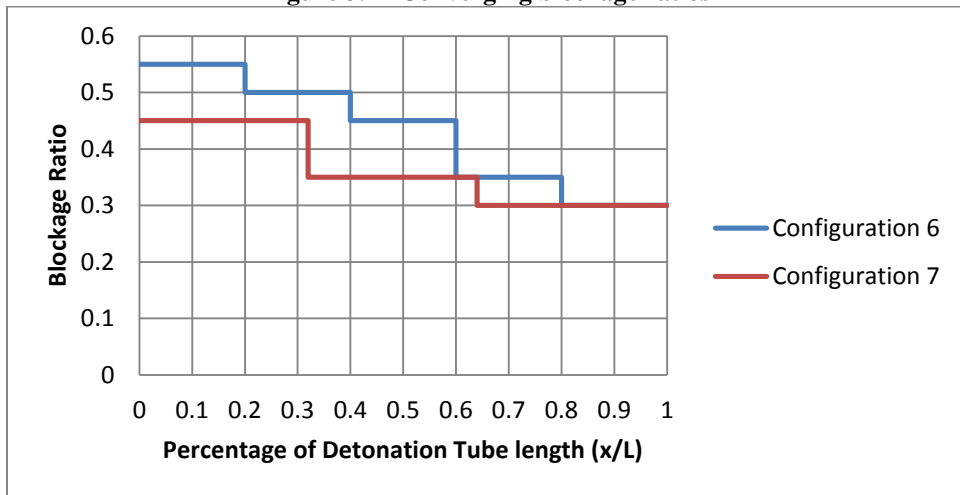


Figure 3.22 Diverging blockage ratios

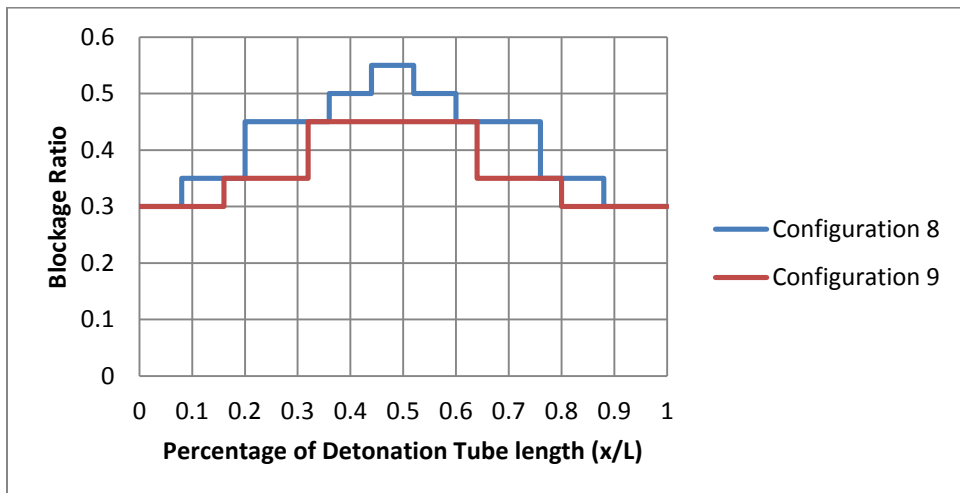


Figure 3.23 Converging-diverging blockage ratios

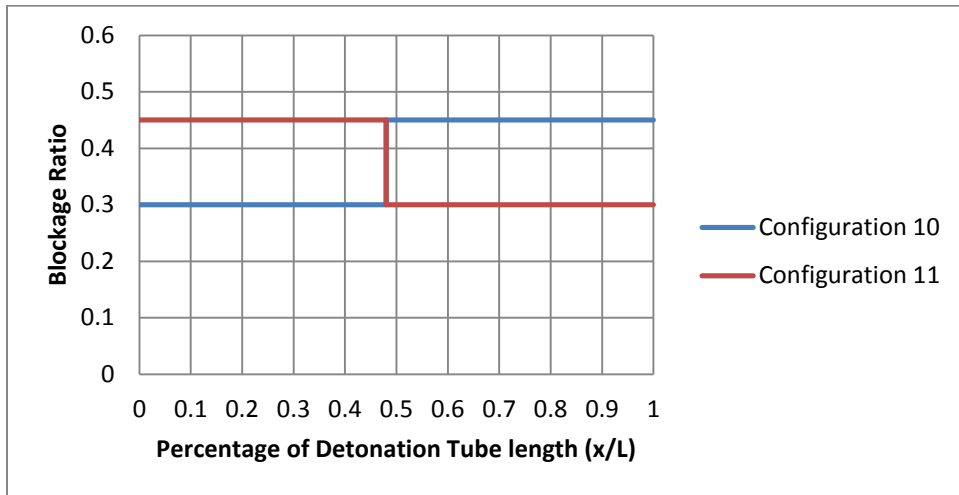


Figure 3.24 Alternating blockage ratios at 50% of tube length

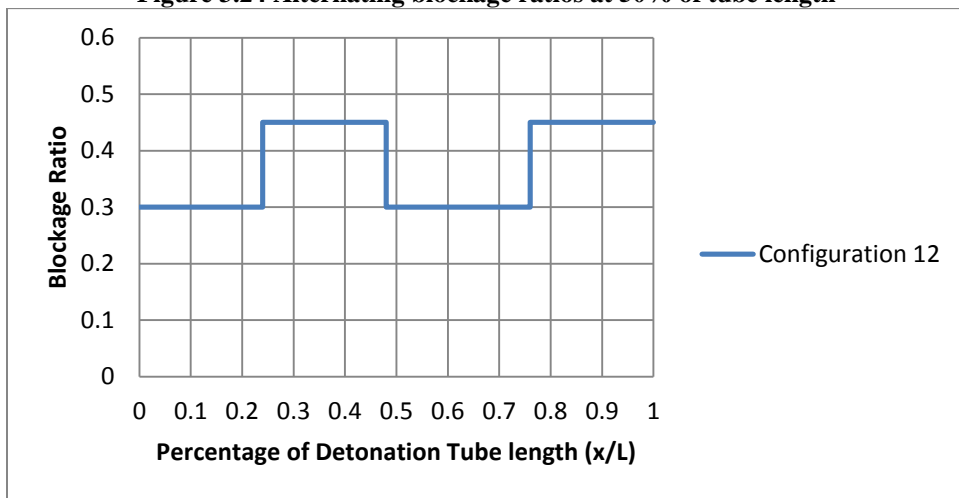


Figure 3.25 Alternating blockage ratios at 25% of tube length

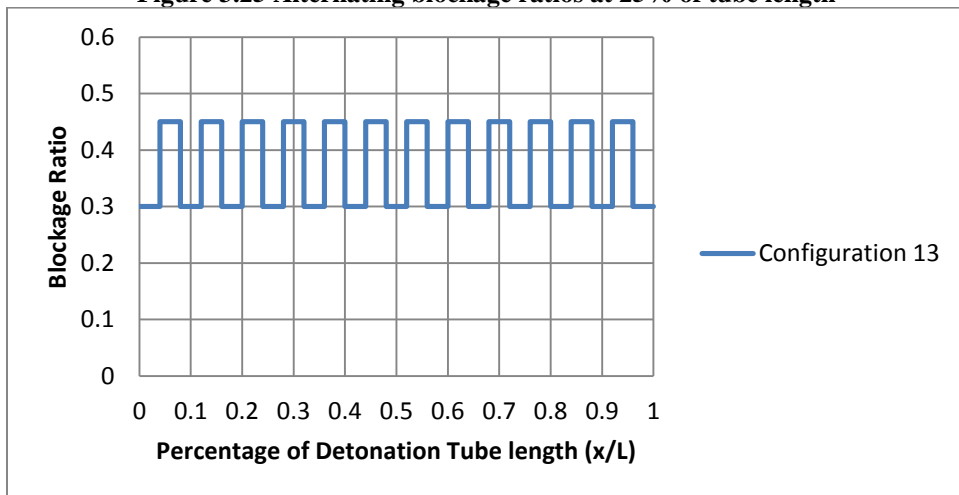


Figure 3.26 Alternating blockage ratios at every obstacle

4. EXPERIMENTAL RESULTS

4.1. Theoretical Results

Using NASA's CEA tool, the relation between detonation pressure and velocity versus equivalence ratio was plotted for ethylene-air mixtures. This gives a theoretical detonation velocity of 1876 m/s and a pressure of 287 psig for an equivalence ratio of 1.3 which was used in all cases.

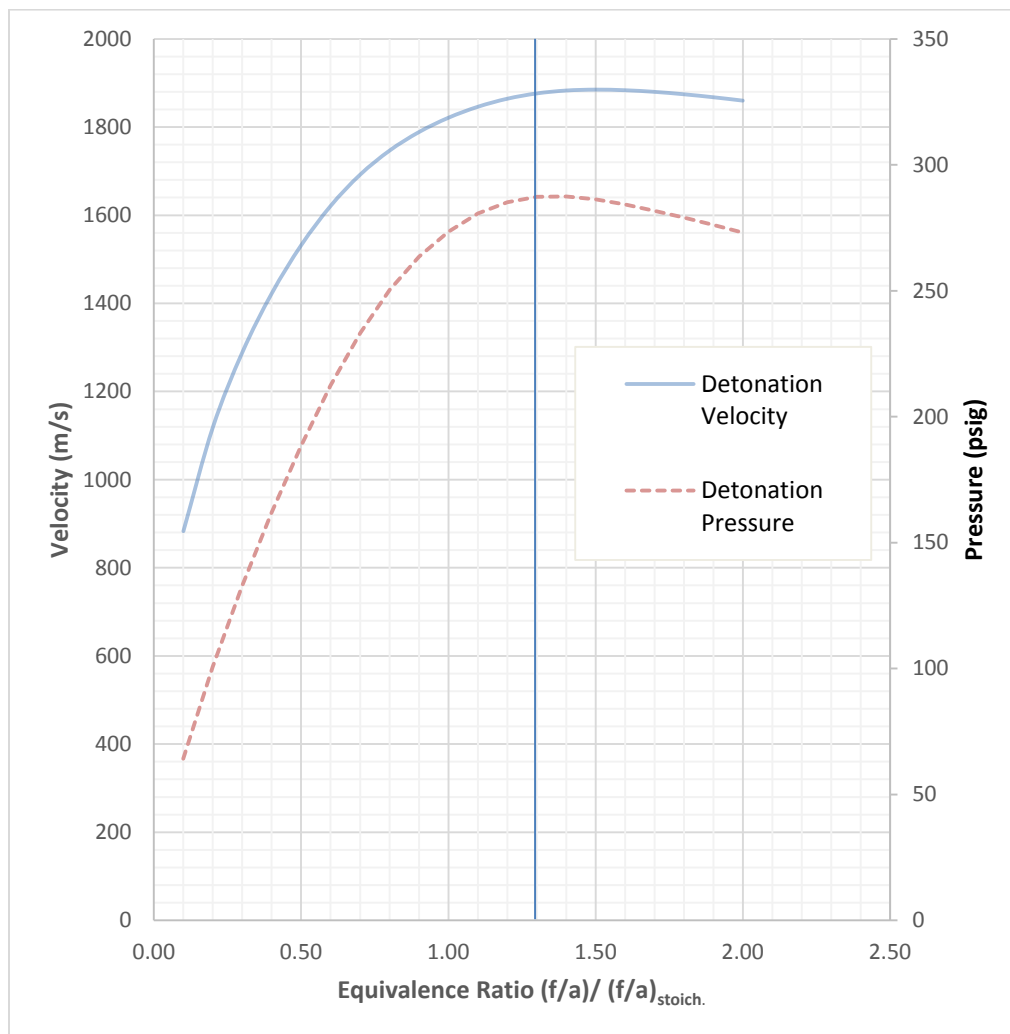


Figure 4.1 Detonation Velocity and Pressure vs. Equivalence Ratio

Theoretically, a decreasing blockage ratio function such as cases 6, 7, 8, 9, and 11 would give the best performance due to larger obstacles increasing turbulence leading to faster flow and flame acceleration earlier in the DDT process leading a more open flow path toward the open end of the tube producing fewer losses and reducing the weakening of shocks due to diffraction. Since Gamzeo, Ogawa, and Oran showed these competing effects of blockage ratio, this was the logical hypothesis.

4.2. Results

The detonation performance varied with both firing cycle and blockage ratio configuration. For firing cycle 1 deflagrations were consistent for most firings and some test fires failed to ignite. Firing cycle 2 yielded a much higher detonation success rate and giving interesting comparisons between blockage ratio functions. It was easy to differentiate between the deflagrations and detonations for many reasons. The first is looking at the peak pressure levels where the predicted C-J pressure was 287 psi. The pressure for successful detonations always fell above 250psi where deflagration pressure levels were close to the 100psi mark. The next indication of detonation was the wave velocity calculated as the times the wave took to move from one pressure sensing location to the next. The C-J velocity is 1876 m/s and detonations typically fell within 200m/s of this. Typical deflagration velocities were around 1000 m/s. The third indication of detonation was using ion sensors. The delay between the ion sensors and the third and fourth pressure sensor indicate whether the combustion wave is actually coupled to the shock pressure wave. Typical deflagration and detonation tests can be seen in Figure 4.2 and Figure 4.3. The positive values are pressure traces where the negative values are ion traces. The magnitudes of ion sensors used in this experiment have no meaning. A voltage is supplied to each sensor and in

the presence of ionized combustion products, current is able to flow from the post to the body of the spark plug. Therefore any recorded voltage is an indication of the combustion wave.

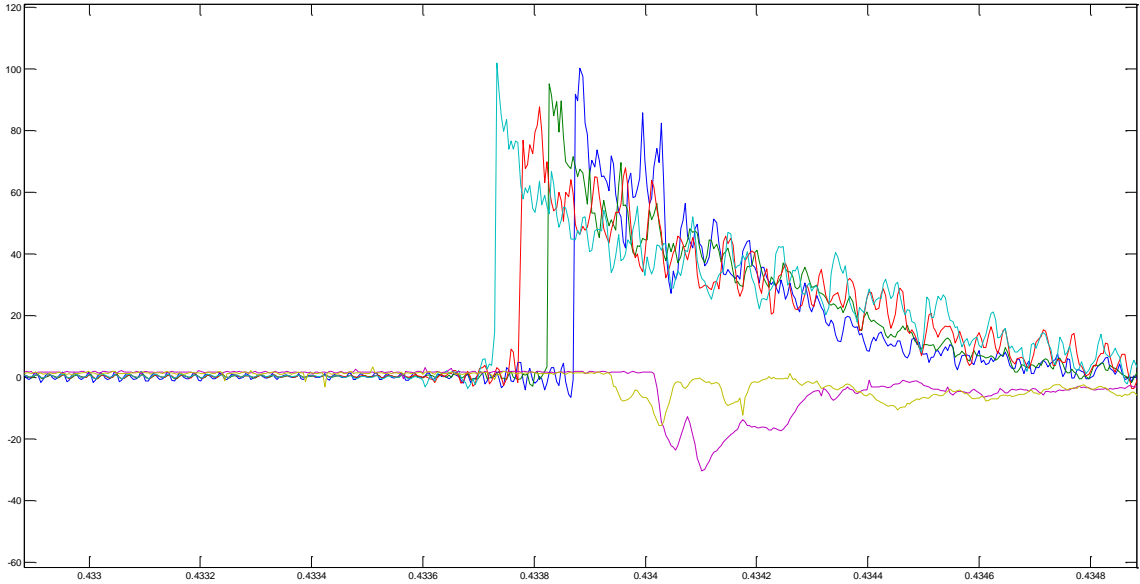


Figure 4.2 Typical deflagration sensor traces

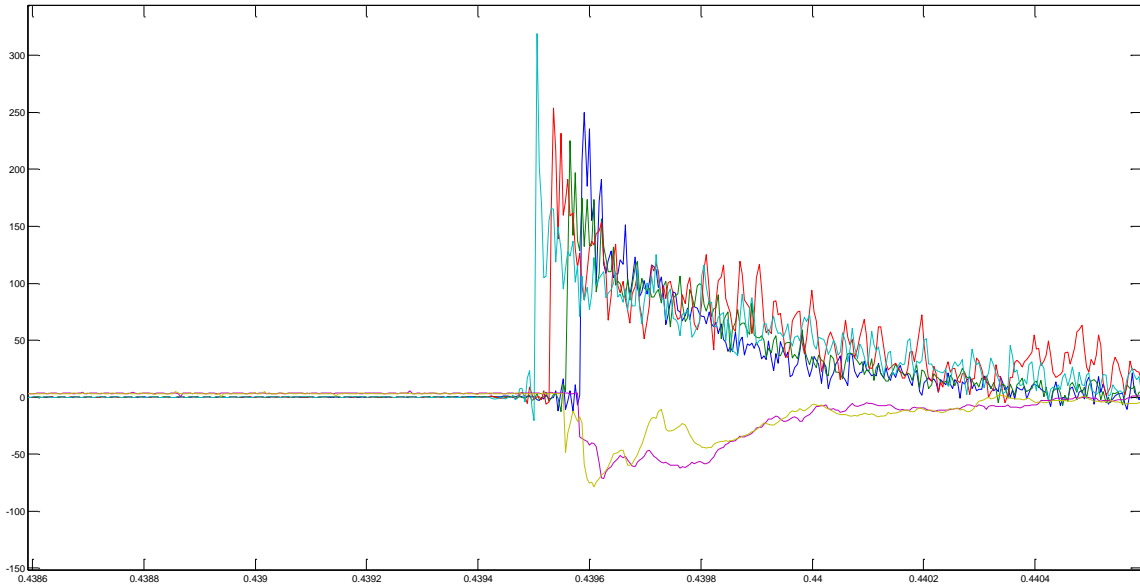


Figure 4.3 Typical detonation sensor traces

4.3. Firing Cycle 1

Firing cycle 1 was not a great representation of the effects variable blockage ratio had on detonation performance since 12 out of 13 cases produce no detonations. Only Case 1 produced detonations and the success rate was only 2%. The averages of detonation peak pressure and velocity are 261.7 psi and 1912.7 m/s respectively. Detonation performance is not able to be studied with this firing cycle however, there are some interesting trends revealed in the strength of the deflagrations showing that some cases were much closer to detonation transition than others. A comparison of the measured pressures and velocities can be found in Table 4.1. The configuration with the clear advantage is Case 1 with a constant blockage ratio of 30%. When looking at the distribution of pressures and velocities seen in Figure 4.4 and Figure 4.5 it is noticed that many of the recorded pressures for case 1 fall above the C-J predicted pressures and the majority of velocities are close to the C-J velocity. This at first may seem indicative of detonations but with the use of ion sensors, it was determined that only two samples had the pressure and combustion waves coupled resulting in a detonation wave. The other cases are examples of a strong deflagration just before the onset of detonation.

Table 4.1 Velocity and Peak Pressure Overview for Firing Cycle 1

Case	P_{\max} Avg	P_{\max} Std. Dev.	Vel Avg	Vel Std. Dev.	Misfire %
1	234.1	83.6	1440.5	269.5	1.0%
2	67.8	12.5	807.3	46.9	0.0%
4	55.0	5.8	785.1	27.4	0.0%
5	155.6	35.5	1142.6	134.9	16.7%
6	79.7	18.5	868.1	71.2	1.0%
7	67.1	9.4	853.1	48.8	0.0%
8	134.6	32.7	1118.2	80.4	16.7%
9	90.8	17.4	966.6	91.5	2.1%
10	74.3	16.5	813.2	48.3	0.0%
11	93.5	15.9	967.5	104.6	12.5%
12	118.0	44.0	1048.1	143.5	2.1%
13	121.5	39.4	1062.1	150.2	16.7%

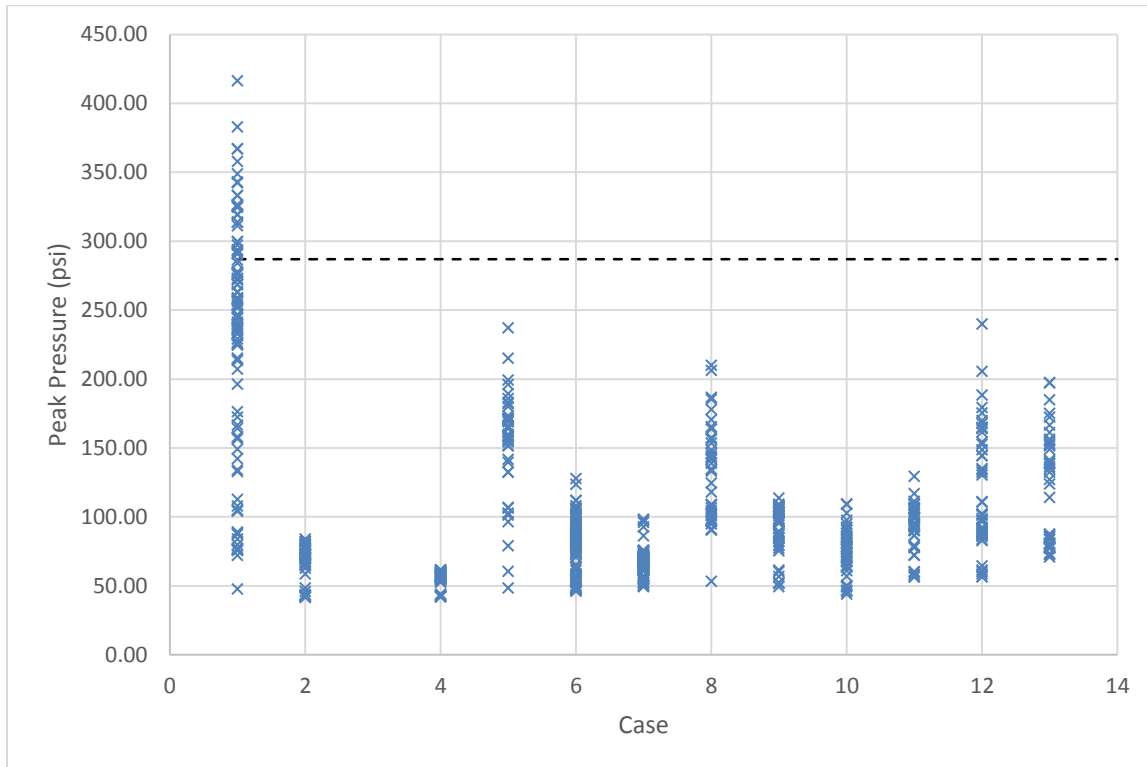


Figure 4.4 Distribution of peak pressures for firing cycle 1

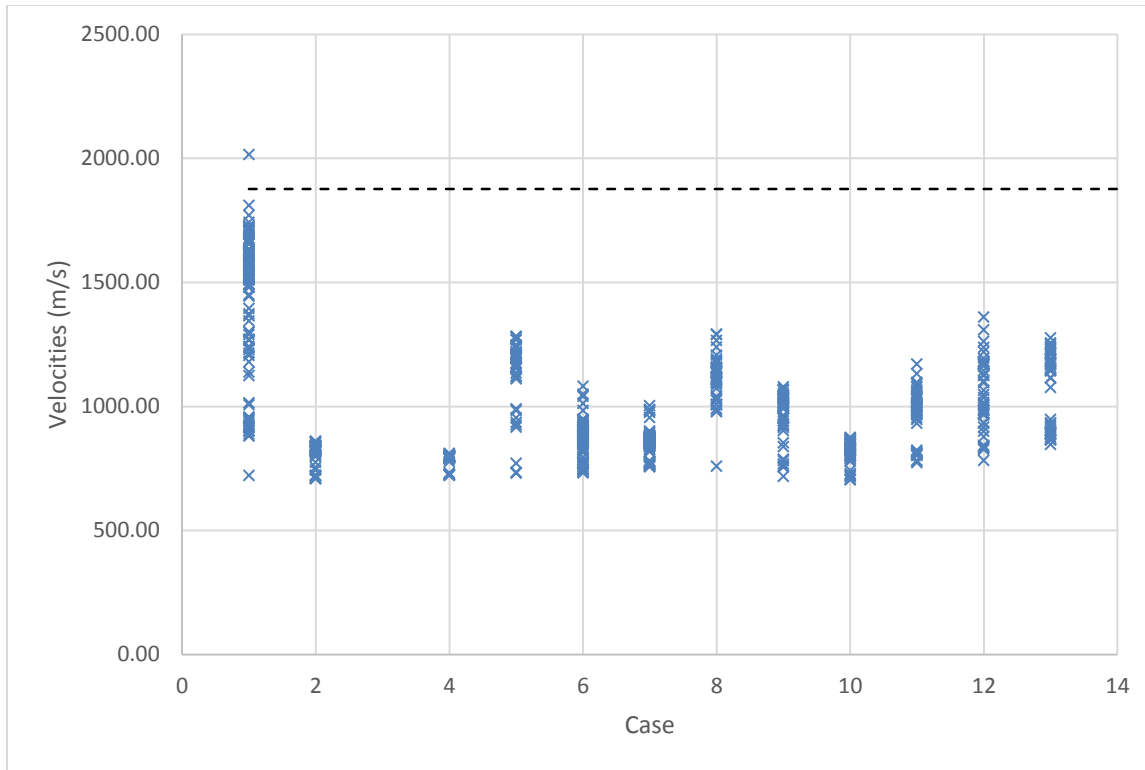


Figure 4.5 Distribution of wave velocities for firing cycle 1

Other cases that performed above average were 5, 8, 11, and 13. This is true for both pressure and velocity measurements. There is no clear commonality between the blockage ratio function of these cases or between the cases that performed at a lower level.

An interesting trend relating to firing a sequence of several pulses was revealed. Table 4.1 gives the number of misfires where the fuel air mixture failed to ignite completely. Of the 34 misfires, 33 of them occurred on the first firing in the sequence of 6. It was unexpected that the first firing in a sequence would not be the same as all of the rest. When comparing pressure and velocity measurements over the 6 firing pulses of a single firing cycle a clear trend emerged and that was that the velocities and pressures of the first pulse of each firing cycle is consistently between 25% to 90% of the following 5 pulses of the cycle. See APPENDIX C: RAW DATA & RESULTS. This trend can be seen in Figure 4.6 where some sample runs were randomly

selected from various cases. The reason behind why the first fire performs worse than the pulses succeeding it is not known for certain. It is believed that transient pressure variations within a detonation tube as outlined in (Endo, Kasahara, Matsuo, Inaba, & Sato, 2004) give a favorable pressure gradient to draw injected fuel and air from the closed end towards the exit. This can assist in uniformly filling and mixing the fuel air mixture throughout the volume of detonation tube. Since the time of transition was not accounted for in the firing sequence, filling for the next fire begins immediately as the fuel air mixture is ignited as shown by the digital signals in Figure 3.18. The large amount of misfires of initial firings led to a search for a filling sequence that would ensure proper and complete mixing as it was clear there was insufficient mixing in simply filling the detonation tube 100% in a single pulse.

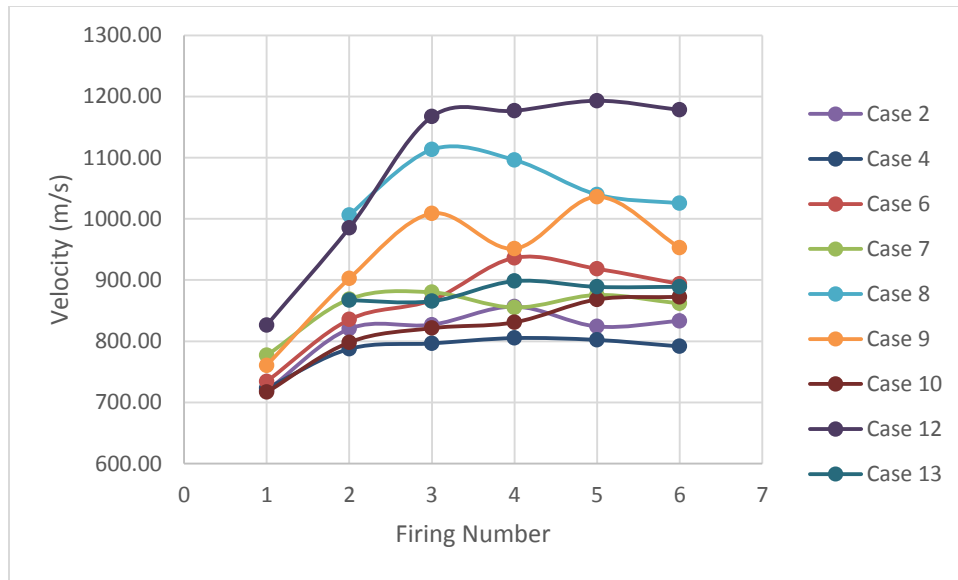


Figure 4.6 Firing number vs. Velocity

4.4. Firing Cycle 2

Firing cycle 2 shows the best results for the effect of blockage ratio on detonation performance and returns some interesting results. The detonation performance was analyzed and there were

cases that had 100% successful detonations and some less, all the way down to no successful detonations. Table 4.2 shows an overview of average velocities and peak pressure for the successful detonations of each case. For cases 3 and 4, there were no successful detonations achieved. A commonality between these two cases; a large blockage ratio of 55% for at least the last 25% of the tube length. The blockage ratio of 55% gives an obstacle diameter of just over 1” which is also the cell width of ethylene-air at an equivalence ratio of 1.3. This shows that using obstacles with the critical tube diameter, detonation could not be achieved.

Table 4.2 Detonation Velocity and Peak Pressure overview for Firing Cycle 2

Case	Occurrence	Average Velocity (m/s)	Velocity Standard Deviation	% of C-J Velocity	Average Pressure (psig)	Pressure Standard Deviation	% of C-J Pressure
1	55%	2042.5	269.7	109%	334.28	59.86	116%
2	90%	1746.7	64.7	93%	335.19	57.85	117%
3	0%	-	-	-	-	-	-
4	0%	-	-	-	-	-	-
5	100%	1841.7	111.5	98%	309.24	50.35	108%
6	70%	1809.8	55.5	96%	312.53	50.09	109%
7	100%	1940.9	39.0	103%	318.80	25.22	111%
8	100%	1809.6	59.8	96%	340.66	47.66	119%
9	100%	1851.1	49.0	99%	324.52	50.94	113%
10	25%	1819.5	206.2	97%	307.20	17.08	107%
11	45%	1922.6	58.8	102%	302.58	34.53	105%
12	85%	1941.2	151.1	103%	296.56	40.33	103%
13	70%	1929.5	58.5	103%	306.95	48.39	107%

Table 4.3 Deflagration Velocity and Peak Pressure overview for Firing Cycle 2

Case	Occurrence	Average Velocity (m/s)	Velocity Standard Deviation	Average Pressure (psig)	Pressure Standard Deviation
1	45%	1437	142.87	144.8	30.32
2	10%	807	3.81	58.9	4.18
3	100%	913	40.51	65.48996	4.86
4	60%	803	12.80	57.59741	2.82
5	0%	-	-	-	-
6	30%	999	15.95	90.1861	7.90
7	0%	-	-	-	-
8	0%	-	-	-	-
9	0%	-	-	-	-
10	75%	845	202.16	88.91253	6.28
11	55%	1011	222.06	135.9937	15.16
12	15%	919	20.14	86.69323	8.46
13	30%	911	19.40	79.0	4.59

Pressure Trends

For pressure, the average peak pressures for all of the cases are all similar and generally speaking cases with a higher percentage of successful detonations recorded high average pressures. The one exception is case 1 which recorded high pressures and velocities for both detonations and deflagrations. Looking at the average pressures for each case found in Table 4.2, all of them are above the C-J predicted pressure of 287 psig with a maximum of 340.7 psig. When looking at each run for each case, the average was not always above the C-J pressure and can be seen in Figure 4.7. In this figure the average pressure of each run is represented by a point where detonations are filled circles and deflagrations are unfilled circles and the C-J pressure is represented by the dashed line. There is a clear distinction between deflagrations and detonations when looking at these pressure trends.

While the peak pressure averages are relatively similar and all fall within 20% above the C-J pressure, Figure 4.8 through Figure 4.20 shows a rather wide variation among individual pressure measurements from run to run. This variation can be attributed to the complex 3-d structure of a detonation wave consisting of transverse shock waves that propagate in a helical pattern. Creating surfaces of intersecting shocks and triple points which change location as they propagate and lead to slightly different pressure measurements from sensor to sensor. When looking at runs that resulted in deflagrations and no transverse shock waves, there is clearly a close grouping of pressure measurements when compared to detonation. Figure 4.8 through Figure 4.20 show this relationship as well as the average standard deviations in Table 4.2 and Table 4.3. For detonations, the average standard deviation is 43.8psi and for deflagrations it is a mere 9.4psi.

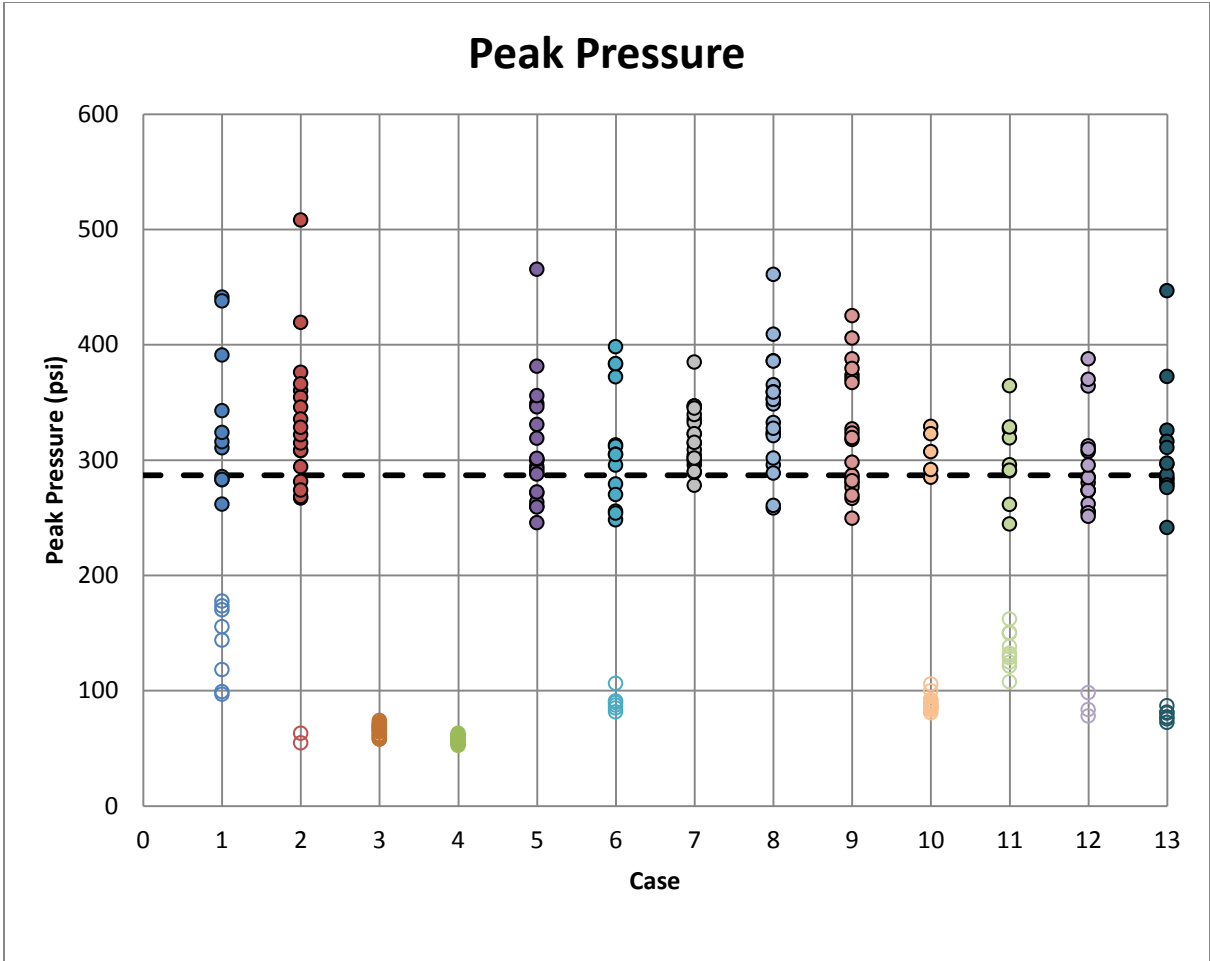


Figure 4.7 Average peak pressures for Firing Cycle 2

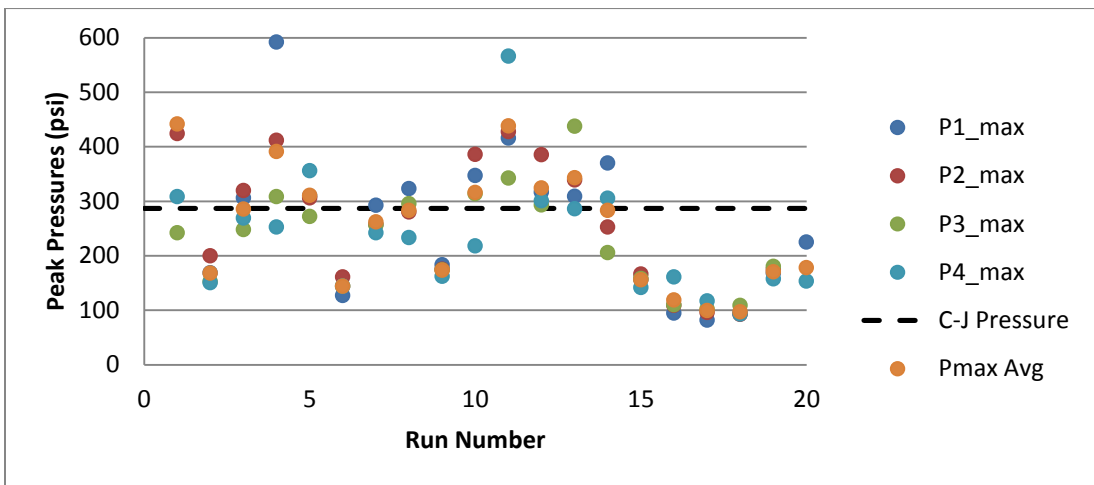


Figure 4.8 Measured peak pressures for each run of Case 1

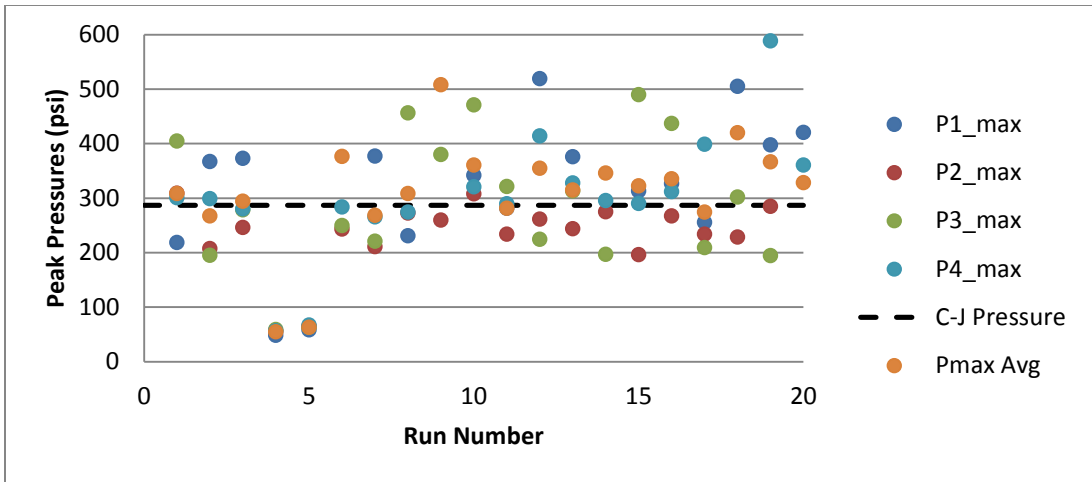


Figure 4.9 Measured peak pressures for each run of Case 2

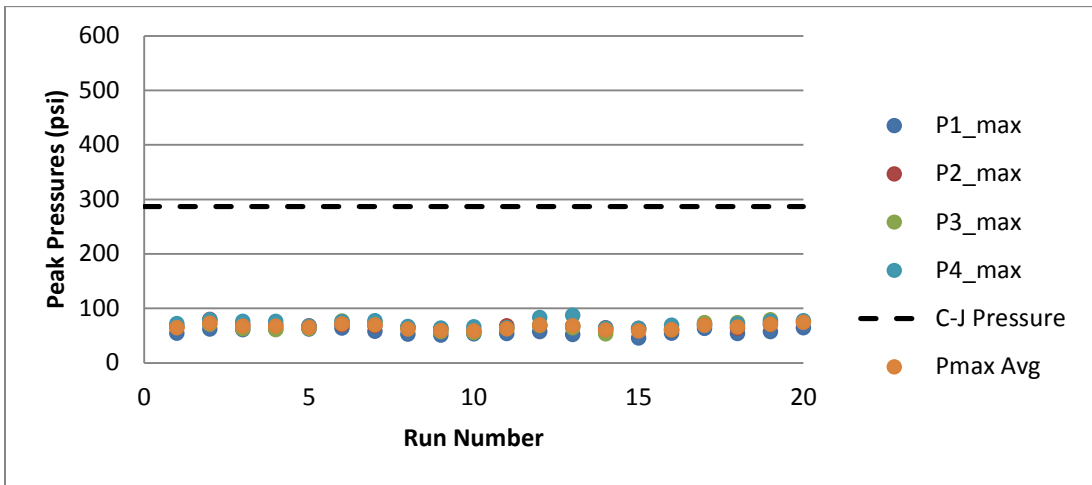


Figure 4.10 Measured peak pressures for each run of Case 3

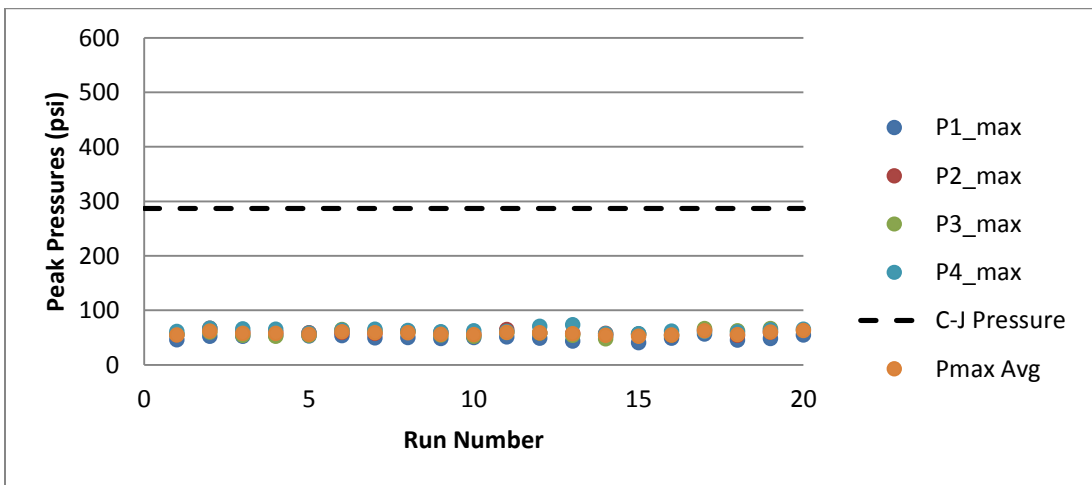


Figure 4.11 Measured peak pressures for each run of Case 4

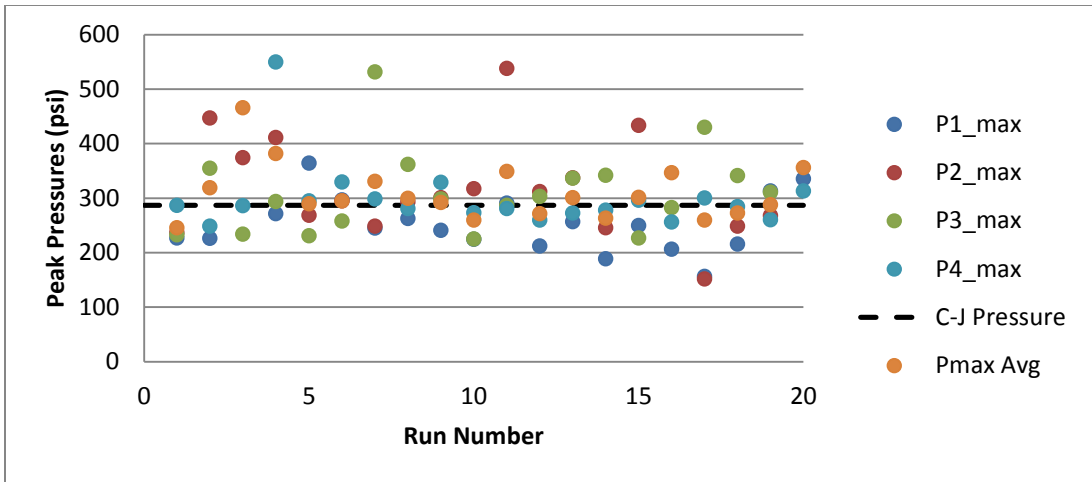


Figure 4.12 Measured peak pressures for each run of Case 5

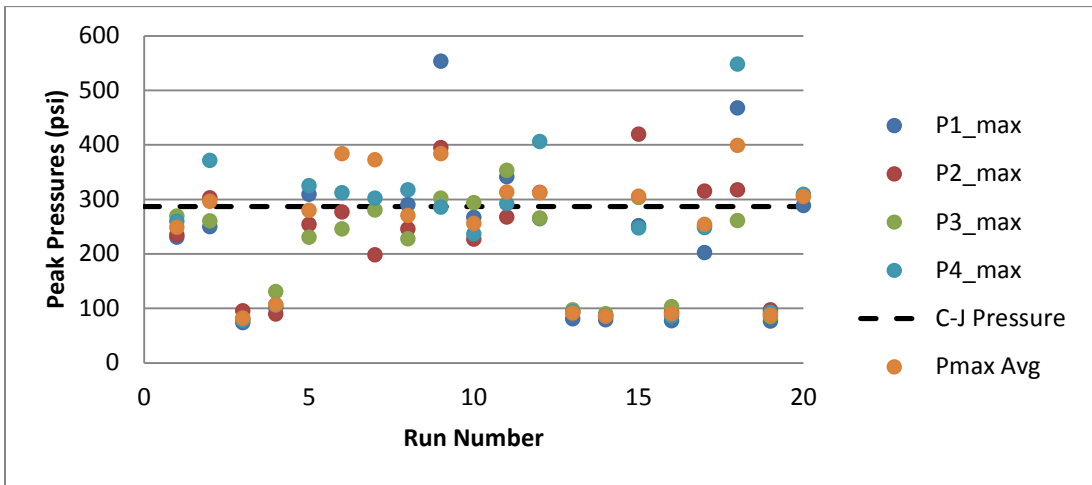


Figure 4.13 Measured peak pressures for each run of Case 6

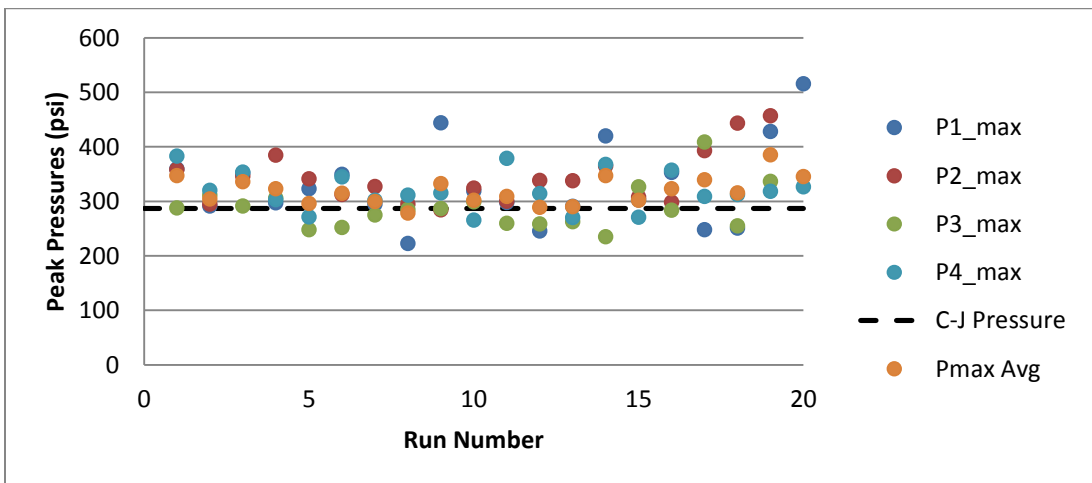


Figure 4.14 Measured peak pressures for each run of Case 7

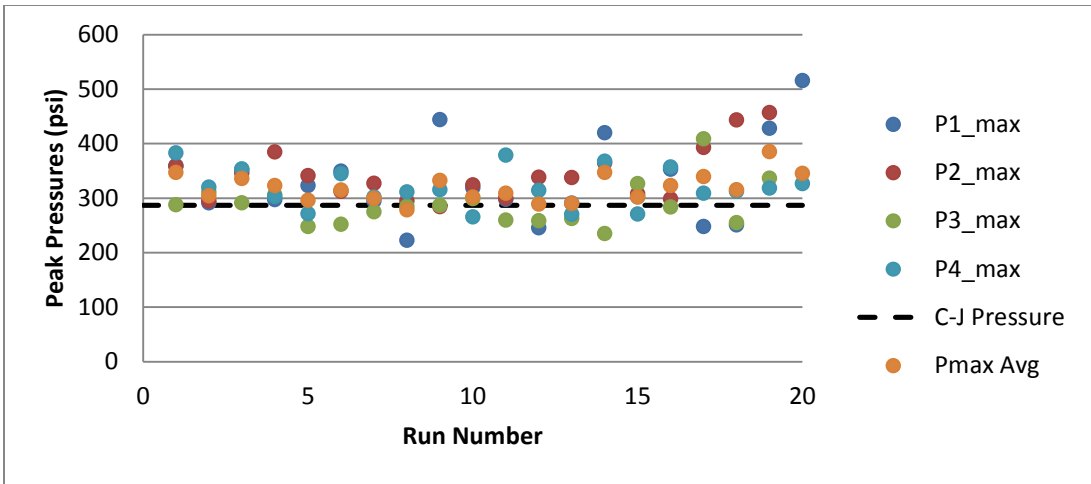


Figure 4.15 Measured peak pressures for each run of Case 8

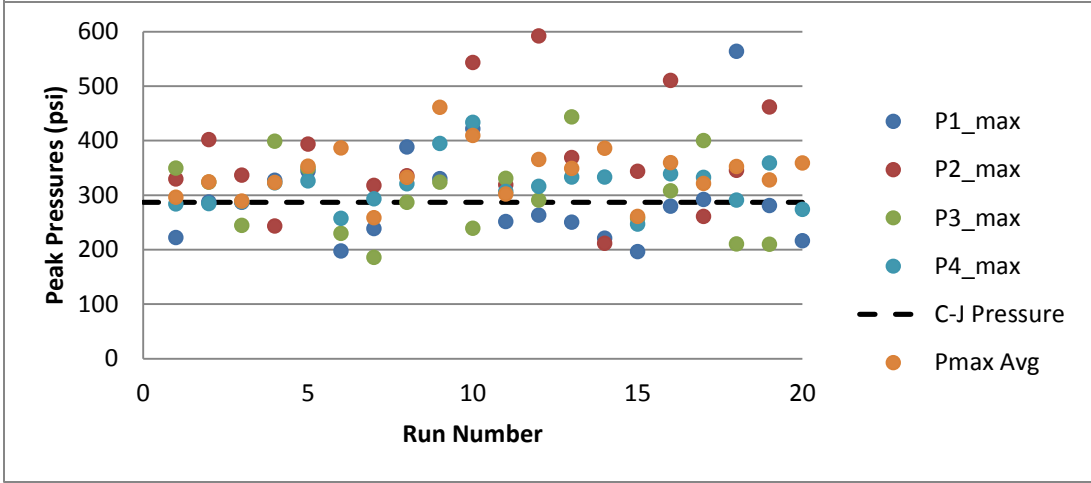


Figure 4.16 Measured peak pressures for each run of Case 9

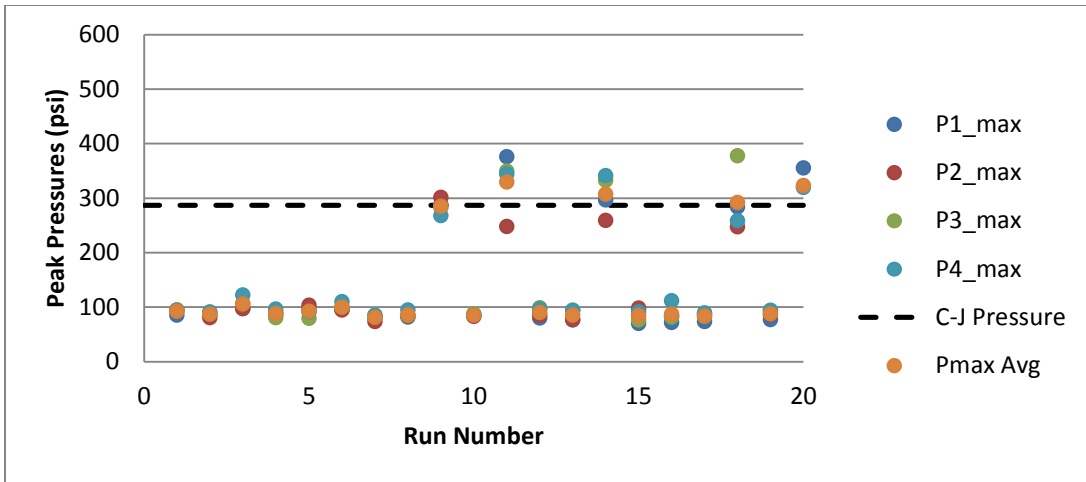


Figure 4.17 Measured peak pressures for each run of Case 10

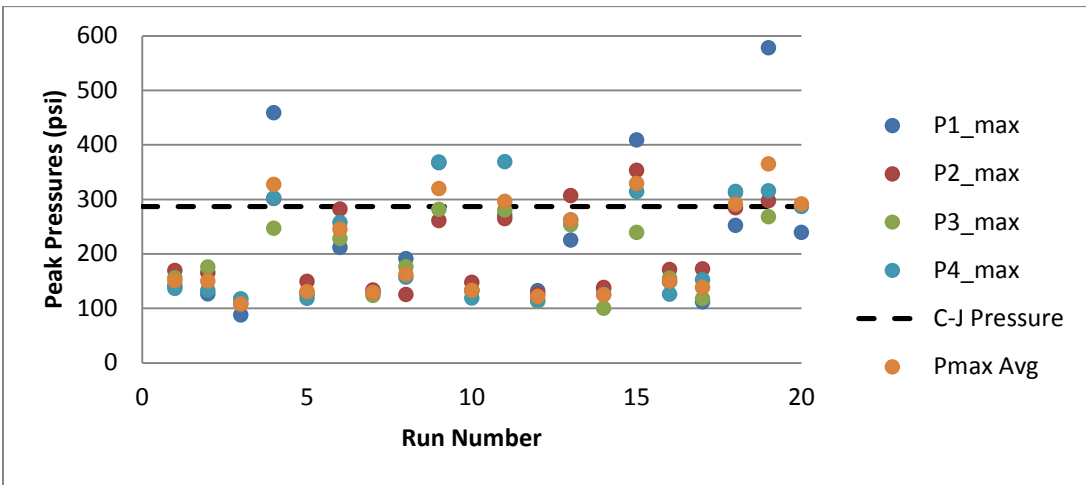


Figure 4.18 Measured peak pressures for each run of Case 11

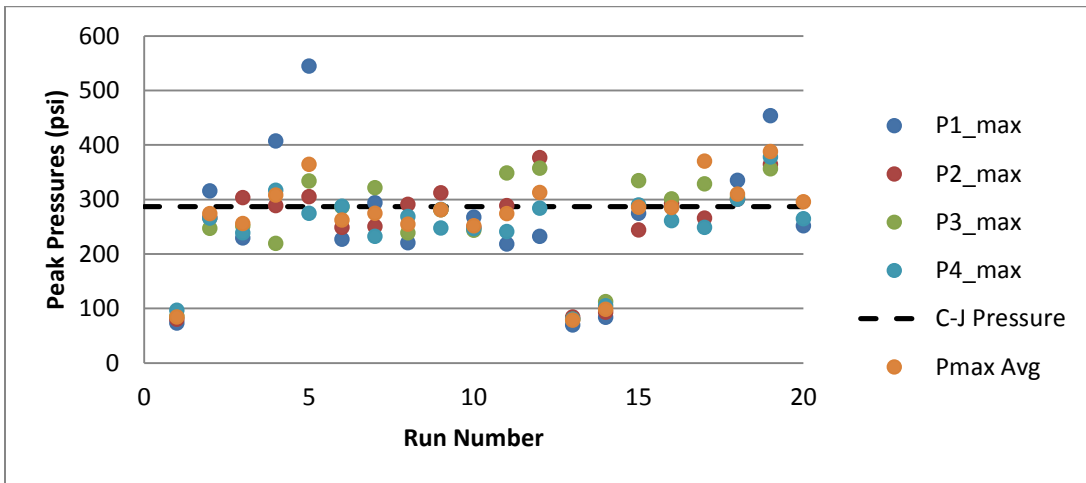


Figure 4.19 Measured peak pressures for each run of Case 12

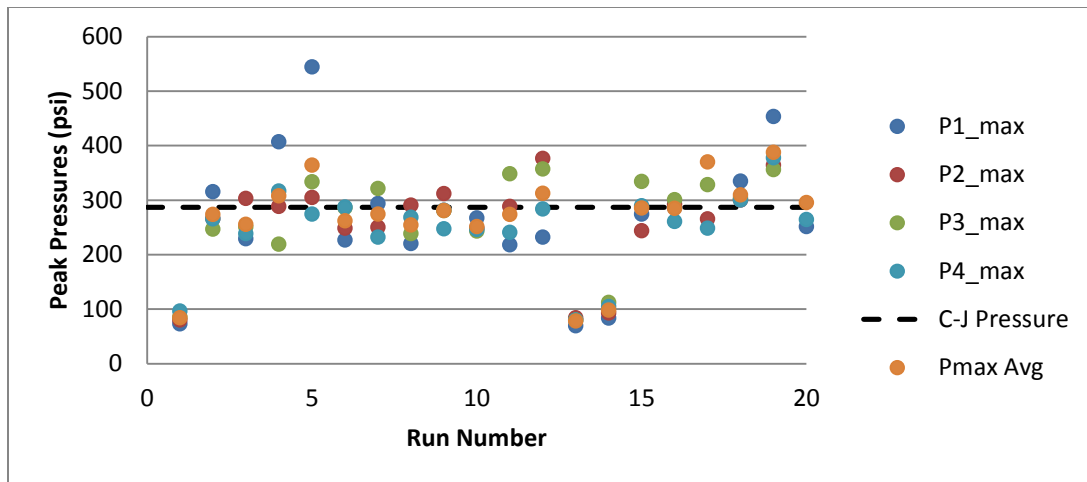


Figure 4.20 Measured peak pressures for each run of Case 13

Velocity Trends

The average velocities for each case, like the pressures, were all similar and fell within 10% of the expected C-J Velocity. When looking at the average velocity on a case by case basis as laid out in Table 4.2 there appears to be no correlation. However a higher success rate correlates with a lower standard deviation of velocities and this can be seen graphically in Figure 4.22 through Figure 4.34 with a focus on cases 5, 7, 8, and 9 since they had a 100% success rate and low variation in individual pressure measurements when compared to the other configurations. This is an important finding for looking at how variable blockage ratio affects the detonation transition and detonation performance. While the existing test rig is not capable of determining when the detonation transition occurs, it does show more consistencies with certain configurations.

Without the use of schlieren imagery or a similar imaging method to look at the shock-wave and combustion phenomena, it is difficult to say with certainty what the mechanism is for these consistencies. The simplest and most probable theory is that the detonation wave is highly unstable in cases of a larger deviation in velocity. It has been shown numerically and experimentally that in unstable detonations, local explosions may occur at triple points creating

highly irregular pressure fields that influence local velocity. As a part of this theory, is that the fuel-air mixture may not be uniformly mixed in some cases creating instabilities in combustion and therefore an unstable detonation wave. Since mixing has been a concern it is more than possible that certain configurations are more likely to promote uniform mixing. In studies varying the ratio of specific heats (γ) changing that value by a small amount (between 1.15 and 1.35) it has been shown to highly change the stability of the detonation wave (Khokhlov, Austin, Pintgen, & Shepherd, 2004). With ethylene at $\gamma = 1.24$ and air at $\gamma = 1.4$ with an equivalence ratio of 1.3, a mixture $\gamma = 1.38$ should give stable detonation waves unless there is a non-uniform mixture of reactants. This issue of mixing has been a persistent problem which is what drove changing the filling-firing cycle.

Initially it was thought a decreasing blockage ratio function such as cases 6, 7, 8, 9, and 11 would give the best performance due to higher turbulence earlier in the DDT process and fewer losses and a more open flow path toward the open end of the tube and in fact, these particular cases do hold the smallest deviation in velocities. This is ignoring success rate as a measure of performance since case 5 with an increasing blockage ratio had a 100% success rate. The decreasing blockage ratio functions do result in the smallest deviations in velocity as expected so the theory is plausible.

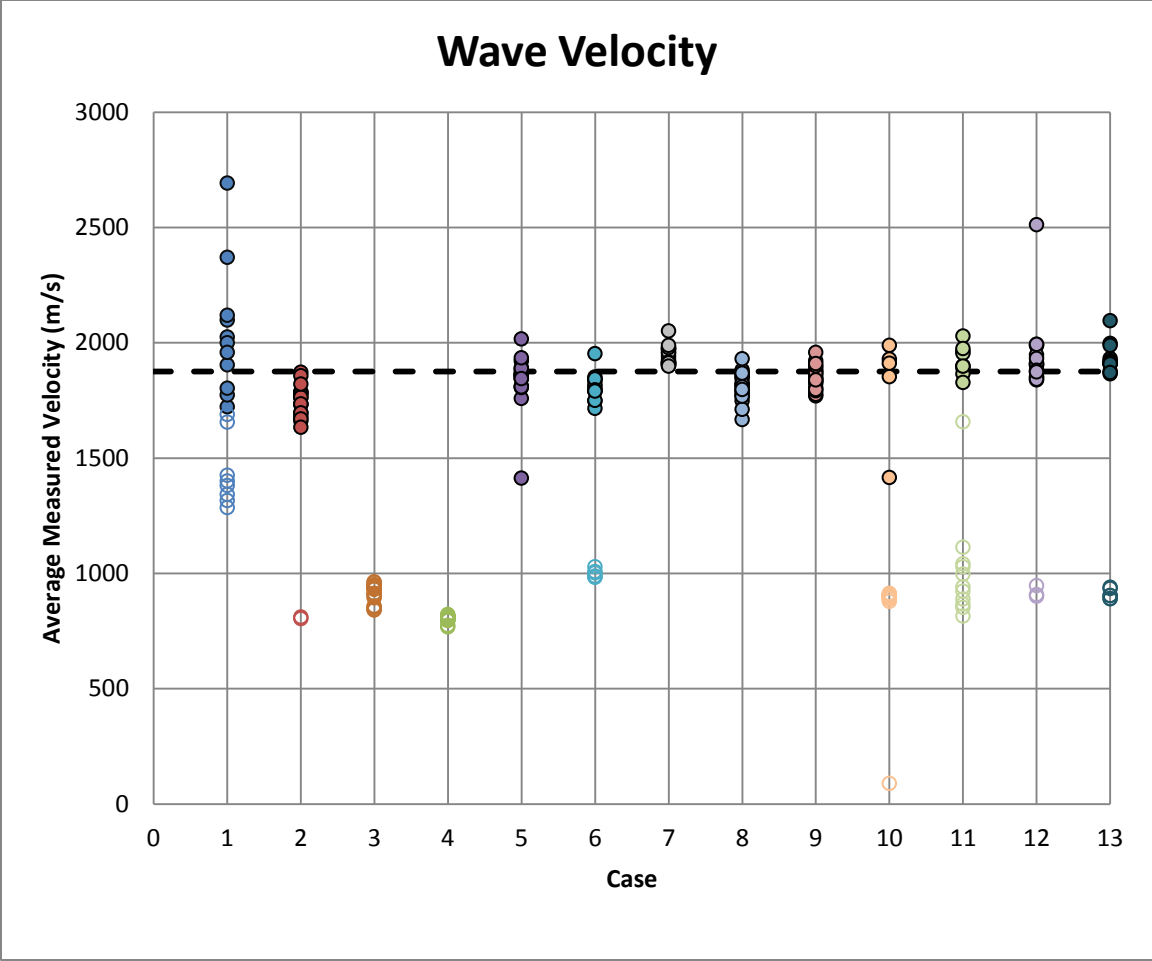


Figure 4.21 Average wave velocities for Firing Cycle 2

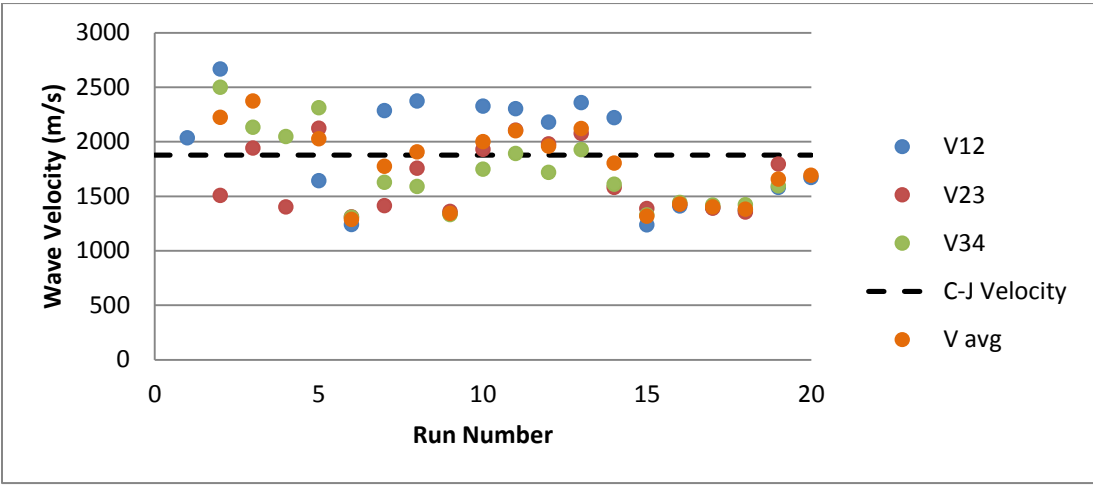


Figure 4.22 Measured wave velocities for each run of Case 1

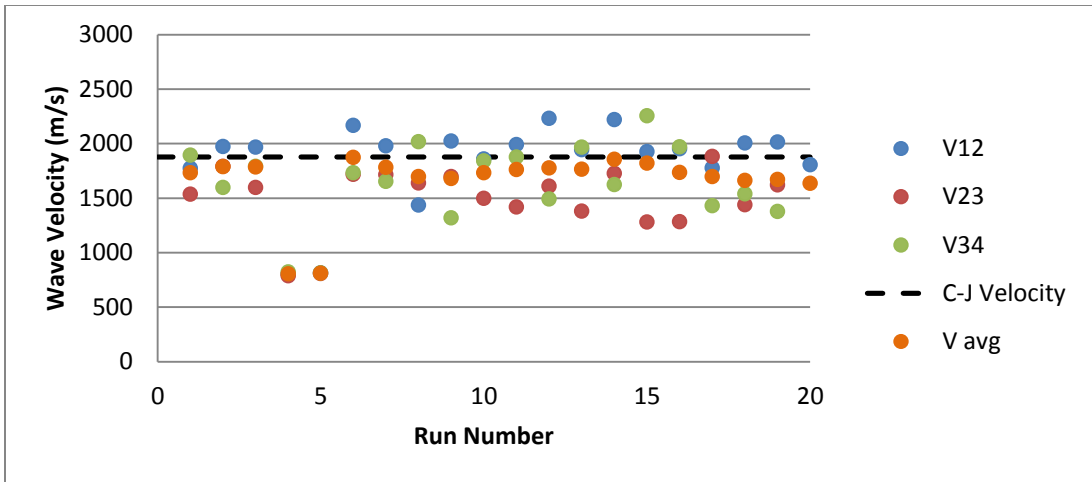


Figure 4.23 Measured wave velocities for each run of Case 2

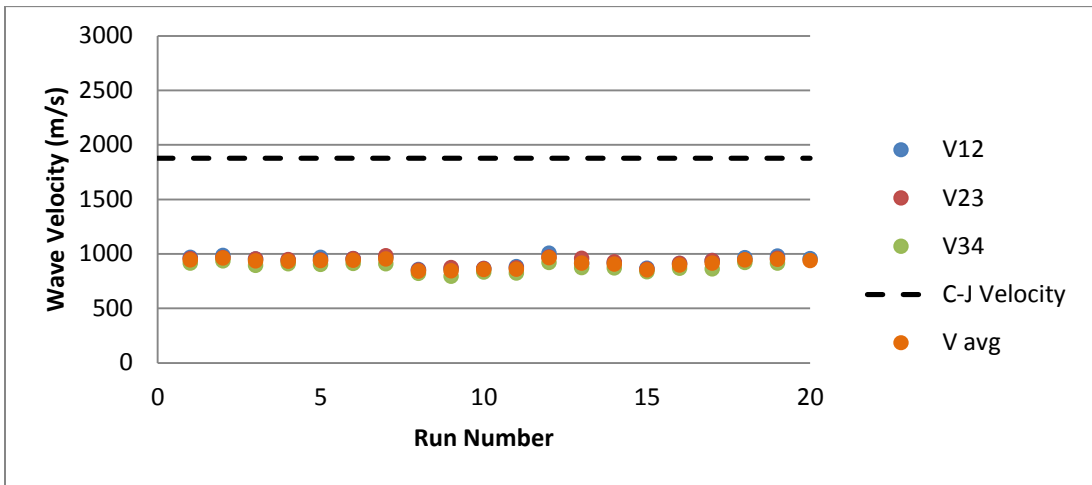


Figure 4.24 Measured wave velocities for each run of Case 3

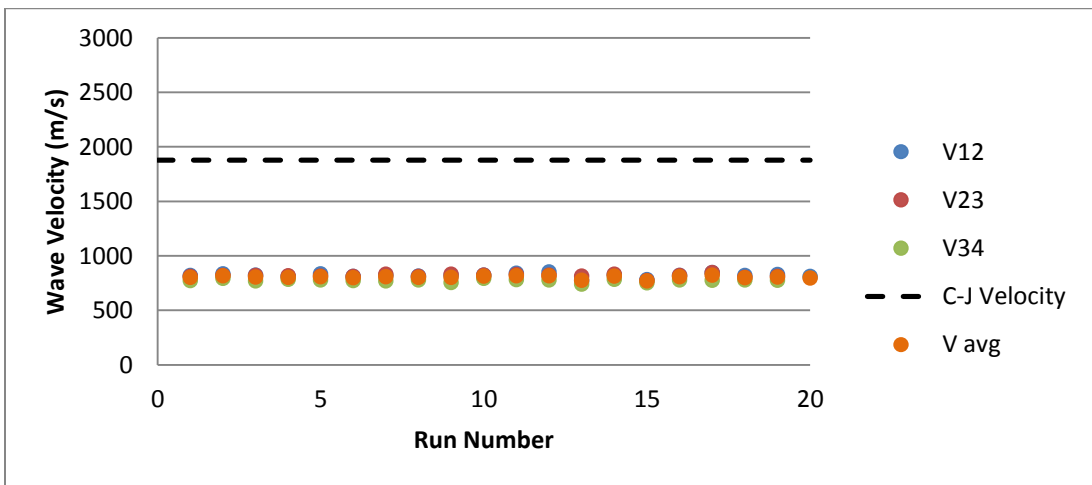


Figure 4.25 Measured wave velocities for each run of Case 4

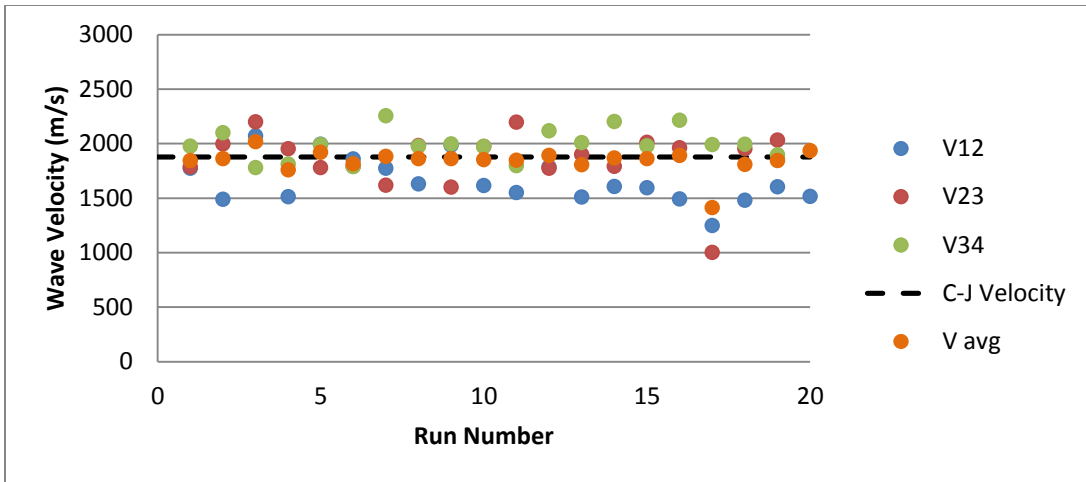


Figure 4.26 Measured wave velocities for each run of Case 5

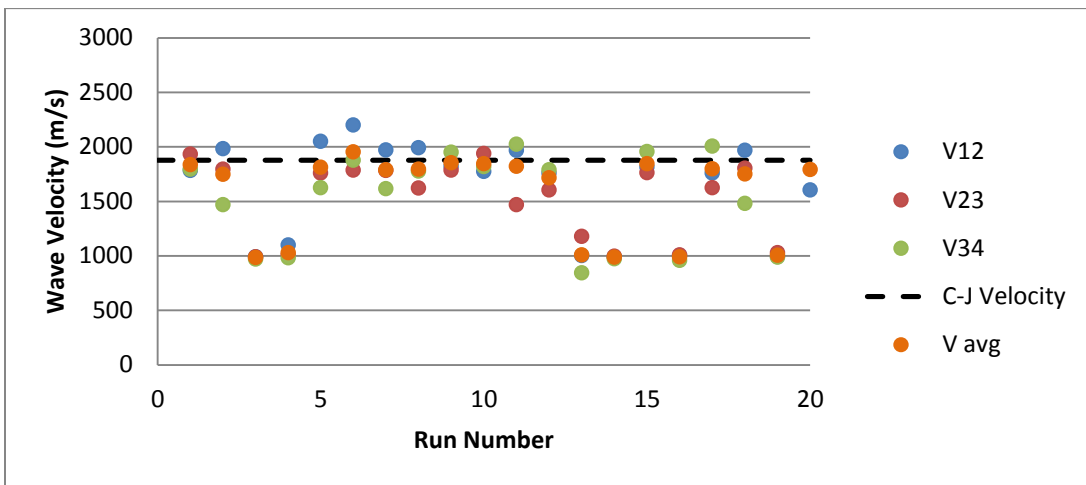


Figure 4.27 Measured wave velocities for each run of Case 6

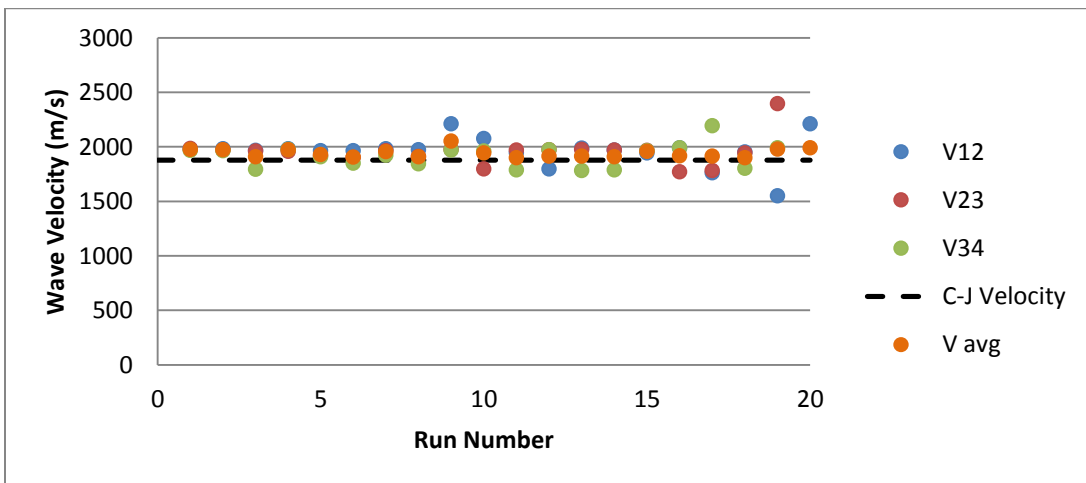


Figure 4.28 Measured wave velocities for each run of Case 7

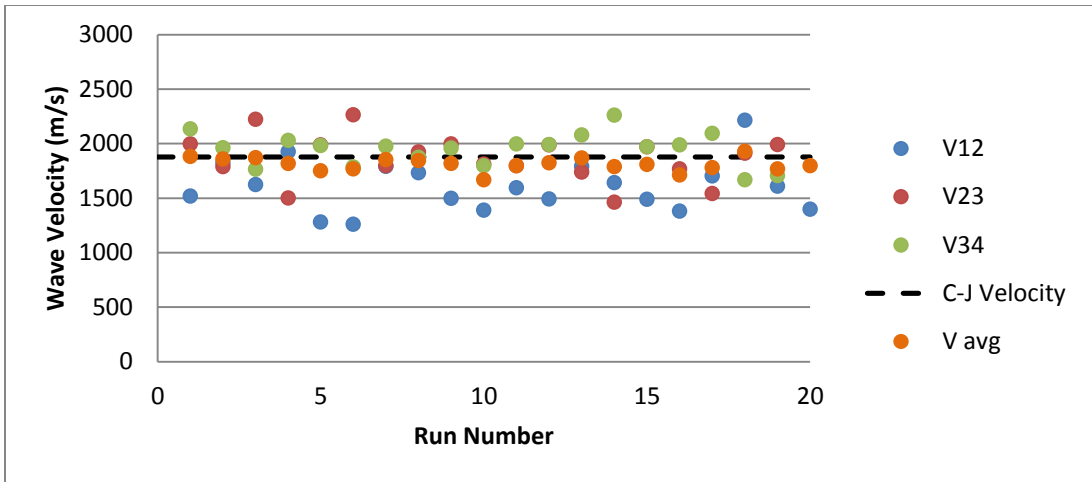


Figure 4.29 Measured wave velocities for each run of Case 8

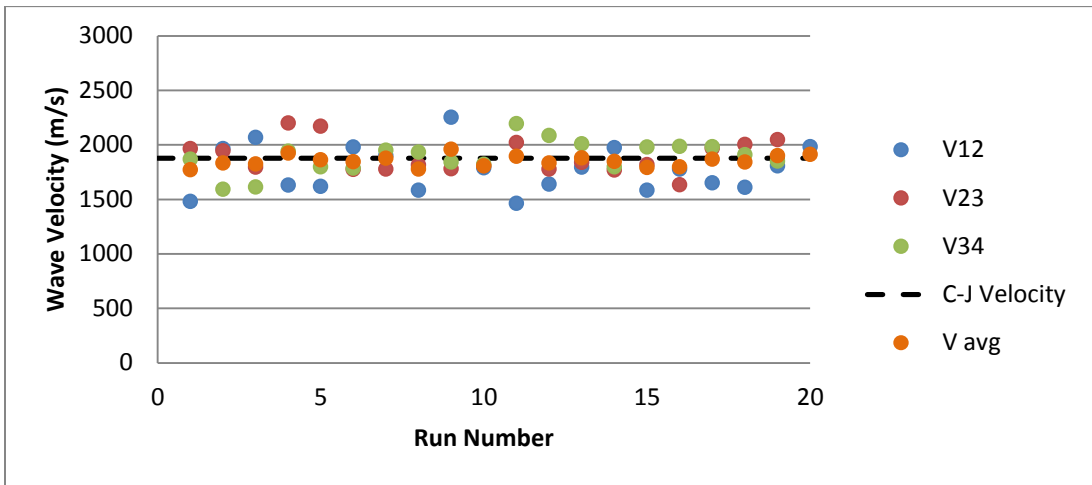


Figure 4.30 Measured wave velocities for each run of Case 9

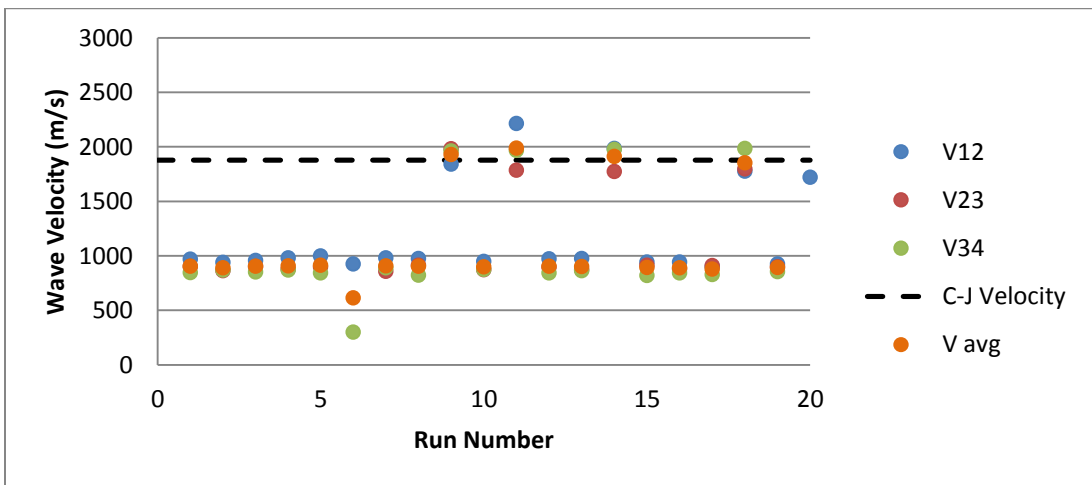


Figure 4.31 Measured wave velocities for each run of Case 10

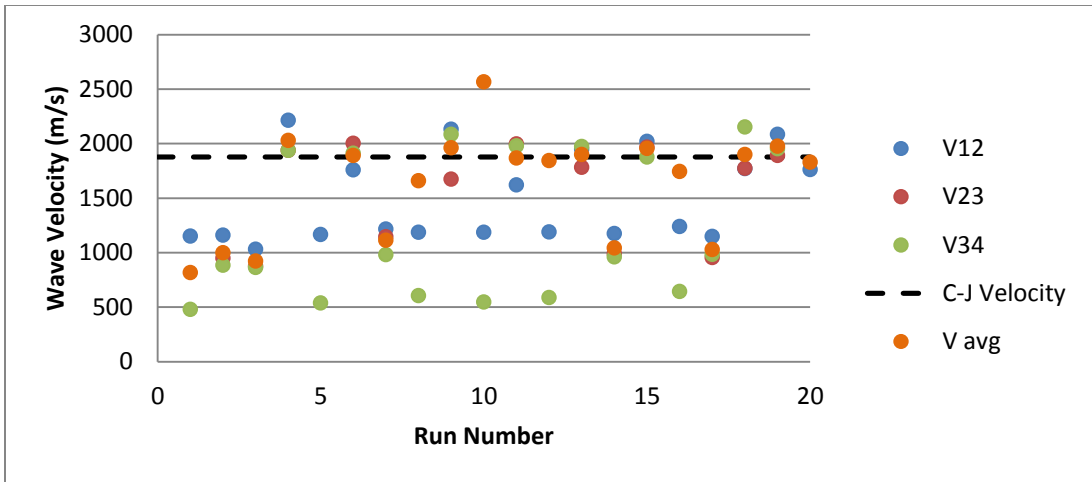


Figure 4.32 Measured wave velocities for each run of Case 11

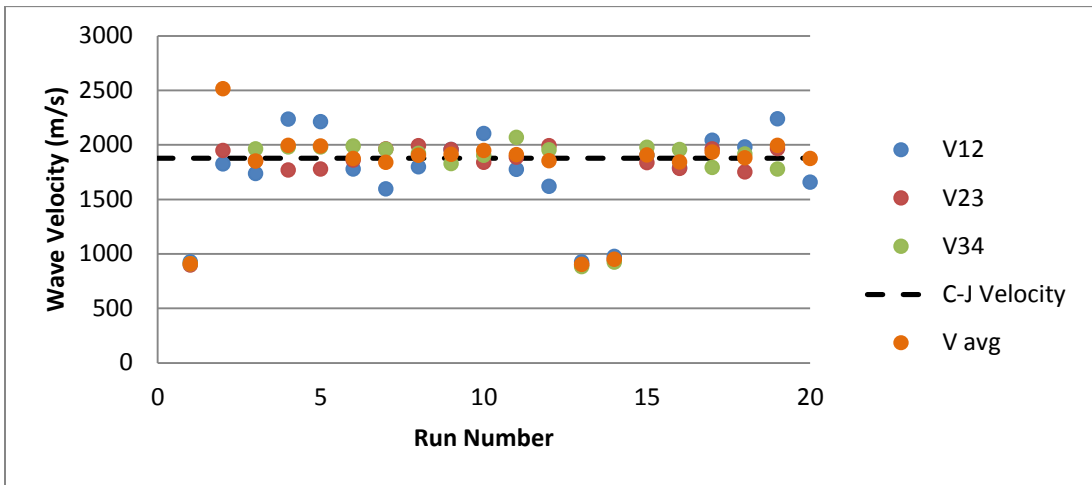


Figure 4.33 Measured wave velocities for each run of Case 12

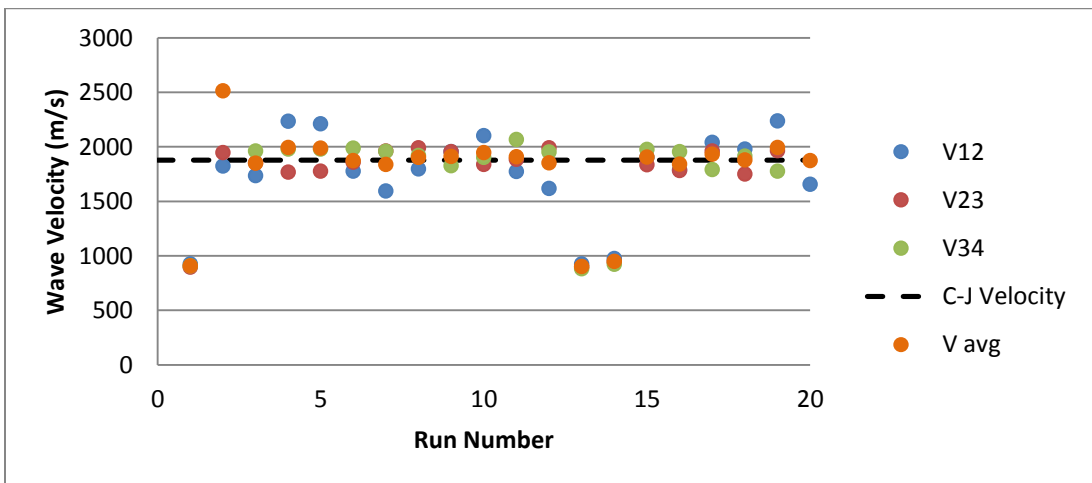


Figure 4.34 Measured wave velocities for each run of Case 13

5. CONCLUSIONS

5.1. Summary

There have been many numerical and experimental investigations into detonation transition mechanisms using regularly spaced obstacles. Many of these numerical investigations came to the same conclusion that obstacles affect the flame and shock differently where large blockage ratios are conducive to flame acceleration, they hinder the strength of shock. It has been the suggestion of these many studies to optimize geometry to increase the rate of flame acceleration and keep a strong shock by varying obstacle shape, pitch or blockage ratio over the length of a detonation tube.

The goal of this investigation was to identify an optimal blockage ratio function and correlation between variable blockage ratio and detonation performance characteristics. Therefore, thirteen configurations were tested that covered a wide range of blockage ratio function patterns. Two different firing cycles were used due to issues with mixing. The findings showed that there are variable blockage ratio functions that outperform the commonly used constant blockage ratio. These cases outperformed constant blockage ratios by percentage of successful detonations, peak pressure levels, wave velocities, as well as having a higher degree of predictability in performance due to less variability in pressures and velocities. This gives grounds for further investigation to further optimize variable blockage ratio. This can lead to shortened DDT sections and more consistent performance.

5.2. Recommendations

Monitoring Onset of Detonation Transition

While it is clear that certain blockage ratio functions produce better and more consistent results, these results would be more useful if the detonation transition was monitored over the length of

the tube. This could be done using schlieren photography or simply recording pressure and velocity measurements along the length of the detonation tube with more instrumentation. If detonation transition is monitored over the length of the tube, the DDT run-up time and distance would be known and would lead to shorter more efficient detonation tubes more practical to applications. A shorter DDT section will also increase frequency at which the detonation tube can be pulsed by reducing the time to inject the necessary amount of fuel and oxidizer.

Filling

The limiting factor in cycle frequency was the time pulse width of oxidizer as well as a spark delay time added to when filling was complete. To increase the cycle frequency these two issues should be addressed. The oxidizer (air) filling time is limited by the flow capacity of the injector solenoid as well as the number of injection locations. The injector solenoids are being operated at the maximum recommended pressure and this prompts the need for either more injector locations or injector solenoids with a higher flow rate capacity.

The injection site closest to the exit of the tube is effectively useless. With or without this injection site of both fuel and air the detonation performance remains the same. Since the injection site is downstream of the DDT section, with three other injection sites upstream, it is directly exhausting out of the detonation tube. It would be beneficial to move this injection site upstream of the DDT section to ensure all of the expected fuel and air move through the DDT section proceeding to mix.

Continued research with this test rig would benefit from using a flow meter to measure the flow through each injector. There are many fittings and exceedingly long hoses that both the fuel and air travel through that introduce losses. The injector curves were constructed assuming the exit of the injector is at atmospheric pressure and with the added pressure losses, the curve fits may not

be accurate and would benefit from a calibration factor found by measuring the actual flow and comparing it to the ideal flow based on injector curves.

Mixing

A proper and consistent fuel-air mixture is critical in the success and stability of detonation transition as shown to play a role in the performance of detonation transition in this study. In an ideal test rig, the fuel and oxidizer would be premixed and then injected into the detonation tube, however this can be dangerous in certain environments if the proper care and safety measures are not taken and would most likely require a test cell. In the case of the test rig used for this research, better mixing could be achieved if the fuel and oxidizer pulses were of the same duration. In experimentation, the fuel pressure was as low as possible to accurately inject a known amount in order to increase the pulse time. On the other hand, the air pressure was at the high limit of recommended pressures in order to decrease the pulse time. Even with these measures, the fuel pulse width was about one third that of the air. Even though the fuel pulse was centered within the air pulse, there is still a lot of time that only air is being injected which can lead to an irregular mixture. This extended oxidizer pulse time is likely why a spark delay time is required. The oxidizer most likely blows most of the fuel down the tube and a delay is needed while allowing for mixing and diffusion of fuel back towards the ignition end of the detonation tube.

Future Studies

With clear advantages of variable blockage ratios, more studies and refinements can take place to further optimize the DDT section. With the use of schlieren photography, more instrumentation and numerical analysis an optimum blockage ratio function can be attained that can produce consistent detonations with predictable performance characteristics. The predictability of these

characteristics can be paramount in detonation tubes that have the potential to be integrated with turbomachinery in order to extract power from the high enthalpy flow.

REFERENCES

- Brophy, C. M., Dvorak, W. T., Dausen, D. F., & Myers, C. B. (2012). *Detonation Initiation Improvements Usin Swept-Ramp Obstacles*. Orlando: 48th AIAA Aerospace Sciences Meeting.
- Bussing, T., & Pappas, G. (1994). *An Introduction to Pulse Detonation Engines*. Nevada: AIAA 94-0263. 32nd Aerospace Sciences Meeting & Exhibit.
- Bychkov, V., Akkerman, V., Valiev, D., & Law, C. K. (2010). Influence of Gas Compression on Flame Acceleration in Channels with Obstacles. *157*.
- California Institute of Technology. (n.d.). *Glossary on Explosion Dynamics*. Retrieved from Explosion Dynamics Laboratory:
<http://www.galcit.caltech.edu/EDL/projects/JetA/Glossary.html>
- Coleman, M. L. (2001). *Overview of Pulse Detonation Propulsion Technology*. Chemical Propulsion Information Agency.
- Davis, W. C., Craig, B. G., & Ramsay, J. B. (1965). Failure of the Chapman-Jouguet Theory for Liquid and Solid Explosives. *Phys. Fluids* 8.
- Endo, T., Kasahara, J., Matsuo, A., Inaba, K., & Sato, S. (2004). Pressure History at the Thrust Wall of a Simplified Pulse Detonation Engine. *AIAA Journal*, Vol.42: 1921-1930.
- Explosion Dynamics Laboratory. (2007, April 2). *Spectral Analysis for Cell Size Measurement*. Retrieved July 2012, from Explosion Dynamics Laboratory:
<http://www2.galcit.caltech.edu/EDL/CellImageProcessing/cellsize.html>
- Frolov, S. M. (2008). Fast Deflagration-to-Detonation Transition. *Russain Journal of Physical Chemistry B*, Vol. 2, No 3, pp. 442-455.

- Frolov, S. M., Aksenov, V. S., & Shamshin, I. O. (2007). Shock Wave and Detonation Propagation Through U-bend Tubes. *Proceedings of the Combustion Institute* 31.
- Frolov, S. M., Aksenov, V. S., & Skripnik, A. A. (2011). Detonation Initiation in a Natural Gas - Air Mixture in a Tube with a Focusing Nozzle. *Doklady Physical Chemistry*, Vol. 436, Pt 1, pp.10-14.
- Frolov, S. M., Basevich, V. Y., Aksenov, V. S., & Polikhov, S. A. (2003). Detonation Initiation by Controlled Triggering of Electric Discharges. *19*(4).
- Gamezo, V. N., Ogawa, T., & Oran, E. S. (2007). Numerical simulations of flame propagation and DDT in obstructed channels filled with hydrogen-air mixture. *31*(2).
- Gamezo, V. N., Ogawa, T., & Oran, E. S. (2009). *Deflagration-to-Detonation Transition in H₂-Air Mixtures: Effect of Blockage Ratio*. Orlando: 47th AIAA Aerospace Sciences Meeting.
- Gamezo, V. N., Ogawa, T., & Oran, E. S. (2009). *Deflagration-to-Detonation Transition in H₂-Air Mixtures: Effect of Blockage Ratio*. Orlando: 47th AIAA Aerospace Sciences Meeting.
- Gamezo, V. N., Ogawa, T., & Oran, E. S. (2012). The Influence of Chemical Kinetics on the Structure of Hydrogen-Air Detonations.
- Glassman, I., & Yetter, R. A. (2008). *Combustion*. San Diego: Elsevier Inc.
- Hsu, K., & Jemcov, A. (2000). Numerical Investigation of Detonation in Premixed Hydrogen-Air-Mixture - Assessment of Simplified Chemical Mechanisms.
- Ishii, K., & Tanaka, T. (2005). A Study on Jet Initiation of Detonation Using Multiple Tubes. *Shock Waves*, *14*(4).
- Jiang, Z., & Han, Z. -Y. (2005). *Shock Waves*. Springer.

- Kailasanath, K. (2009). *Research on Pulse Detonation Combustion Systems - A Status Report*.
Orlando: 47th AIAA Aerospace Sciences Meeting.
- Kaneshige, M., & Shepherd, J. E. (1999). *Detonation Database*. California Institute of
Technology. Explosion Dynamics Laboratory Report, Graduate Aeronautical
Laboratories.
- Khemani, H. (2009, December 17). *The Stoichiometric Air-Fuel Ratio*. Retrieved February 2,
2010, from Bright Hub:
<http://www.brighthub.com/engineering/mechanical/articles/15235.aspx#ixzz0eS3M9wMn>
- Khokhlov, A. M., Austin, J. M., Pintgen, F., & Shepherd, J. E. (2004). *Numerical study of the
detonation wave structure in ethylene-oxygen mixtures*. Reno: AIAA 2004-792. 32nd
Aerospace Sciences Meeting & Exhibit.
- Kuhl, A. L., Leyer, J. -C., & Borisov, A. A. (1993). Progress in Astronautics and Aeronautics.
Dynamic Aspects of Detonations, 153.
- Lam, M., Tillie, D., Leaver, T., & McFadden, B. (2004). *Pulse Detonation Engine Technology:
An Overview*. The University of British Columbia.
- Lee, J. H. (1977). Initiation of Gaseous Detonation. 75(104).
- Lee, J. H. (1984). Dynamic Parameters of Gaseous Detonations. 16.
- Li, J.-M., Lu, F. K., Panicker, P. K., & Wilson, D. R. (2007). Development of a Compact Liquid
Fueled Pulse Detonation Engine with Predetonator. Reno: 45th AIAA Aerospace
Sciences Meeting and Exhibit.
- Lieberman, M. (2003). *Flame, Detonation, Explosion - When Where and How They Occur*.
Uppsala: Department of Physics, Uppsala University.

- New, D. D., Lu, D. F., & Tsai, D. H. (n.d.). *Experimental Investigations on DDT Enhancements by Shchelkin Spirals in a PDE*. Retrieved from Aerodynamics Research Center:
http://arc.uta.edu/publications/pr_files/SchelkinSpiral.pdf
- Paxon, D. E., Schauer, F., & Hopper, D. (2009). *Performance Impact of Deflagration to Detonation Transition Enhancing Obstacles*. Orlando: 47th AIAA Aerospace Sciences Meeting.
- Radulescu, M. I. (1999). *Experimental Investigation of Direct Initiation of quasi-cylindrical detonations*. Montreal, Canada: Master's Thesis, McGill University.
- Romo, F. X. (2012). *Design, Construction, and Optimization of a Pulse Detonation Engine DDT Section*. Daytona Beach, FL: Embry-Riddle Aeronautical University.
- Saretto, S. R., Lee, S. -Y., Conrad, C., Brumberg, J., Pal, S., & Santoro, R. J. (n.d.). *Predetonator to Thrust Tube Detonation Transition Studies for Multi-Cycle PDE Applications*.
- Schultz, E., Wintenberger, E., & Shepherd, J. E. (1999). *Investigation of Deflagration to Detonation Transition for Application to Pulse Detonation Engine Ignition Systems*. Pasadena: California Institute of Technology.
- Shepherd, J. E. (2005). *Pulse Detonation Engines: Initiation, Propagation, and Performance*. Pasadena: Graduate Aeronautical Laboratories California Institute of Technology.
- Sinibaldi, J. O., Rodriguez, J., Channel, B., Brophy, C., Wang, F., Cathey, C., & Gundersen, M. A. (2005). *Investigation of Transient Plasma Ignition for Pulse Detonation Engines*. Tucson: 41st AIAA/ASME/SAE/ASEE Joint Propulsion Conference & Exhibit.
- Sun, G., Akbari, P., Gower, B., & Müller, N. (2012). *Thermodynamics of the Wave Disk Engine*. Atlanta: AIAA 2012-3704. 48th AIAA/ASME/SAE/ASEE Joint Propulsion Conference.

- Valiev, D., Bychkov, V., Akkerman, V., Law, C. K., & Eriksson, L.-E. (2010). Flame acceleration in channels with obstacles in the deflagration-to-detonation transition. *157*.
- Vasil'ev, A. A., Roy, G., Frolov, S., Santoro, R., & Tsyganov, S. M. (2003). Confined Detonations and Pulse Detonation Engines. In A. A. Vasil'ev, *Optimization of Accelerators of Deflagration-to-Detonation Transition* (pp. 41-48). Moscow: Torus Press.
- Vizcaino, J. (2013). *Investigation of Pulse Detonation Engines; Theory, Design, and Analysis*. Daytona Beach: Master's Thesis, Department of Aerospace Engineering, Embry-Riddle Aeronautical.
- Wintenberger, E. (2004). *Application of Steady and Unsteady Detonation Waves to Propulsion*. Pasadena: California Institute of Technology.
- Wintenberger, E., & Shepherd, J. E. (2004). *Detonation Waves and Pulse Detonation Engines*. California Institute of Technology Graduate Aeronautical Laboratories.
- Wintenberger, E., & Shepherd, J. E. (2005). *Thermodynamic Cycle Analysis for Propagating Detonations*. Pasadena: Graduate Aeronautical Laboratories California Institute of Technology.

APPENDIX A: CALCULATION OF FILLING PARAMETERS

Given: Ethylene + Air

Ethylene:

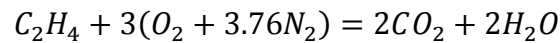
- Formula: C_2H_4
- Mass Fraction: 3.0
- Molecular Weight(kg/kmol): 28.054
- Density(kg/m³): 1.187
- Mass AFR (stoich): 13.353

Calculating density at specified conditions

C_2H_4 has a molecular weight of 28.054 g/mol, using ideal gas law we have $\frac{P}{RT} = \rho$, where

$$R = \frac{\bar{R}}{mw} \bar{R} = 8314 \frac{j}{gmol K}$$
$$\rho = \frac{101325 Pa}{\frac{8314}{28.054} * 288.15} = 1.187 \frac{kg}{m^3}$$

Volumetric Air – to – Fuel Ratio (AFR) is simply the ratio of the number of moles in a balanced chemical equation, i.e.



And the Volumetric AFR is then for pure oxygen is

$$\frac{3}{1}$$

To find AFR by Mass

$$\frac{3 mw_{O_2}}{1 mw_{C_2H_4}} = 3 * \frac{28.97}{28.054} * \frac{1}{0.232} = 13.353$$

*Note we use divide by 0.232 because air is roughly 23.2% oxygen by mass.

To determine mass of air required to fill volume:

Total mass of mixture is then equal to

$$m_{mix} = \rho_{mix} V_{mix}$$

Where V_{mix} is equal to the tube volume

Noting that $AFR = \frac{m_{Air}}{m_{Fuel}}$ and $m_{mix} = m_{Air} + m_{Fuel}$ we have

$$m_{mix} = (AFR * m_{Fuel}) + m_{Fuel}$$

Or

$$m_{mix} = m_{Fuel}(AFR + 1)$$

Solving for m_{Fuel} we get:

$$m_{Fuel} = \frac{m_{mix}}{(AFR + 1)}$$

Accordingly m_{Air} is simply:

$$m_{Air} = m_{Fuel} * AFR$$

To calculate necessary pulse width for the fuel and air injectors one must reference the mass vs. time curves provided by the manufacturer. For example, if we are to use a combination of ethylene and air at 29 psi_g (200 kPa_g) and 87 psi_g respectively (600 kPa_g) to deliver 160 mg of air and 50 mg of fuel per injector. We simply reference the injector curves (shown in Figure 7.1, Figure 7.2, and Figure 7.3) using the required mass in milligrams and pressure to find the required pulse width of air to be roughly 18 ms and fuel to be 14 ms. Unfortunately no injector curves were given for ethylene. For ethylene, the values were interpolated between methane and LPG based on gas density.

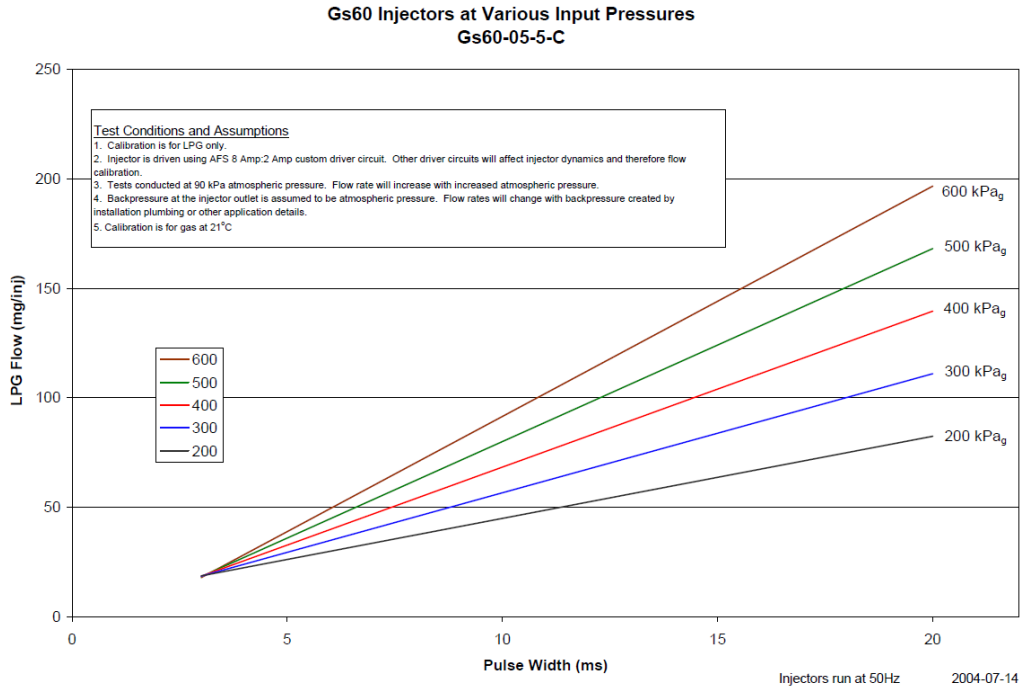


Figure 7.1: Mass vs. Pulse Width curves for Propane

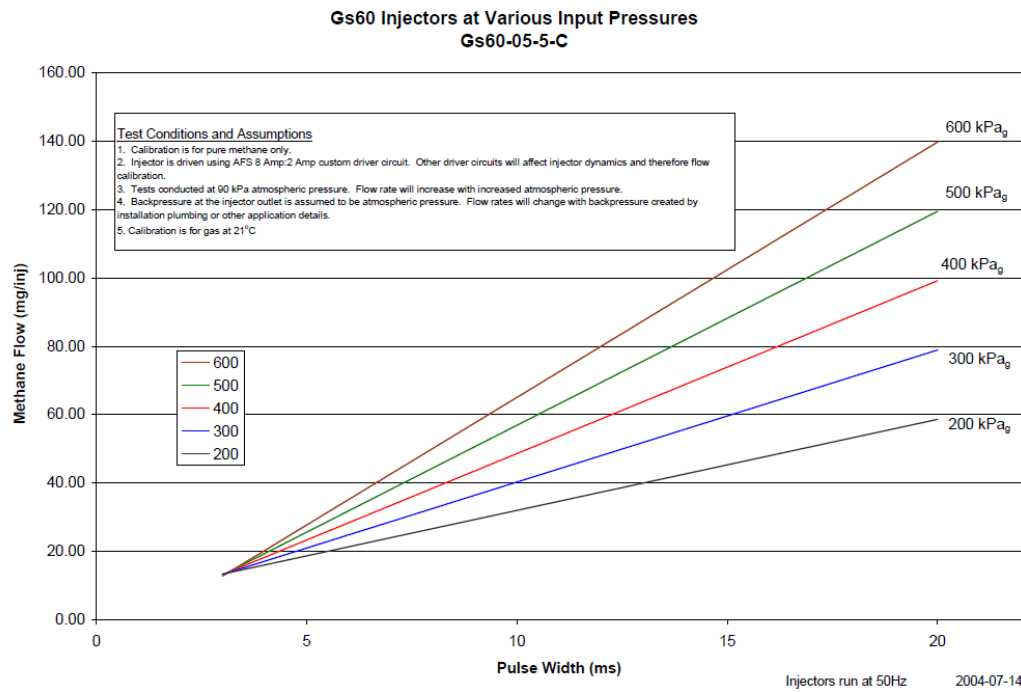


Figure 7.2 Mass vs. Pulse Width curves for Methane

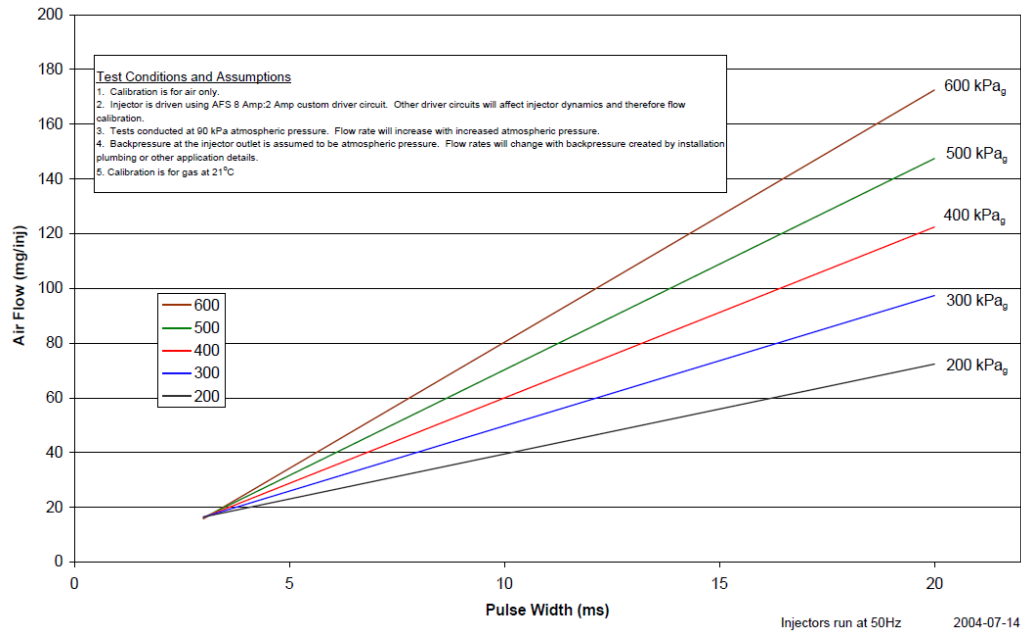
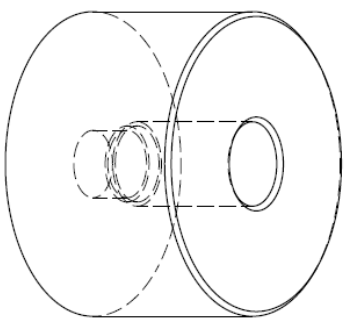
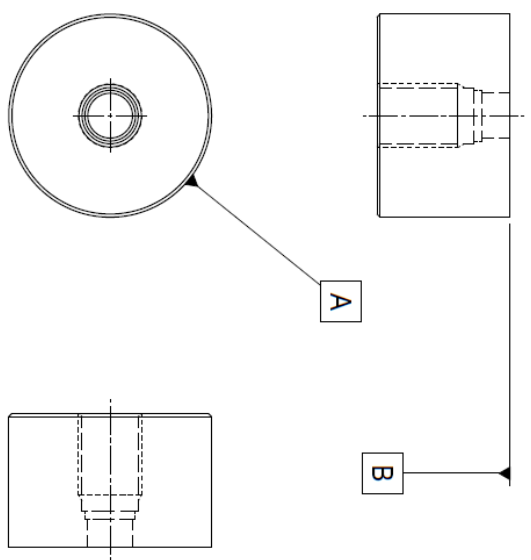


Figure 7.3: Mass vs. Pulse Width curves for Air

APPENDIX B: DRAWINGS AND DIAGRAMS

THIS DRAWING AND/OR ANY OF THE EXCLUSIVE PROPERTY OF DANIEL STEVENS, INC. IS UNCLASSIFIED AND NOT CONTROLLED. IT IS THE PROPERTY OF DANIEL STEVENS, INC. AND IS NOT TO BE REPRODUCED, COPIED, OR TRANSMITTED IN ANY FORM OR BY ANY MEANS, ELECTRONIC OR MECHANICAL, INCLUDING PHOTOCOPYING, RECORDING, OR BY ANY INFORMATION STORAGE AND RETRIEVAL SYSTEM, WITHOUT PERMISSION IN WRITING FROM DANIEL STEVENS, INC.

- NOTES: 1. UNLESS OTHERWISE SPECIFIED:
 -DRAWING INTERPRETED PER ANSI Y14.5M-1994
 -CORNERS TO HAVE FILLETS 1/64"
 -TOTAL RIMOUT OF ALL DIAMETERS RELATIVE TO [A] SHALL NOT EXCEED 1/16"
 2. MATERIAL: COLD ROLLED STEEL ROD (PROVIDED)



Isometric view

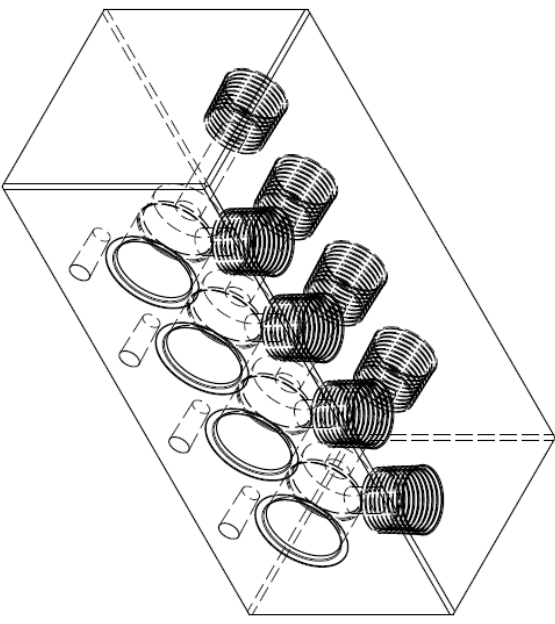
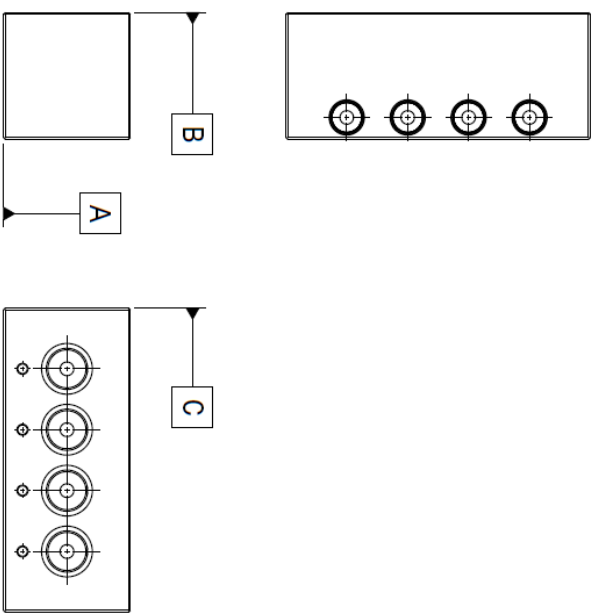
REVISIONS		
REV	DESCRIPTION	DATE
IR		

UNLESS OTHERWISE SPECIFIED DIMENSIONS ARE IN INCHES DECIMALS: 0.01 ANGLES: XX° ± Y' ± Z"		DATE 07 MAY 2015	DRAWN D. STEVENS	
THIRD ANGLE PROJECTION		DATE 17 MAR 2015	CHECKED JEFF VIZCAINO	
APPROVED		DATE 17 MAR 2015	DESIGNED DANIEL STEVENS	
TITLE DES ENGINEERING PRESSURE SENSOR PLUG PRE-WELDED		DATE 17 MAR 2015	SCALE NONE	
CAGE CODE N/A		DATE 17 MAR 2015	REVISION IR	
SIZE B		DATE 17 MAR 2015	DRAWN BY JPDE 0001	

SOLID MODEL:
 APPLICATION: CATIA V5R20
 CATIA MODEL FILE NAMES: N/A
 CATIA MODEL FILE DATE: N/A

THIS DRAWING AND/OR DATA IS THE EXCLUSIVE PROPERTY OF DANRELL STEVENS, INC. IT IS TO BE USED ONLY FOR THE PROJECT AND/OR FOR WHICH IT WAS PREPARED. NO PARTS OR COMPONENTS HAVE BEEN ENTERED INTO THE SMALL PARTS AND SUPPLIERS CATALOG, OR LISTED IN THE SMALL PARTS AND SUPPLIERS CATALOG. ANY REPRODUCTION OF THIS DRAWING WITHOUT THE EXPRESS WRITTEN AUTHORIZATION FROM DANRELL STEVENS, INC. IS PROHIBITED.

- NOTES: 1. UNLESS OTHERWISE SPECIFIED:
 -DRAWING INTERPRETED PER ANSI Y14.5M-1994
 -CORNERS TO HAVE FILLETS 1/64"
 2. MATERIAL: ALUMINUM 2.5 X 2.5 IN BLOCK 6061 (PROVIDED)



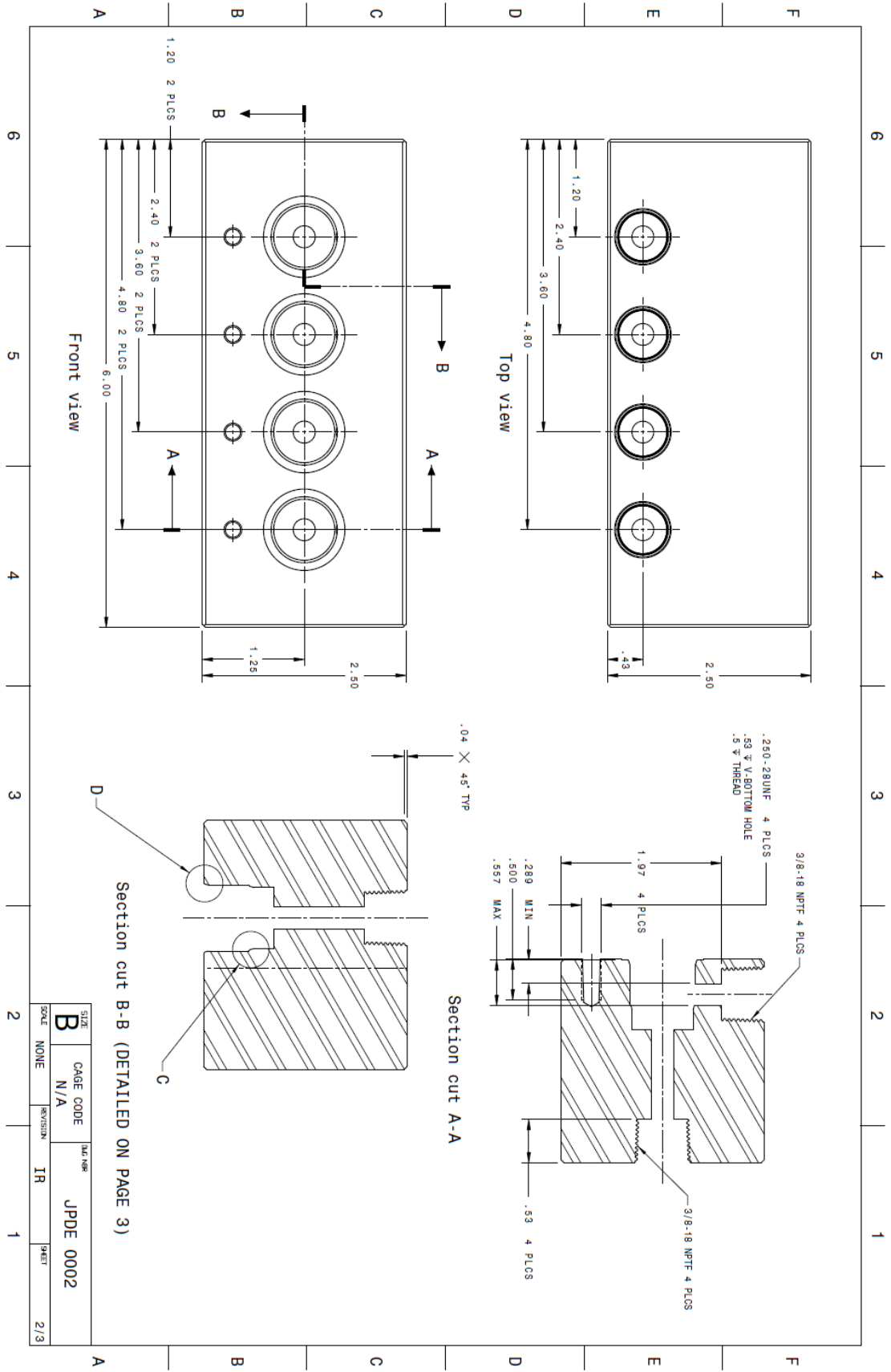
Isometric view

SOLID MODEL:
 APPLICATION: CATIA V5R20
 CATIA MODEL FILE NAMES: N/A
 CATIA MODEL FILE DATE: N/A

6 5 4 3 2 1

REVISIONS		
REV	DESCRIPTION	DATE
IR		

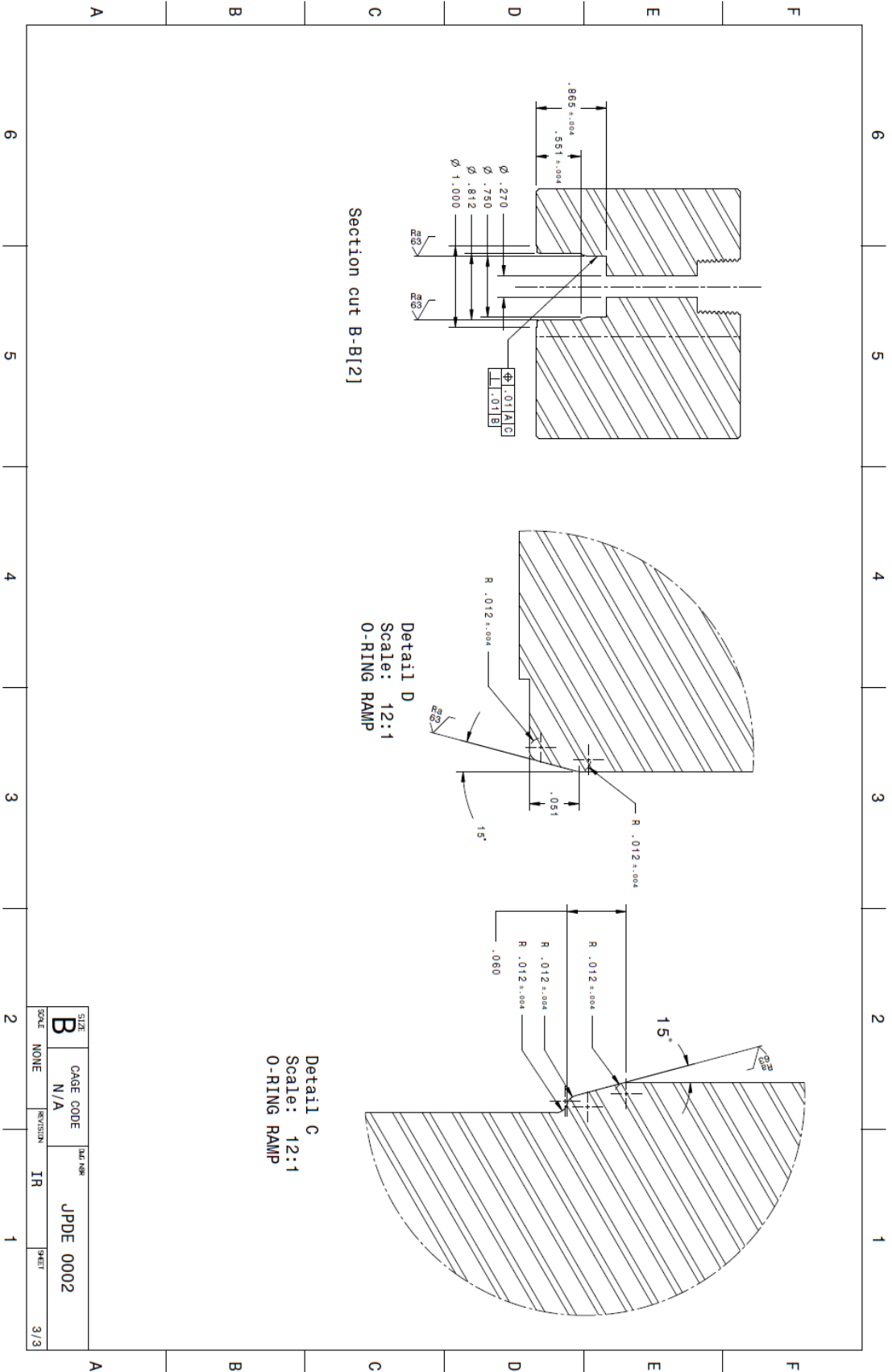
UNLESS OTHERWISE SPECIFIED DIMENSIONS ARE IN INCHES DECIMALS - FRACTIONS ANGULAR .XX +.01 X -.01 X +.2° .XXX DO NOT SCALE DRAWING 0.5"		DATE 07 MAY 2012	TITLE DES ENGINEERING
THIRD ANGLE PROJECTION	DESIGNER DANRELL STEVENS	DATE 08 MAY 2012	SIZE B
	PROPOSED ENGINEER	DATE 08 MAY 2012	CAGE CODE N/A
		SCALE NONE	REV. NO. 1
		REVISION IR	DATE 1/3



SIZE	B	CAGE CODE	N/A	3RD YEAR	JPDE 0002
SCALE	NONE	REVISION	IR	9/87	2/3

Section cut B-B (DETAILED ON PAGE 3)

Section cut A-A



PROPRIETARY NOTICE
 THIS DRAWING AND/OR DATA IS THE EXCLUSIVE PROPERTY OF DANIEL STEVENS, AND IS NOT TO BE REPRODUCED, COPIED, OR TRANSMITTED IN ANY FORM OR BY ANY MEANS, ELECTRONIC OR MECHANICAL, INCLUDING PHOTOCOPYING, RECORDING, OR BY ANY INFORMATION STORAGE AND RETRIEVAL SYSTEM, WITHOUT PERMISSION IN WRITING FROM DANIEL STEVENS.

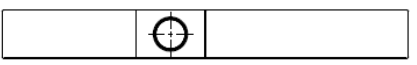
NOTES: 1. UNLESS OTHERWISE SPECIFIED:
 -DRAWING INTERPRETED PER ANSI Y14.5M-1994
 -ALL SURFACES SHALL NOT EXCEED 124 MICRONS RA (MEASURED I.A.W. ASME B46.1)
 -BREAK SHARP EDGES .003 - .008
 -TOTAL RIMOUT OF ALL DIAMETERS RELATIVE TO A SHALL NOT EXCEED .005

2. MATERIAL: STAINLESS STEEL 304 (PROVIDED)

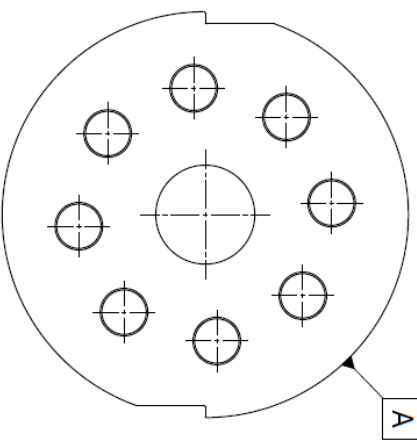
REVISIONS			
REV	DESCRIPTION	DATE	APPROVED
IR			



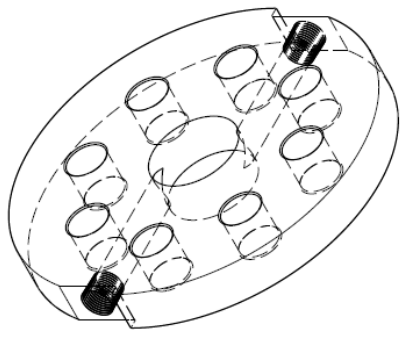
Top view



Right view



Front view

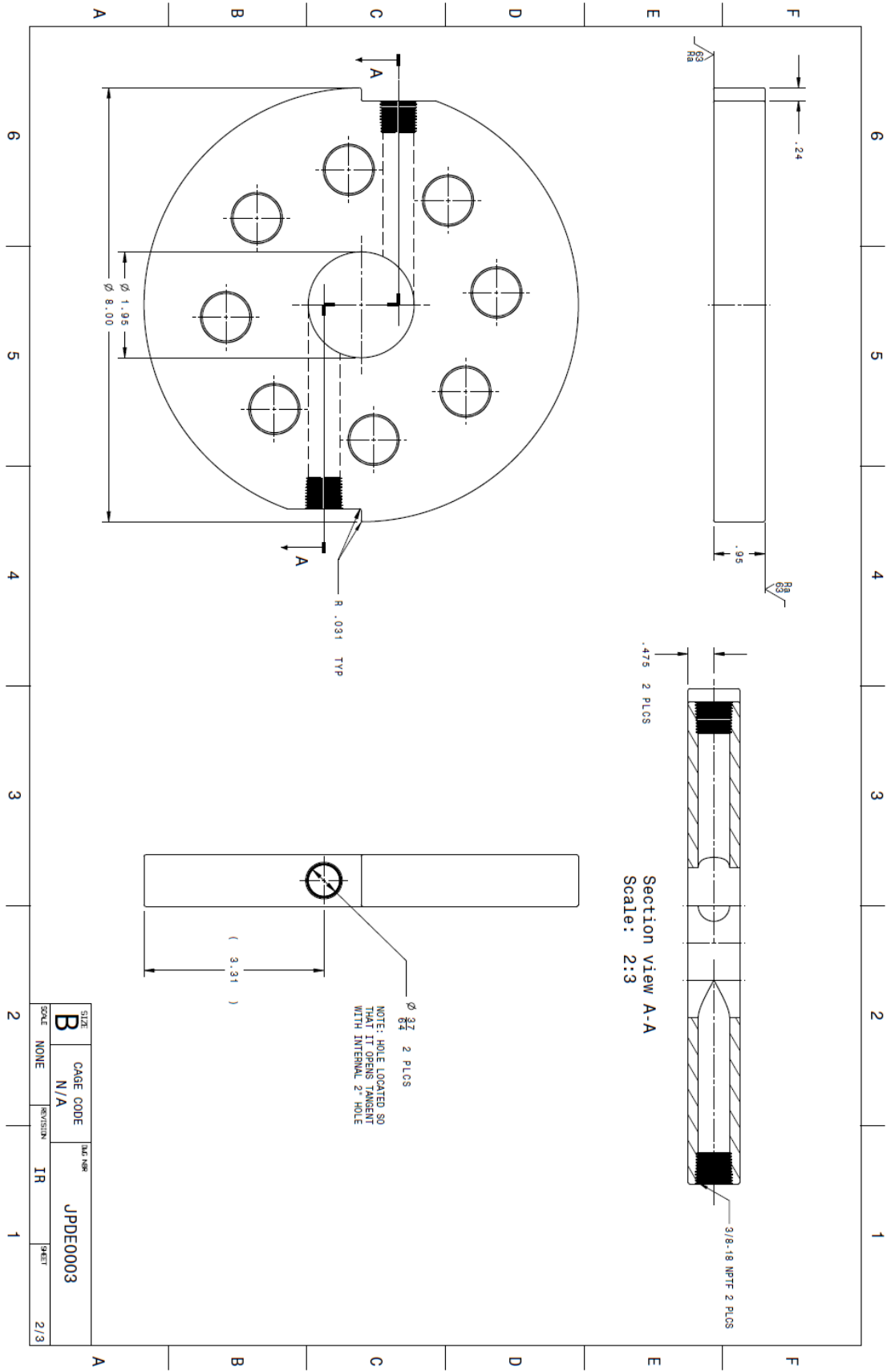


Isometric view
 Scale: 1:2

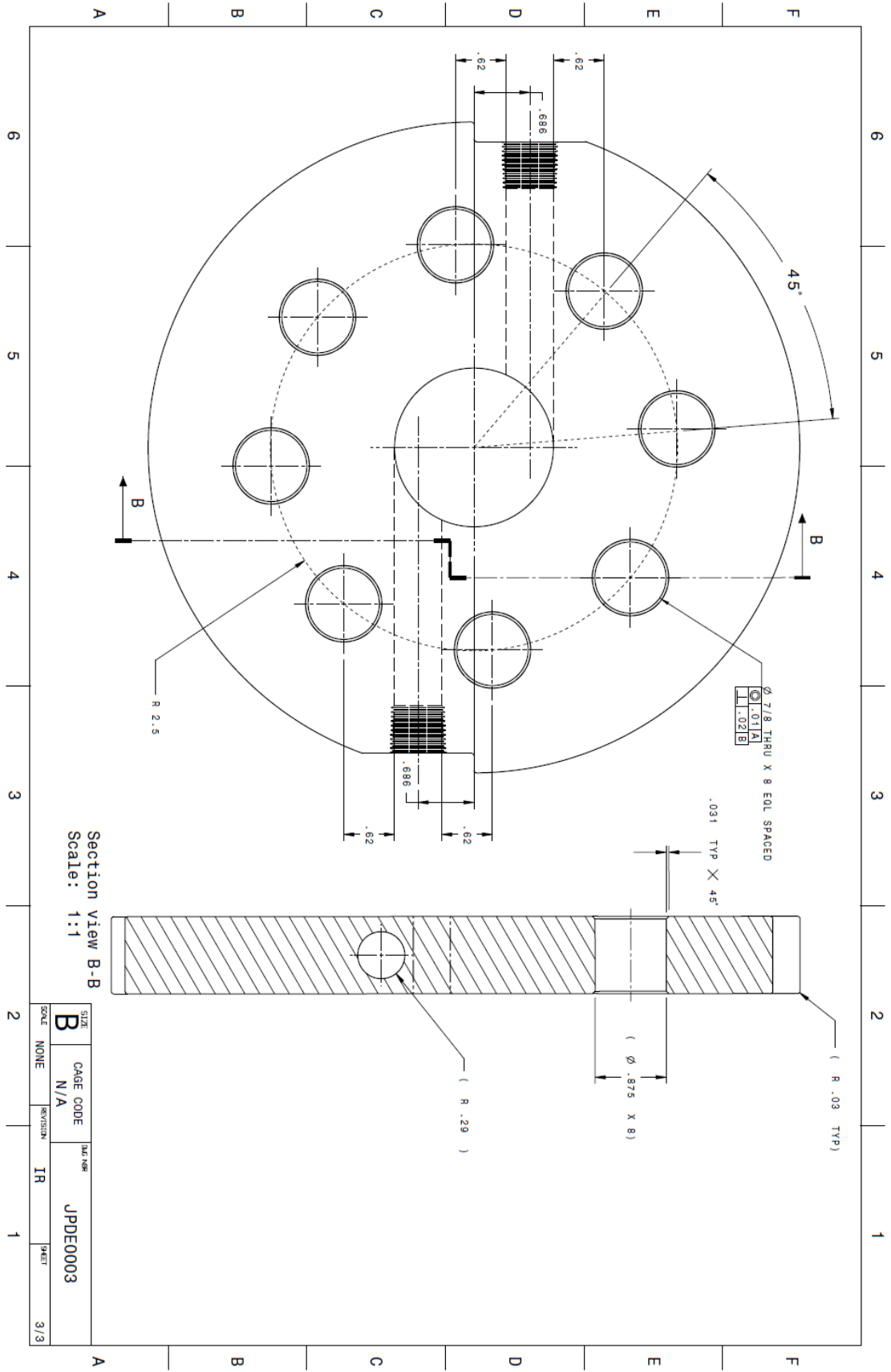
SOLID MODEL:
 APPLICATION: CATIA V20
 CATIA MODEL FILE NAMES: N/A
 CATIA MODEL FILE DATE: N/A

UNLESS OTHERWISE SPECIFIED DIMENSIONS ARE IN INCHES		DECIMALS		ANGULARS	
.XX	+/- 0.01	X'	+/- 2"	DO NOT SCALE DRAWING	
.XXX	DO NOT SCALE DRAWING	THIRD ANGLE PROJECTION			
DESIGNER: DARRELL STEVENS		CHECKED: JEFF VIZCAINO		APPROVED: ENGINEER	
DATE: 08 MAY 2012		DATE: 08 MAY 2012		DATE: 08 MAY 2012	
TITLE: DES ENGINEERING		SIZE: B		CAGE CODE: N/A	
INJECTOR PLATE W SWIRL		SCALE: NONE		REVISON: IR	
JPDE 0003		1/3			

6 5 4 3 2 1

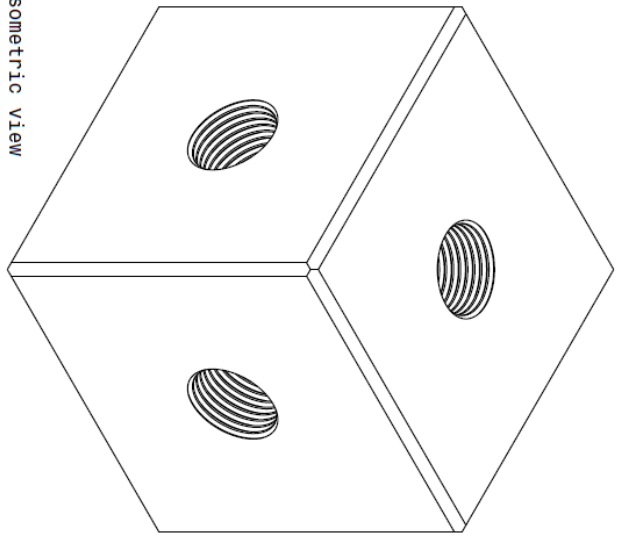
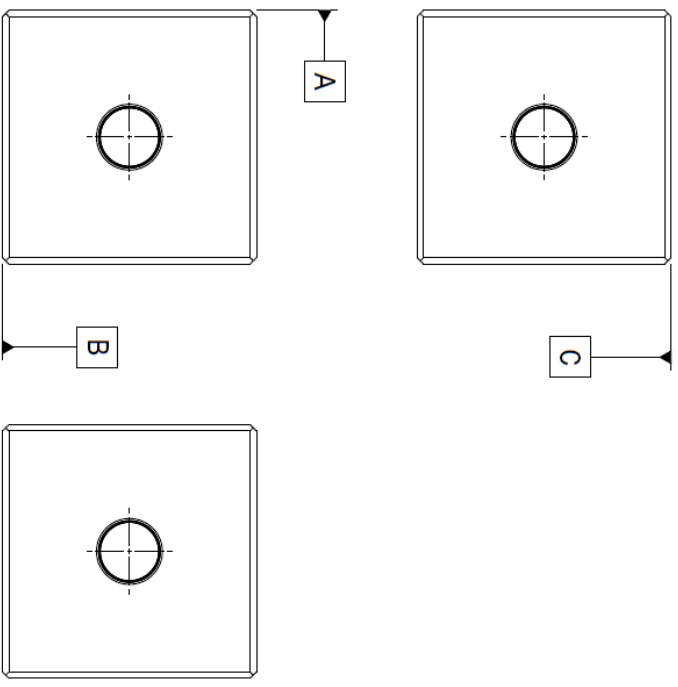


SIZE	CAGE CODE	3RD YEAR	
B	N/A	JPDE0003	
SCALE	REVISION	SHEET	
NONE	IR	2/3	



THIS DRAWING AND/OR DATA IS THE EXCLUSIVE PROPERTY OF DANRELL STEVENS, INC. IT IS TO BE USED ONLY FOR THE PROJECT AND/OR PART IDENTIFIED HEREIN. NO PARTS, COMPONENTS, MATERIALS, OR SERVICES SHALL BE USED IN THE MANUFACTURE OF THIS DRAWING WITHOUT THE EXPRESS WRITTEN AUTHORIZATION FROM DANRELL STEVENS.

- NOTES: 1. UNLESS OTHERWISE SPECIFIED:
 -DRAWING INTERPRETED PER ANSI Y14.5M-1994
 -ALL SURFACES SHALL NOT EXCEED 124 MICRONS RA (MEASURED I.A.W. ASME B46.1)
2. MATERIAL: 6041 ALUMINUM (PROVIDED)

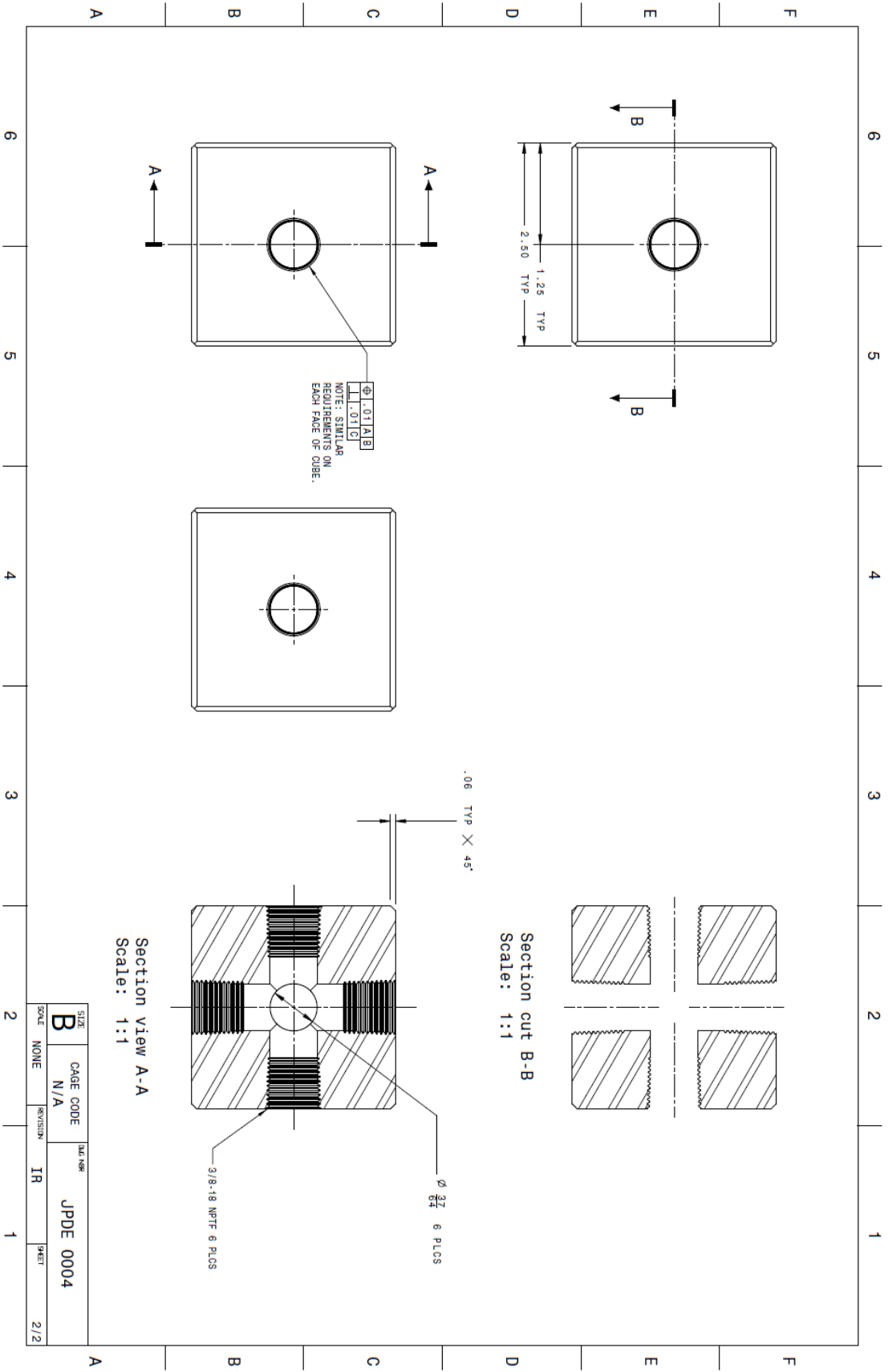


Isometric view
 Scale: 3:2

REVISIONS		
REV	DESCRIPTION	DATE
IR		

UNLESS OTHERWISE SPECIFIED DIMENSIONS ARE IN INCHES DECIMALS ANGLES XX +/-.0.01 X +/-.2° XXX DO NOT SCALE DRAWING 0.5"		DESIGNER DANRELL STEVENS	APPROVED ENGINEER	DATE 00 NOV 2012	SCALE NONE
THIRD ANGLE PROJECTION	THIRD ANGLE PROJECTION	DESIGNER DANRELL STEVENS	APPROVED ENGINEER	DATE 00 NOV 2012	SCALE NONE
TITLE DES ENGINEERING 2.5 X 2.5 X 2.5 INJECTOR BALANCING MANIFOLD		DATE 00 NOV 2012	DATE 00 NOV 2012	DATE 00 NOV 2012	DATE 00 NOV 2012
SIZE B	CAGE CODE N/A	DATE 00 NOV 2012	DATE 00 NOV 2012	DATE 00 NOV 2012	DATE 00 NOV 2012
REV	IR	REV	IR	REV	IR
1		2		3	

SOLID MODEL:
 APPLICATION: CATIA V5R20
 CATIA MODEL FILE NAMES: N/A
 CATIA MODEL FILE DATE: N/A



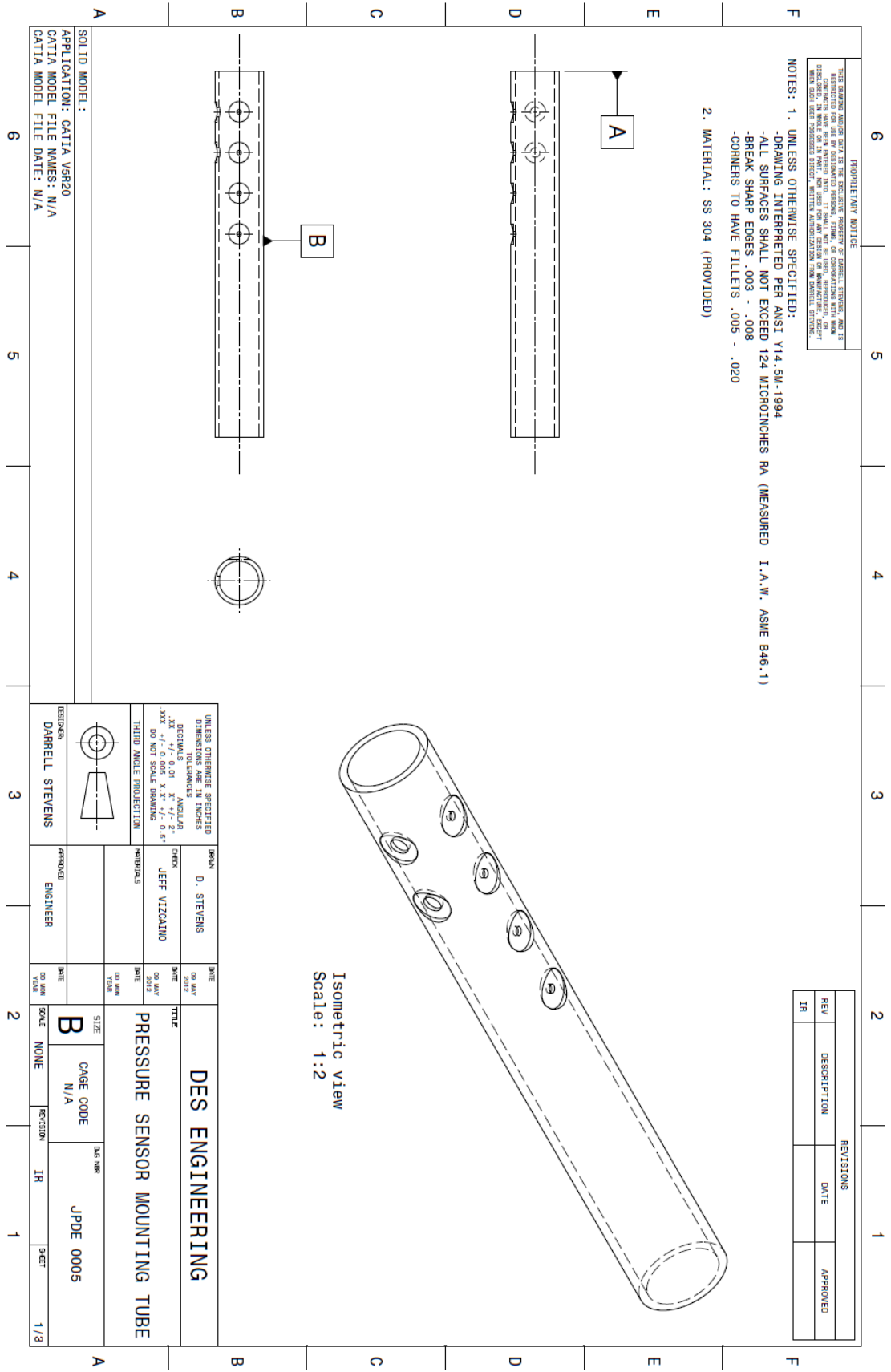
SIZE	CAGE CODE	3RD REV
B	N/A	JPDE 0004
SCALE	REVISION	SHEET
NONE	IR	2/2

THIS DRAWING AND/OR DATA IS THE EXCLUSIVE PROPERTY OF DARRELL STEVENS, AND IS NOT TO BE REPRODUCED, COPIED, EITHER WHOLLY OR IN PART, OR TRANSMITTED IN ANY FORM OR BY ANY MEANS, WITHOUT THE WRITTEN AUTHORIZATION FROM DARRELL STEVENS.

NOTES: 1. UNLESS OTHERWISE SPECIFIED:

- DRAWING INTERPRETED PER ANSI Y14.5M-1994
- ALL SURFACES SHALL NOT EXCEED 124 MICRONS RA (MEASURED I.A.W. ASME B46.1)
- BREAK SHARP EDGES .003 - .008
- CORNERS TO HAVE FILLETS .005 - .020

2. MATERIAL: SS 304 (PROVIDED)

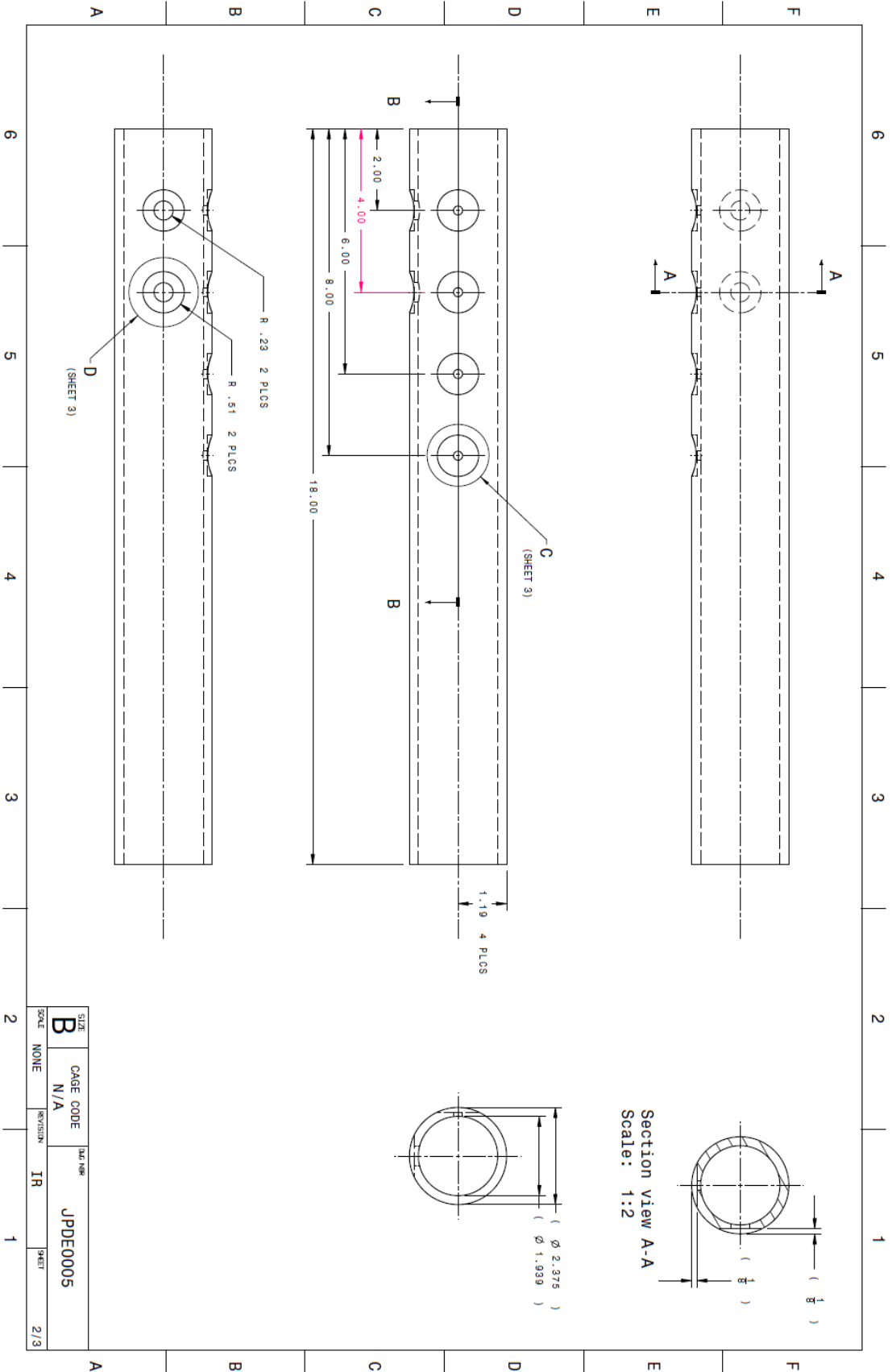


REVISIONS		
REV	DESCRIPTION	DATE
IR		
		APPROVED

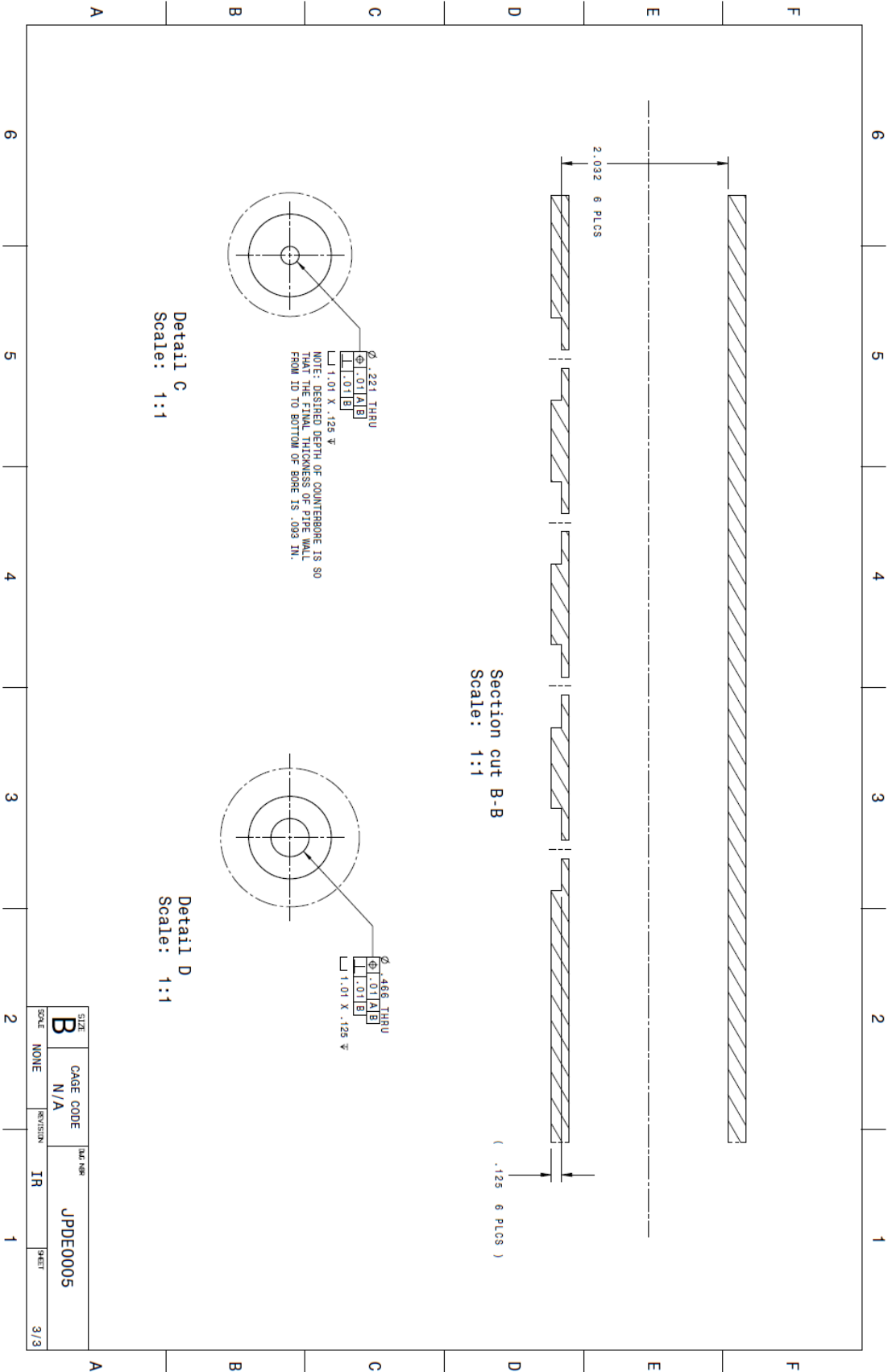
Isometric view
Scale: 1:2

UNLESS OTHERWISE SPECIFIED DIMENSIONS ARE IN INCHES DECIMALS .XX ±.01 X ±.2° ANGLES .XX ±.01 X ±.2° DO NOT SCALE DRAWING		DATE 09 MAY 2012	TITLE DES ENGINEERING
THIRD ANGLE PROJECTION	DESIGNER DARRELL STEVENS	DATE 09 MAY 2012	SIZE B
	APPROVED ENGINEER	SCALE NONE	CAGE CODE N/A
		REVISION IR	DWG. NO. JPDE 0005
			1/3

SOLID MODEL:
APPLICATION: CATIA V5R20
CATIA MODEL FILE NAMES: N/A
CATIA MODEL FILE DATE: N/A



SIZE	B	CAGE CODE	N/A	REV. NO.	IR	SHEET	2/3
SCALE	NONE	REVISION					
		JPDEC0005					

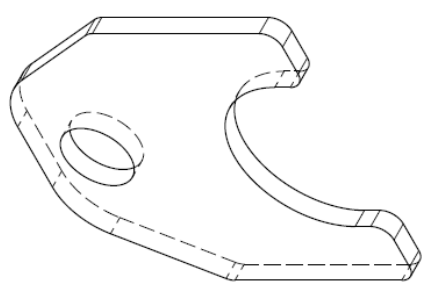
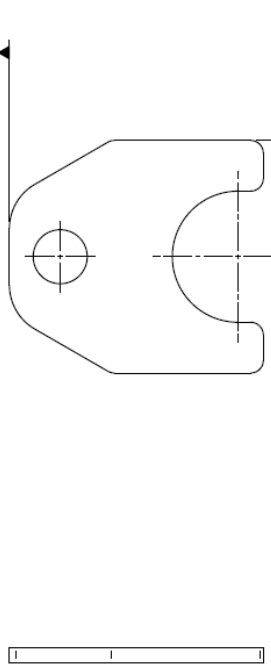
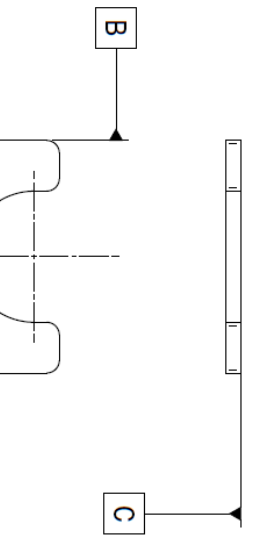


SIZE	CAGE CODE	3RD REV	
B	N/A		JPDEC0005
SCALE	REVISION	IR	SHEET
NONE			3/3

THIS DRAWING AND/OR DATA IS THE EXCLUSIVE PROPERTY OF DANRELL STEVENS, INC. IT IS UNLAWFUL TO REPRODUCE, TRANSMIT, OR DISSEMINATE THIS INFORMATION IN ANY MANNER WITHOUT THE WRITTEN AUTHORIZATION FROM DANRELL STEVENS. CONTRACTS HAVE BEEN ENTERED INTO BY SMALL AND MEDIUM BUSINESSES, OR BY INDIVIDUALS, TO OBTAIN THIS INFORMATION FROM DANRELL STEVENS. THESE CONTRACTS ARE SUBJECT TO THE TERMS AND CONDITIONS OF SUCH CONTRACTS.

- NOTES: 1. UNLESS OTHERWISE SPECIFIED:
 -DRAWING INTERPRETED PER ANSI Y14.5M-1994
 -ALL SURFACES SHALL NOT EXCEED 124 MICRONS RA (MEASURED I.A.W. ASME B46.1)
 -BREAK SHARP EDGES .003 - .008
 -CORNERS TO HAVE FILLETS .005 - .020
2. MATERIAL: MILD STEEL

REVISIONS		
REV	DESCRIPTION	DATE
IR		



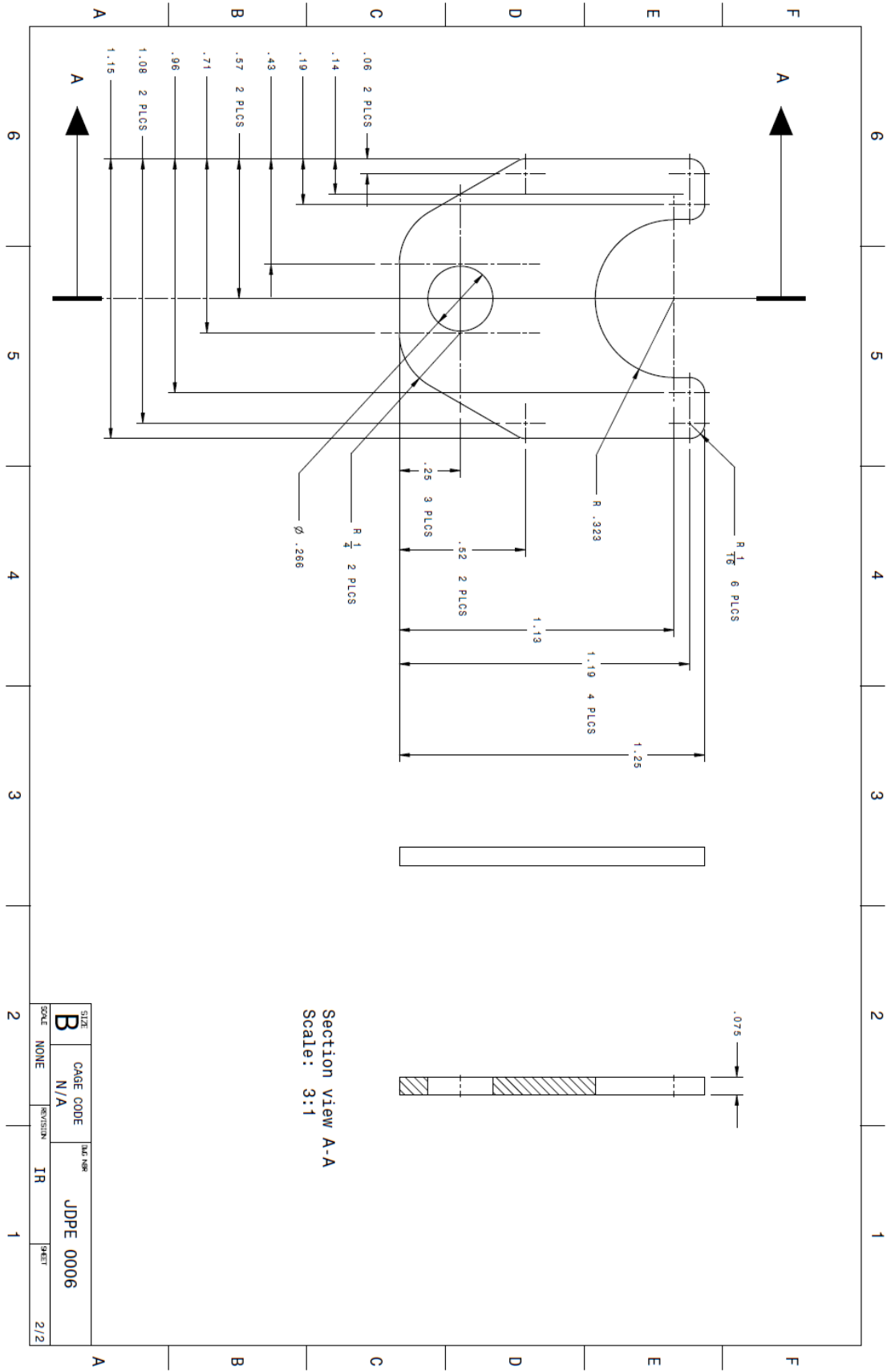
Isometric View
 Scale: 3:1

SOLID MODEL:
 APPLICATION: CATIA V20
 CATIA MODEL FILE NAMES: N/A
 CATIA MODEL FILE DATE: N/A

UNLESS OTHERWISE SPECIFIED		DIMENSIONS ARE IN INCHES	
DECIMALS	.XX	ANGULAR	+/- .01
ANGLES	X° Y' Z"	ANGLES	+/- .2°
DO NOT SCALE DRAWING		DO NOT SCALE DRAWING	
THIRD ANGLE PROJECTION		THIRD ANGLE PROJECTION	
DESIGNER	DANRELL STEVENS	APPROVED	ENGINEER
DATE	16 MAY 2012	DATE	16 MAY 2012
TIME	10:00 AM	TIME	10:00 AM
SCALE	NONE	SCALE	NONE
SIZE	B	SIZE	B
CAGE CODE	N/A	CAGE CODE	N/A
REV	IR	REV	IR
DATE	1/2	DATE	1/2

DES ENGINEERING
 INJECTOR PLATE
 INSTALL BRACKET

JDPE 0006

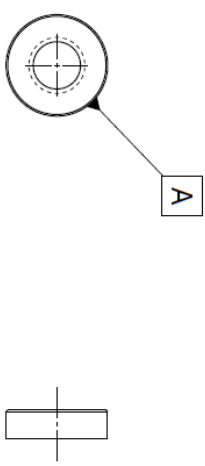


THIS DRAWING AND/OR DATA IS THE EXCLUSIVE PROPERTY OF DANRELL STEVENS, INC. IT IS TO BE KEPT CONFIDENTIAL AND NOT TO BE REPRODUCED, COPIED, OR TRANSMITTED IN ANY FORM OR BY ANY MEANS, ELECTRONIC OR MECHANICAL, INCLUDING PHOTOCOPYING, RECORDING, OR BY ANY INFORMATION STORAGE AND RETRIEVAL SYSTEM, WITHOUT PERMISSION IN WRITING FROM DANRELL STEVENS.

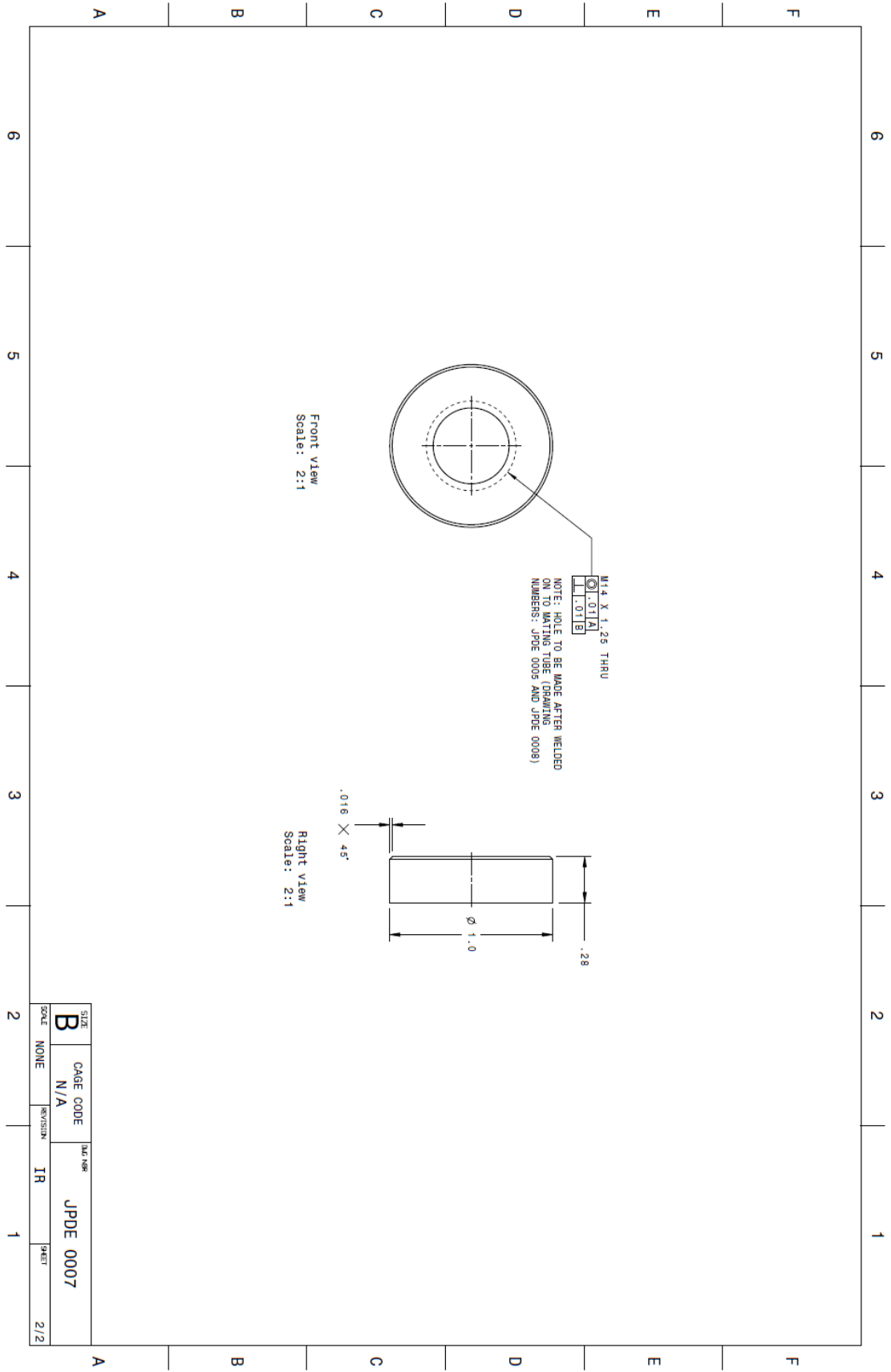
NOTES: 1. UNLESS OTHERWISE SPECIFIED:
 -DRAWING INTERPRETED PER ANSI Y14.5M-1994
 -ALL SURFACES SHALL NOT EXCEED 124 MICRONS RA (MEASURED I.A.W. ASME B46.1)
 -BREAK SHARP EDGES .003 - .008
 -CORNERS TO HAVE FILLETS .005 - .020
 -TOTAL RUNOUT OF ALL DIAMETERS RELATIVE TO **A** SHALL NOT EXCEED .01

2. MATERIAL: STAINLESS STEEL 316 (PROVIDED).

REVISIONS		
REV	DESCRIPTION	DATE
1R		



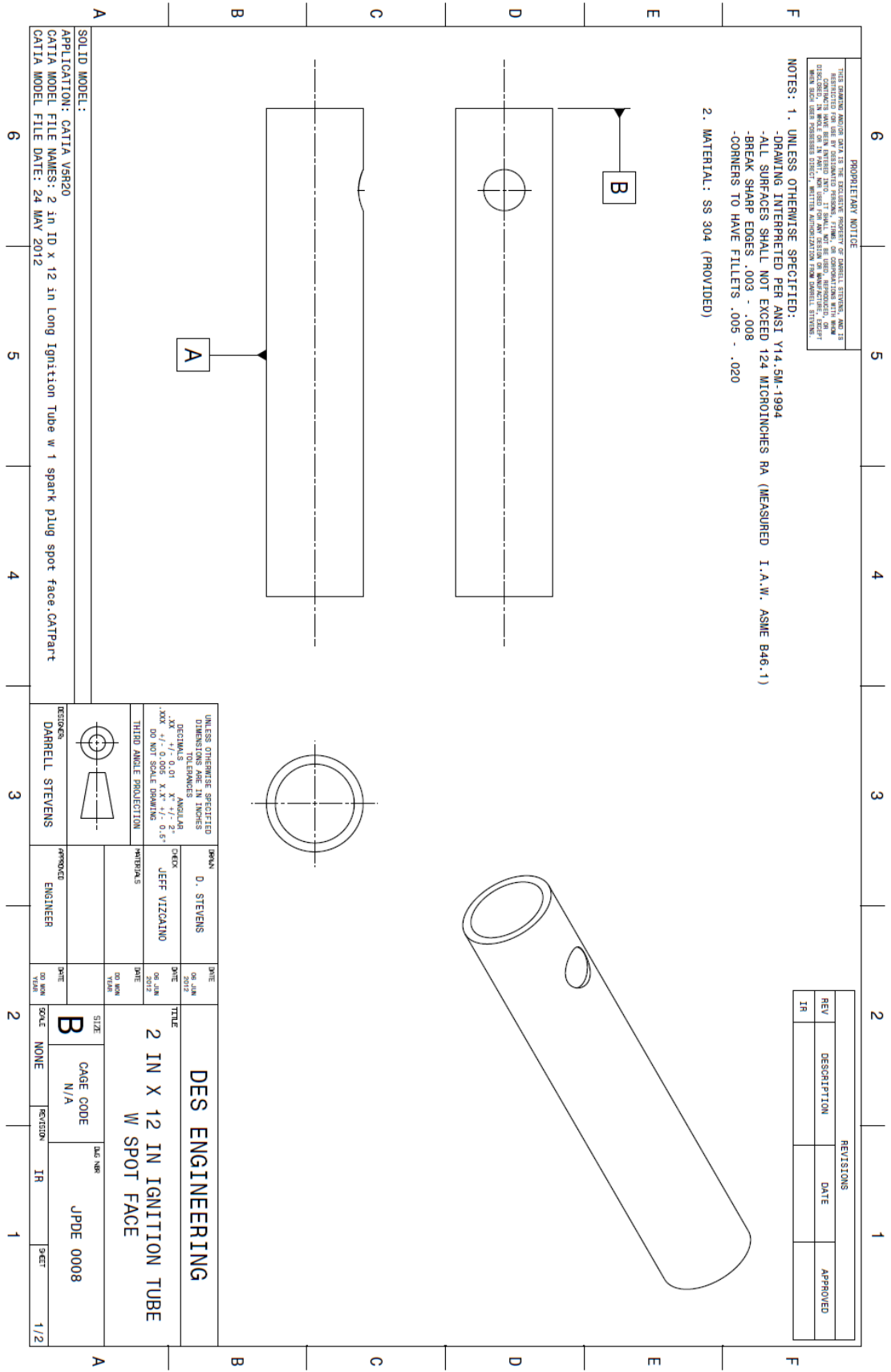
SOLID MODEL: APPLICATION: CATIA V5R20 CATIA MODEL FILE NAMES: N/A CATIA MODEL FILE DATE: N/A		UNLESS OTHERWISE SPECIFIED DIMENSIONS ARE IN INCHES DECIMALS: .005 ANGULARS: .01 .XX +.01 X -.01 .XXX DO NOT SCALE DRAWING		UNLESS OTHERWISE SPECIFIED DIMENSIONS ARE IN INCHES DECIMALS: .005 ANGULARS: .01 .XX +.01 X -.01 .XXX DO NOT SCALE DRAWING	
THIRD ANGLE PROJECTION		THIRD ANGLE PROJECTION		THIRD ANGLE PROJECTION	
DESIGNS: DANRELL STEVENS		CHECKED: JEFF VIZCAINO		DATE: 2012	
APPROVED: ENGINEER		DATE: 2012		TITLE: SPARK PLUG SLUG PRE-WELDED	
SCALE: NONE		SIZE: B		CAGE CODE: N/A	
REVISION: IR		DATE: JPD 0007		DRAWN BY: JPD 0007	



THIS DRAWING AND/OR DATA IS THE EXCLUSIVE PROPERTY OF DARRELL STEVENS, AND IS NOT TO BE REPRODUCED, COPIED, EITHER WHOLLY OR IN PART, OR TRANSMITTED IN ANY FORM OR BY ANY MEANS, ELECTRONIC OR MECHANICAL, INCLUDING PHOTOCOPYING, RECORDING, OR BY ANY INFORMATION STORAGE AND RETRIEVAL SYSTEM, WITHOUT PERMISSION IN WRITING FROM DARRELL STEVENS.

NOTES: 1. UNLESS OTHERWISE SPECIFIED:
 -DRAWING INTERPRETED PER ANSI Y14.5M-1994
 -ALL SURFACES SHALL NOT EXCEED 124 MICRONS RA (MEASURED I.A.W. ASME B46.1)
 -BREAK SHARP EDGES .003 - .008
 -CORNERS TO HAVE FILLETS .005 - .020

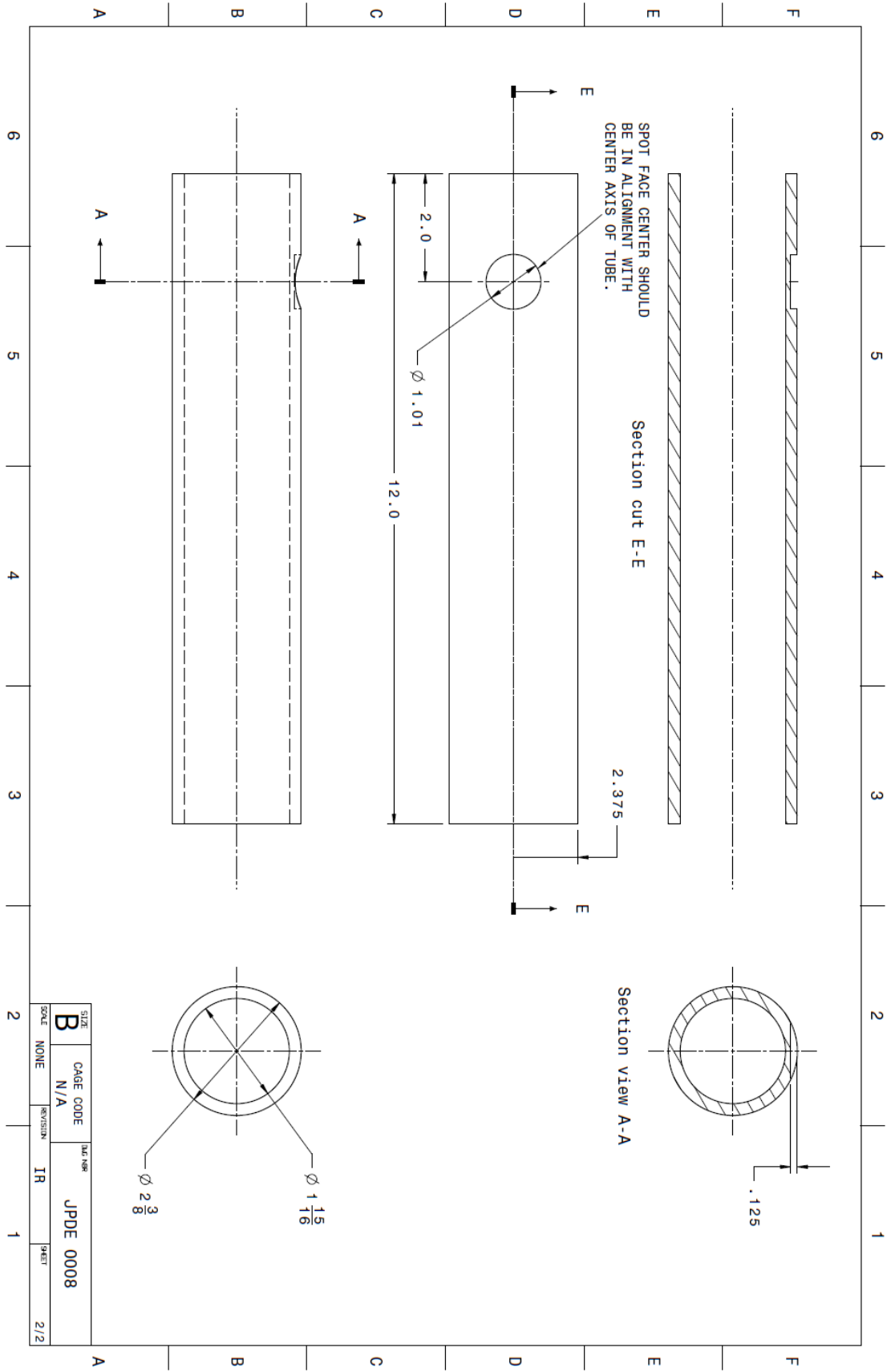
2. MATERIAL: SS 304 (PROVIDED)



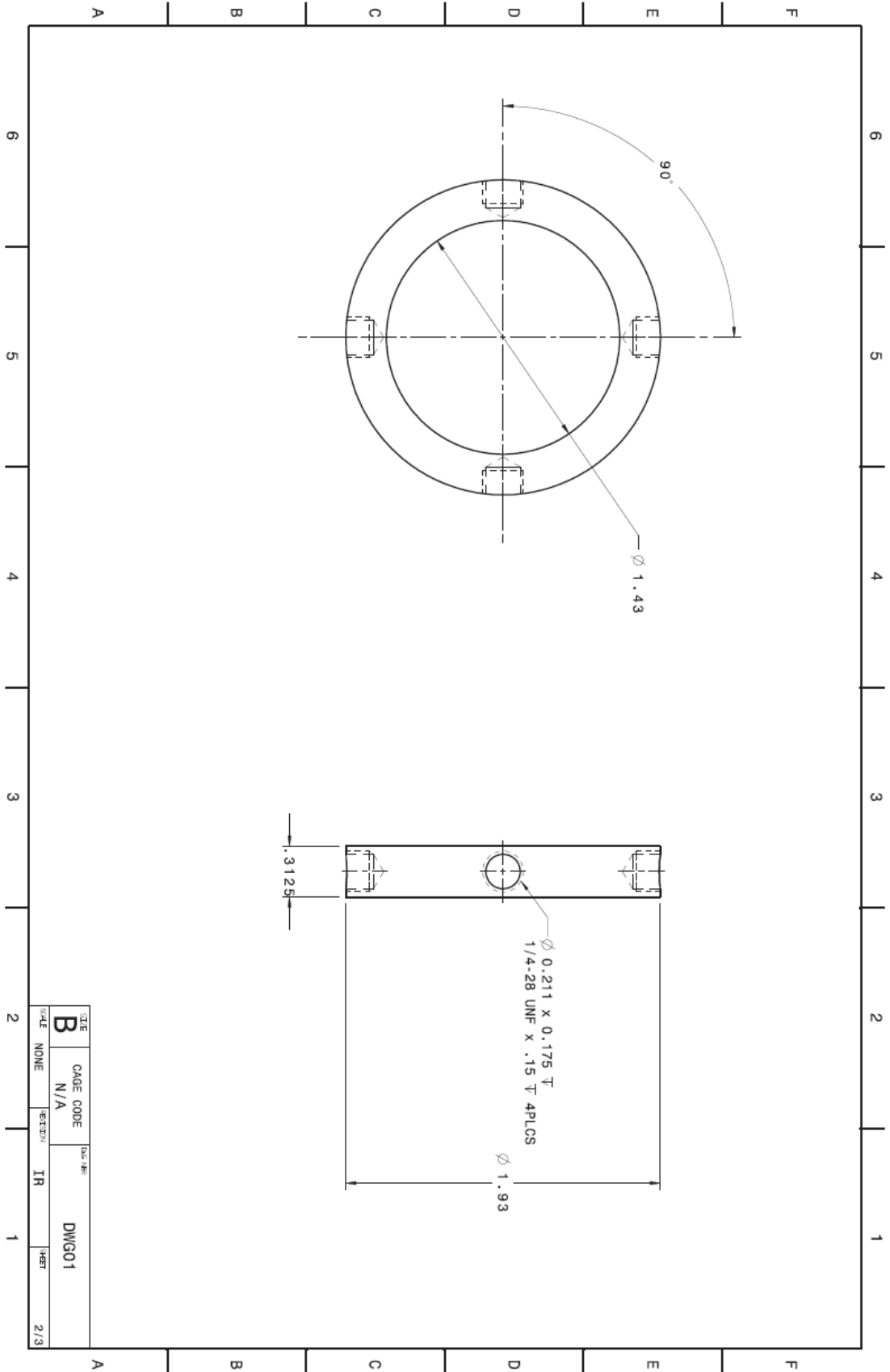
REVISIONS		
REV	DESCRIPTION	DATE
IR		

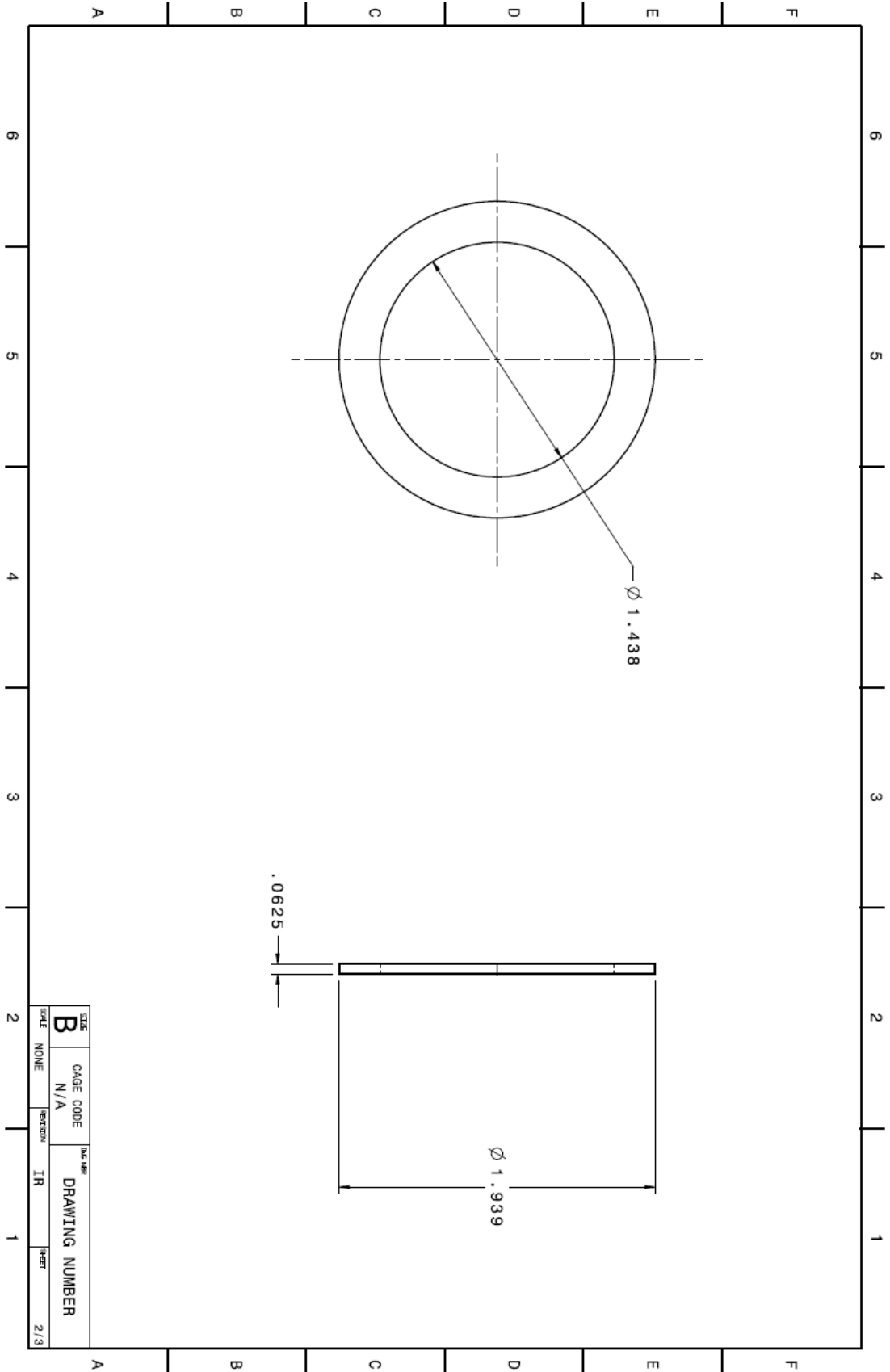
UNLESS OTHERWISE SPECIFIED DIMENSIONS ARE IN INCHES DECIMALS XX +.01 -0.01 X +.2 -2 XXX DO NOT SCALE DRAWING		DATE 06 JUN 2012	DESIGNER DARRELL STEVENS	SCALE NONE
THIRD ANGLE PROJECTION	PROPOSER JEFF VIZCAINO	DATE 06 JUN 2012	APPROVED ENGINEER	SIZE B
				CAGE CODE N/A
				DWG. NO. JPDE 0008
TITLE 2 IN X 12 IN IGNITION TUBE W SPOT FACE			REVISION IR	DATE 1/2

SOLID MODEL:
 APPLICATION: CATIA V2R0
 CATIA MODEL FILE NAMES: 2 in ID x 12 in Long Ignition Tube w 1 spark plug spot face.CATPart
 CATIA MODEL FILE DATE: 24 MAY 2012



SIZE	B	CAGE CODE	N/A	3RD. REV.	IR	JPDE 0008	SHEET	2/2
SCALE	NONE	REVISION						





APPENDIX C: RAW DATA & RESULTS

Firing Cycle 1 Data

Case	Run	Fire	V12	V23	V34	P1	P2	P3	P4	Pmax Avg	V avg
1	1	1	No ignition								
1	1	2	1350.23	1434.1	1118.49	257.912	262.329	231.957	321.333	268.38	1300.94
1	1	3	1392.03	1187.99	1750.79	233.376	327.265	534.681	204.132	324.86	1443.60
1	1	4	1499.79	1126.54	1815.46	264.36	420.994	788.016	192.428	416.45	1480.60
1	1	5	1478.61	1273.69	1788.97	226.476	290.993	629.024	248.465	348.74	1513.76
1	1	6	1192.31	990.785	1232.43	136.488	109.921	162.314	127.622	134.09	1138.51
1	2	1	887.611	864.587	910.572	60.5262	83.9016	82.2894	77.4532	76.04	887.59
1	2	2	1626.34	1378.41	1786.56	318.914	259.169	358.863	227.927	291.22	1597.10
1	2	3	1454.01	1254.04	1853.88	243.693	328.49	660.397	235.794	367.09	1520.64
1	2	4	1495.44	1163.95	1524.36	253.463	194.621	259.427	223.445	232.74	1394.58
1	2	5	1463.14	1274.3	1791.64	276.548	271.293	553.705	270.1	342.91	1509.69
1	2	6	1459.45	1186.39	998.168	189.397	181.788	139.39	146.806	164.35	1214.67
1	3	1	903.879	853.55	949.989	80.8708	97.1208	89.4794	88.4478	88.98	902.47
1	3	2	1606.6	2294.11	1229.4	220.027	265.424	359.379	230.087	268.73	1710.04
1	3	3	1454.9	1287.71	1980.64	262.136	317.173	710.793	241.984	383.02	1574.42
1	3	4	1470.78	1274.99	1808.24	180.724	348.384	556.607	192.428	319.54	1518.00
1	3	5	1605.37	1161.8	1672.99	256.945	301.665	519.269	254.398	333.07	1480.05
1	3	6	1590.74	1305.22	906.626	461.619	137.069	174.856	133.329	226.72	1267.53
1	4	1	911.874	885.073	950.344	65.2658	85.7394	84.1596	83.8048	79.74	915.76
1	4	2	1999.51	1599.76	1371.71	468.004	211.999	197.78	258.267	284.01	1656.99
1	4	3	1466.21	1382.85	1759.15	207.55	186.496	674.229	230.345	324.66	1536.07
1	4	4	1274.88	1587.91	1620.07	178.596	275.355	321.558	209.323	246.21	1494.29
1	4	5	1398.27	1804.33	1242.67	220.995	526.718	186.979	264.876	299.89	1481.76
1	4	6	1189.53	973.828	1207.22	139.712	113.016	146.419	132.49	132.91	1123.53
1	5	1	909.593	908.248	997.518	88.8346	93.7676	123.688	114.048	105.08	938.45
1	5	2	1831.04	1614.43	1588.65	302.89	254.656	287.381	172.47	254.35	1678.04
1	5	3	1786.19	1466.81	1568.15	254.785	235.343	365.763	169.601	256.37	1607.05
1	5	4	1481	1449.2	1773.89	211.806	237.89	609.421	244.145	325.82	1568.03
1	5	5	1430.03	1320.53	1955.87	216.513	246.982	719.466	248.304	357.82	1568.81
1	5	6	1592.88	1180.07	1026.82	453.817	176.533	141.099	161.863	233.33	1266.59
1	6	1	931.588	930.54	988.529	86.6744	91.9298	115.531	122.721	104.21	950.22
1	6	2	1966.73	3038.66	1039.76	207.808	250.174	313.369	234.923	251.57	2015.05
1	6	3	1249.08	1491.34	1609.11	184.045	223.155	443.273	185.077	258.89	1449.84
1	6	4	2263.9	1307.42	1309.39	292.024	225.605	238.567	297.667	263.47	1626.90
1	6	5	2254.28	1064.54	1782.67	237.277	248.82	456.977	224.38	291.86	1700.50
1	6	6	1252.08	1114.31	1171.34	170.891	134.554	140.583	122.495	142.13	1179.24
1	7	1	872.283	858.392	908.288	94.3802	73.423	89.0926	78.4528	83.84	879.65

1	7	2	1989.26	1567.99	1519.49	481.61	242.21	176.501	403.841	326.04	1692.25
1	7	3	1460.92	1472.15	1651.94	241.855	232.28	518.27	196.652	297.26	1528.34
1	7	4	1420.23	1544.93	1611.34	190.333	354.252	302.503	182.433	257.38	1525.50
1	7	5	1594.32	1376.34	1756.76	247.369	228.314	596.04	183.755	313.87	1575.81
1	7	6	1471.49	1230.64	1006.9	232.828	155.672	121.56	121.496	157.89	1236.34
1	8	1	903.562	896.2	946.346	67.426	78.4528	81.9348	77.6466	76.37	915.37
1	8	2	1944.26	1801.17	1478.6	302.181	247.788	224.09	337.067	277.78	1741.34
1	8	3	1403.82	1695.82	1376.4	212.934	254.075	218.673	143.42	207.28	1492.01
1	8	4	1599.12	1563.27	1523.85	227.766	221.446	205.39	205.841	215.11	1562.08
1	8	5	1599.17	1286.85	1878.5	182.949	277.773	469.422	173.728	275.97	1588.17
1	8	6	1789.66	1259.72	11095.5	627.573	169.375	160.734	134.554	273.06	1524.69
1	9	1	882.567	883.579	931.29	57.2376	78.0336	82.1282	70.8114	72.05	899.15
1	9	2	1833.65	1839.27	1317.32	254.656	271.744	203.52	226.669	239.15	1663.41
1	9	3	1558.01	1512.78	1567.32	200.005	320.559	263.941	156.833	235.33	1546.04
1	9	5	1594.13	1512.3	1737.53	237.084	348.513	243.339	221.93	262.72	1614.65
1	9	6	1649.98	1524.87	1353.49	279.063	586.818	203.004	207.389	319.07	1509.45
1	9	7	1783.79	1248.54	1061.68	436.922	181.144	187.85	137.198	235.78	1364.67
1	10	1	938.69	918.586	978.276	72.7136	83.547	100.087	95.6054	87.99	945.18
1	10	2	1777.67	1745.64	1620.13	225.476	320.365	213.805	226.831	246.62	1714.48
1	10	3	2244.84	1115.27	1793.77	238.244	319.366	699.121	210.548	366.82	1717.96
1	10	4	1651.69	1962.1	1167.43	224.219	277.677	184.142	216.062	225.53	1593.74
1	10	5	1551.09	1317.46	1951.58	226.508	211.322	632.378	236.084	326.57	1606.71
1	10	6	1301.76	1053.08	1260.52	178.532	136.585	140.196	175.34	157.66	1205.12
1	11	1	935.263	952.037	987.106	74.9384	81.1288	113.951	148.257	104.57	958.14
1	11	2	1985.28	1612.13	1580.55	321.59	250.561	228.314	211.677	253.04	1725.99
1	11	3	1698.64	1487.5	1438.36	258.363	253.334	255.816	183.143	237.66	1541.50
1	11	4	1464.28	1710.42	1654.97	238.148	225.831	278.966	208.291	237.81	1609.89
1	11	5	1486.5	1484.21	1751.92	247.691	271.389	426.088	229.732	293.73	1574.21
1	11	6	1640.58	1241.61	1011.39	343.644	163.023	137.262	141.421	196.34	1297.86
1	12	1	976.582	1014.36	1052.13	90.4468	111.211	102.408	146.806	112.72	1014.36
1	12	2	1954.42	1633.62	1720.79	207.26	217.029	227.379	264.812	229.12	1769.61
1	12	3	1786.7	1366.08	1695.86	319.946	210.355	389.944	187.689	276.98	1616.21
1	12	4	1608.64	1797.9	1472.92	268.487	543.194	202.262	355.38	342.33	1626.49
1	12	5	1625.39	1765.77	1469.7	217.674	244.209	221.575	169.956	213.35	1620.29
1	12	6	1608.37	1129.95	1075.8	218.48	157.059	122.624	191.106	172.32	1271.37
1	13	1	948.89	1040.33	1031.86	92.2522	99.3778	127.589	112.436	107.91	1007.03
1	13	2	1882.06	1544.09	1739.3	291.057	244.145	397.521	212.289	286.25	1721.82
1	13	3	1611.76	1372.06	1755.55	218.899	230.7	493.959	255.204	299.69	1579.79
1	13	4	1744.01	1501.74	1614.56	276.032	295.055	274.678	257.074	275.71	1620.10
1	13	5	1949	1228.81	1476.53	209.388	184.464	218.609	247.401	214.97	1551.45
1	13	6	1369.48	1919.05	828.805	186.367	135.972	131.684	142.195	149.05	1372.45

1	14	1	910.768	904.379	949.059	65.7494	78.1626	83.4824	81.2578	77.16	921.40
1	14	2	1763.63	1759.46	1497.93	266.231	422.187	231.473	187.689	276.90	1673.67
1	14	3	1613.53	1665.3	1526.55	215.32	258.976	295.926	176.662	236.72	1601.79
1	14	4	1992.46	1327.09	1650.3	215.739	192.009	406.227	172.567	246.64	1656.62
1	14	5	1947.57	1941.27	1241.15	478.902	327.652	217.513	220.35	311.10	1710.00
1	14	6	1404.98	1166.53	1150.88	196.201	150.61	126.59	153.125	156.63	1240.80
1	15	1	919.65	953.78	985.227	89.4472	84.0306	89.6084	86.61	87.42	952.89
1	15	2	1790.18	1617.68	1766.16	274.162	203.036	225.122	195.975	224.57	1724.67
1	15	3	1790.98	1491.8	1619.7	347.03	247.304	204.648	232.473	257.86	1634.16
1	15	4	1652.02	1450.72	1747.72	341.71	346.675	357.863	208.517	313.69	1616.82
1	15	5	1768.52	1600.37	2062.37	263.587	210.065	409.419	204.358	271.86	1810.42
1	15	6	1778.89	1257.22	996.709	711.728	168.15	128.686	154.737	290.83	1344.27
1	16	1	891.351	896.84	950.203	58.5916	80.1292	85.5782	77.6466	75.49	912.80
1	16	2	1806.27	1775.36	1385.5	217.319	257.815	229.603	272.357	244.27	1655.71
1	16	3	1763.35	1636.02	1568.18	205.841	301.471	212.193	181.659	225.29	1655.85
1	16	4	1484.96	1646.66	1456.4	172.019	381.497	249.497	173.857	244.22	1529.34
1	16	5	1611.32	1467.77	1535.12	294.249	309.016	195.104	166.635	241.25	1538.07
1	16	6	1307.54	1210.02	1169.83	173.502	158.864	170.084	163.894	166.59	1229.13
1	17	1	907.723	913.61	967.373	69.425	80.0326	75.0674	80.3872	76.23	929.57
1	17	2	1780	1778.84	1555.2	286.092	263.877	315.851	222.252	272.02	1704.68
1	17	3	1570.02	1773.68	1651.18	228.281	294.926	261.91	246.692	257.95	1664.96
1	17	4	1495.84	1496.59	1750.32	217.126	204.39	354.8	169.762	236.52	1580.92
1	17	5	1705.94	1299.53	1747.75	218.738	209.678	693.253	211.709	333.34	1584.41
1	17	6	1444.25	1134.89	9091.58	295.152	131.878	132.49	145.677	176.30	1289.57
2	1	1	739.407	726.688	700.295	39.4722	48.5	53.2396	49.2416	47.61	722.13
2	1	2	824.548	831.756	827.908	66.3942	79.8068	90.0276	91.285	81.88	828.07
2	1	3	855.076	866.222	846.146	58.237	80.226	81.7736	96.2826	79.13	855.81
2	1	4	824.918	869.473	825.315	58.9464	72.0044	70.8758	84.6432	71.62	839.90
2	1	5	819.068	838.59	792.537	56.7216	73.165	89.0926	90.608	77.40	816.73
2	1	7	856.526	886.583	832.293	62.622	76.2924	77.292	102.602	79.70	858.47
2	2	1	715.777	730.773	710.416	36.6026	44.7598	51.0794	50.628	45.77	718.99
2	2	2	823.601	704.887	932.274	65.4914	67.8774	71.295	77.5176	70.55	820.25
2	2	3	826.905	835.535	818.41	58.7852	79.6778	70.7468	85.6104	73.71	826.95
2	2	4	851.113	894.668	823.976	58.5272	73.423	88.9636	82.2572	75.79	856.59
2	2	5	813.779	839.482	819.139	53.2718	75.8088	71.7142	73.294	68.52	824.13
2	2	6	826.909	836.049	836.585	59.4944	76.905	95.9278	89.8342	80.54	833.18
2	3	1	698.612	723.485	708.608	36.7962	43.3734	46.0496	43.7926	42.50	710.24
2	3	2	828.321	817.747	800.836	55.8512	66.1362	74.7772	83.4824	70.06	815.63
2	3	3	844.917	841.105	827.625	61.0098	74.2612	71.0048	85.5136	72.95	837.88
2	3	4	835.746	875.499	821.717	59.978	79.968	65.3948	78.7752	71.03	844.32
2	3	5	852.164	865.835	835.15	62.106	72.6492	79.2266	87.7384	75.43	851.05

2	3	6	834.306	864.841	821.941	66.1686	72.1656	77.8724	86.8678	75.77	840.36
2	4	1	702.66	716.171	716.372	40.8586	42.503	43.2446	47.694	43.58	711.73
2	4	2	784.532	777.985	760.514	52.8848	53.7232	62.0738	65.9106	58.65	774.34
2	4	3	836.168	875.51	814.665	50.0154	73.9388	80.7418	76.1312	70.21	842.11
2	4	4	844.332	838.473	822.49	64.5242	78.227	96.4114	96.9274	84.02	835.10
2	4	5	848.287	851.135	880.842	61.5902	76.2602	83.031	81.419	75.58	860.09
2	4	6	826.865	825.101	816.542	60.623	75.0674	75.2286	81.2256	73.04	822.84
2	5	1	693.005	730.613	704.206	35.4098	43.6314	43.9538	43.2446	41.56	709.27
2	5	2	741.968	735.036	752.653	39.7302	51.4018	50.4344	51.8532	48.35	743.22
2	5	3	825.922	840.974	821.453	71.1338	82.1606	76.357	86.9324	79.15	829.45
2	5	4	816.553	831.428	828.104	63.4602	79.6456	75.9378	90.1242	77.29	825.36
2	5	5	825.451	836.199	822.619	71.0694	78.904	84.5464	94.5092	82.26	828.09
2	5	6	844.307	827.35	828.455	61.6224	77.292	70.9726	78.7752	72.17	833.37
2	6	1	711.494	710.067	737.355	34.9584	41.9226	44.3086	45.7272	41.73	719.64
2	6	2	808.589	801.218	800.267	64.7822	78.3238	71.7786	77.1952	73.02	803.36
2	6	3	810.899	850.346	824.132	53.2072	68.0708	64.9756	72.3268	64.65	828.46
2	6	4	836.7	846.655	820.747	68.5866	84.7722	75.6154	82.7086	77.92	834.70
2	6	5	831.185	847.92	842.965	55.7544	71.5852	67.426	85.417	70.05	840.69
2	6	6	832.292	847.348	824.977	60.8486	86.8034	70.0376	89.1248	76.70	834.87
2	7	1	714.213	732.822	712.016	35.5064	42.5996	42.4708	49.048	42.41	719.68
2	7	2	779.397	754.078	727.934	57.7534	61.1066	72.359	60.236	62.86	753.80
2	7	3	823.277	809.284	829.174	51.8208	60.1392	71.1016	78.227	65.32	820.58
2	7	4	826.005	864.134	817.921	53.2072	69.0702	75.1318	72.0044	67.35	836.02
2	7	5	819.15	824.492	810.059	51.7242	59.1398	70.5212	81.0644	65.61	817.90
2	7	7	805.439	799.692	815.251	57.1408	72.4558	80.2582	79.1298	72.25	806.79
2	8	1	703.767	678.551	744.849	38.8274	44.5986	42.2128	46.2108	42.96	709.06
2	8	2	800.942	787.89	805.584	65.5882	60.5262	74.906	67.7484	67.19	798.14
2	8	3	817.741	838.252	822.243	66.4588	91.6396	79.7102	82.902	80.18	826.08
2	8	4	828.581	817.638	818.101	52.7558	72.907	62.235	80.226	67.03	821.44
2	8	5	828.361	839.777	794.825	64.9434	77.034	68.1998	82.7732	73.24	820.99
2	8	6	854.338	851.299	823.487	65.427	80.4194	73.3908	86.2876	76.38	843.04
4	1	1	721.921	731.894	713.231	38.3116	45.0178	47.049	42.8576	43.31	722.35
4	1	2	813.021	823.152	758.79	51.5952	60.3004	56.6894	59.7202	57.08	798.32
4	1	3	799.302	819.819	771.981	51.982	66.7166	55.98	61.4612	59.03	797.03
4	1	4	812.031	812.483	772.366	50.7568	63.0732	64.7498	67.426	61.50	798.96
4	1	5	819.43	823.244	765.628	49.048	58.1402	65.6526	64.0728	59.23	802.77
4	1	6	815.764	821.537	759.132	55.7866	61.8804	59.1398	62.7186	59.88	798.81
4	2	1	737.858	727.156	704.296	42.0838	46.0496	46.2108	41.8582	44.05	723.10
4	2	2	790.968	820.416	750.944	43.8572	58.0436	56.625	58.9464	54.37	787.44
4	2	3	805.064	828.962	755.279	48.5966	61.4612	63.6536	59.9136	58.41	796.44
4	2	4	828.225	830.472	756.657	50.1766	64.2662	66.7488	63.8148	61.25	805.12

4	2	5	813.192	832.592	760.519	50.8214	68.2964	56.7538	55.6254	57.87	802.10
4	2	6	807.039	817.18	750.391	50.37	59.7846	52.9494	62.622	56.43	791.54
4	3	1	734.419	722.083	709.118	40.8264	42.8254	42.2772	43.1478	42.27	721.87
4	3	2	792.297	789.165	748.513	46.9846	57.8824	61.6546	62.2028	57.18	776.66
4	3	3	797.404	819.796	762.488	48.5966	67.3938	60.0748	70.5534	61.65	793.23
4	3	4	813.652	806.312	762.553	48.0486	57.3664	57.3342	56.2058	54.74	794.17
4	3	5	804.231	827.058	743.439	49.8864	61.3	59.559	58.108	57.21	791.58
4	3	6	802.49	821.617	770.753	49.6284	59.2042	61.9126	58.0114	57.19	798.29
4	4	1	735.553	732.571	705.01	45.1468	43.4058	41.987	43.2768	43.45	724.38
4	4	2	806.033	817.707	757.513	48.371	65.6204	65.0078	62.912	60.48	793.75
4	4	3	828.286	807.414	772.133	54.5292	57.3988	59.559	56.915	57.10	802.61
4	4	4	820.34	809.436	774.265	53.7876	62.0738	61.7192	62.7186	60.07	801.35
4	4	5	823.543	800.148	754.387	51.0148	59.4944	65.7494	64.2018	60.12	792.69
4	4	6	811.59	825.82	757.722	50.241	62.2672	52.5946	61.9448	56.76	798.38
4	5	1	722.934	737.777	713.615	35.8288	45.1146	47.049	40.375	42.09	724.78
4	5	2	815.462	807.495	761.324	45.7916	51.9498	61.1066	56.625	53.87	794.76
4	5	3	827.688	801.22	765.6	51.982	63.0088	59.7202	59.043	58.44	798.17
4	5	4	801.775	802.855	765.168	52.4658	61.3968	57.56	64.1696	58.90	789.93
4	5	5	818.817	811.318	761.711	49.4994	59.8168	57.3988	57.9146	56.16	797.28
4	5	6	817.78	815.591	759.56	51.305	62.1706	58.6884	57.6888	57.46	797.64
4	6	1	731.111	726.705	724.04	39.1498	43.0188	42.3096	43.18	41.91	727.29
4	6	2	819.685	819.134	750.413	48.7256	67.3292	58.8174	59.1076	58.49	796.41
4	6	3	821.542	826.159	750.801	46.9524	57.2698	60.5584	57.7856	55.64	799.50
4	6	4	830.326	815.676	742.648	48.9836	59.4944	56.2702	56.238	55.25	796.22
4	6	5	812.208	826.529	766.158	50.499	63.2668	58.6562	58.3014	57.68	801.63
4	6	6	820.257	817.164	752.895	49.2092	55.3674	57.4632	65.298	56.83	796.77
4	7	1	720.792	728.32	725.376	41.5356	46.501	41.0844	42.8254	42.99	724.83
4	7	2	832.173	811.606	761.063	47.178	54.8194	54.2068	56.5926	53.20	801.61
4	7	3	814.328	818.094	772.642	51.982	58.3982	56.3024	57.5276	56.05	801.69
4	7	4	826.308	825.827	748.177	53.2718	59.6556	59.043	58.9786	57.74	800.10
4	7	5	824.839	823.241	775.649	51.3694	63.6536	54.3358	56.5926	56.49	807.91
4	7	6	825.266	834.39	771.295	55.045	63.5892	60.1716	59.043	59.46	810.32
4	8	1	739.764	738.923	715.179	42.6642	45.7916	40.9232	41.052	42.61	731.29
4	8	2	804.295	822.721	740.29	46.5976	64.363	55.2708	60.3328	56.64	789.10
4	8	3	826.195	810.072	753.948	53.0784	57.8178	66.3298	54.5936	57.95	796.74
4	8	4	821.811	801.388	761.386	51.2728	52.24	54.5292	52.2722	52.58	794.86
4	8	5	817.264	817.329	762.663	46.7912	61.6546	59.8492	55.303	55.90	799.09
4	8	6	805.287	820.009	751.133	48.1776	57.0118	61.2678	54.9484	55.35	792.14
5	1	1	No ignition								
5	1	2	1243.8	1124.88	1269.78	134.006	160.38	210.032	151.545	163.99	1212.82
5	1	3	1166.01	1058.97	1249.07	137.971	132.168	150.288	138.552	139.74	1158.02

5	1	4	1305.97	1393.16	1113.01	225.605	348.126	147.644	139.326	215.18	1270.71
5	1	5	1216.65	1082.47	1157.69	132.329	128.267	149.417	119.561	132.39	1152.27
5	1	6	1459.93	1183.39	951.272	236.955	156.93	109.889	123.624	156.85	1198.20
5	2	1	No ignition								
5	2	2	1280.33	1422.68	1144.92	200.424	425.734	162.637	159.638	237.11	1282.64
5	2	3	1071.83	1083.37	1213.97	142.872	135.328	150.256	138.81	141.82	1123.06
5	2	4	1086.31	1285.29	1142.6	124.365	164.636	179.499	139.519	152.00	1171.40
5	2	5	1281.49	1177.55	1159.04	137.842	152.384	206.228	109.147	151.40	1206.03
5	3	6	No ignition								
5	3	1	800.314	748.992	762.734	63.8794	61.2356	54.6582	62.4608	60.56	770.68
5	3	2	924.984			106.858	102.441	102.183	94.1868	101.42	924.98
5	3	3	983.565			108.148	93.0584	122.914	103.311	106.86	983.57
5	3	4	953.89	910.151	884.027	77.7112	77.8724	78.3238	82.1606	79.02	916.02
5	3	5	989.438			100.216	117.175	99.3454	94.219	102.74	989.44
5	3	6	730.68			86.6422	98.8296	140.035	99.8614	106.34	730.68
5	4	1	No ignition								
5	4	2	1151.79	1076.78	1359.59	154.608	140.067	229.7	158.252	170.66	1196.05
5	4	3	953.46			97.282	99.41	103.279	85.546	96.38	953.46
5	4	4	1329.76	1041.89	1289.12	172.245	158.123	169.601	179.402	169.84	1220.26
5	4	5	1478.58	1249.05	1007.78	240.018	205.648	129.298	118.046	173.25	1245.14
5	4	6	1323.55	1103.08	1046.28	165.7	130.298	141.389	238.438	168.96	1157.64
5	5	1	No ignition								
5	5	2	1182.85	1355.39	1109.24	128.267	225.541	148.289	158.929	165.26	1215.83
5	5	3	1166.42	1120.82	1330.79	143.356	201.972	200.908	136.972	170.80	1206.01
5	5	4	1239.22	1007.73	1105.37	133.586	123.559	167.086	193.396	154.41	1117.44
5	5	5	1253.41	1184.46	1167.49	162.991	128.718	186.109	179.016	164.21	1201.79
5	5	6	1155.96	1105.99	1140.73	124.14	136.263	199.264	163.185	155.71	1134.23
5	6	1	No ignition								
5	6	2	1231.15	1123.3	1349.8	156.382	144.807	163.378	167.924	158.12	1234.75
5	6	3	1380.86	1332.46	1128.42	257.267	241.952	136.166	121.754	189.28	1280.58
5	6	4	1103.72	1199.94	1274.87	136.069	147.451	232.537	169.375	171.36	1192.84
5	6	5	1453.01	1214.9	1077.41	194.814	194.363	137.262	136.746	165.80	1248.44
5	6	6	1109.38	1172.88	1191.91	140.744	146.548	207.002	145.452	159.94	1158.06
5	7	1	No ignition								
5	7	2	1253.74	1464.53	1120.55	172.954	316.851	152.319	154.963	199.27	1279.61
5	7	3	1142.77	1124.3	1306.66	143.291	167.602	245.724	175.211	182.96	1191.24
5	7	4	1154.02	1055.49	1283.57	114.112	138.262	160.638	116.853	132.47	1164.36
5	7	5	1456.7	1242.87	1031.91	247.724	165.603	126.139	147.354	171.71	1243.83
5	7	6	1309.19	1370.5	653.403	180.95	282.545	150.836	128.782	185.78	1111.03
5	8	1	No ignition								
5	8	2	1246.11	1301.94	1165.28	148.031	298.86	149.256	132.748	182.22	1237.78

5	8	3	1166.67		705.285	138.971	174.598	198.715	208.001	180.07	935.98
5	8	4	1322.77	1302.56	1108.15	180.531	164.249	117.401	157.059	154.81	1244.49
5	8	5	1133.89	1084.23	1307.85	151.997	146.193	181.627	154.35	158.54	1175.32
5	8	6	1169	1268.73	1367.3	170.439	184.4	262.523	167.279	196.16	1268.34
6	1	1	750.668	729.617	724.225	44.4698	49.6284	45.6626	54.0134	48.44	734.84
6	1	2	802.702	759.83	759.594	51.0794	55.5932	54.626	57.8178	54.78	774.04
6	1	3	925.59	942.164	858.823	79.3232	80.097	89.8986	80.1616	82.37	908.86
6	1	4	983.844	944.888	910.579	78.6784	81.0644	91.3494	93.0584	86.04	946.44
6	1	5	953.3	913.404	907.343	87.9964	94.348	99.3778	92.5102	93.56	924.68
6	1	6	1011.98	4059.73	556.379	102.602	116.24	108.728	104.375	107.99	1011.98
6	2	1	744.055	737.492	721.44	38.0858	53.8844	61.9448	55.7222	52.41	734.33
6	2	2	858.539	816.097	831.49	59.3654	60.0426	64.4274	67.7162	62.89	835.38
6	2	3	890.967	859.943	850.674	70.0698	85.5782	83.2568	94.6382	83.39	867.19
6	2	4	952.863	947.458	908.446	86.7712	93.4774	109.598	91.8008	95.41	936.26
6	2	5	929.366	882.42	943.311	84.5142	84.0306	78.9686	84.7076	83.06	918.37
6	2	6	945.615	868.851	866.465	81.6446	73.1006	71.8754	82.7086	77.33	893.64
6	3	1	767.214	742.465	752.277	43.9216	50.6602	61.3322	58.5594	53.62	753.99
6	3	2	954.828	933.457	954.568	84.1272	106.149	109.179	93.2196	98.17	947.62
6	3	3	930.822	901.983	904.386	79.033	79.2588	83.9984	88.8346	82.78	912.40
6	3	4	920.209	918.114	880.398	70.102	75.164	93.6386	85.3848	81.07	906.24
6	3	5	956.72	896.793	908.204	82.9344	84.4498	96.7338	92.1878	89.08	920.57
6	3	6	915.707	957.991	893.139	73.6164	83.2246	81.7092	88.7056	81.81	922.28
6	4	1	775.837	766.792	757.484	46.7912	56.5282	66.491	51.7886	55.40	766.70
6	4	2	917.537	896.766	822.616	75.9056	73.294	80.097	92.091	80.35	878.97
6	4	3	953.942	961.611	927.694	74.5192	90.479	89.8342	93.7354	87.14	947.75
6	4	4	945.877	932.628	946.576	73.1328	88.899	83.8372	95.7988	85.42	941.69
6	4	5	983.638	882.848	961.182	80.9354	95.154	91.027	92.5424	89.91	942.56
6	4	6	954.859	1526.07	640.141	92.4134	112.661	144.355	97.7334	111.79	1040.36
6	5	1	747.713	740.486	745.359	40.0204	47.4038	54.626	49.0158	47.77	744.52
6	5	2	778.022	786.909	781.924	48.4354	53.6586	69.5216	59.4622	57.77	782.29
6	5	3	905.28	839.477	865.673	73.7132	92.1878	94.1222	89.3828	87.35	870.14
6	5	4	835.531	819.905	816.107	50.1442	64.3952	65.0078	81.5802	65.28	823.85
6	5	5	935.74	912.143	909.663	74.1322	82.8376	84.224	92.7358	83.48	919.18
6	5	6	920.235	842.561	892.87	77.7756	86.1262	87.287	91.7042	85.72	885.22
6	6	1	760.784	728.448	721.382	41.6324	45.6626	53.4974	47.5326	47.08	736.87
6	6	2	812.18	785.947	785.807	48.5	54.7226	56.6894	61.2356	55.29	794.64
6	6	3	920.11	854.267	886.328	75.0674	91.9298	81.3868	82.1928	82.64	886.90
6	6	4	909.265	888.446	850.415	76.615	87.6416	93.7998	88.351	86.60	882.71
6	6	5	943.781	885.814	873.065	74.8738	76.2924	77.1952	91.8976	80.06	900.89
6	6	6	952.71	885.594	934.758	87.1902	95.412	106.922	97.54	96.77	924.35
6	7	1	739.324	717.606	739.467	42.5996	45.5014	53.4974	53.2396	48.71	732.13

6	7	2	840.095	813.075	824.745	50.8214	65.3624	68.7478	69.7796	63.68	825.97
6	7	3	804.427	757.799	767.286	48.7256	53.0784	55.98	57.3664	53.79	776.50
6	7	4	918.008	943.042	860.806	89.415	93.7998	123.398	119.142	106.44	907.29
6	7	5	890.271	855.508	871.749	74.3902	78.0014	86.1908	76.8084	78.85	872.51
6	7	6	880.64	856.236	863.281	76.5504	88.3188	99.8292	89.544	88.56	866.72
6	8	1	757.421	726.977	725.503	46.3074	45.2758	48.113	51.176	47.72	736.63
6	8	2	789.685	742.13	759.114	46.8234	48.5	53.2396	65.2012	53.44	763.64
6	8	3	910.023	857.411	905.588	72.7136	86.7066	81.7414	101.699	85.72	891.01
6	8	4	955.585	933.212	923.807	80.7418	88.8346	100.023	94.5736	91.04	937.53
6	8	5	912.834	836.994	869.306	77.7434	68.8124	73.6486	77.1952	74.35	873.04
6	8	7	959.03	907.405	883.233	88.4154	107.213	102.183	106.6	101.10	916.56
6	9	1	761.979	740.83	727.693	45.0178	45.3402	49.435	54.2712	48.52	743.50
6	9	2	891.158	822.667	852.578	65.7494	72.8748	80.0648	86.4488	76.28	855.47
6	9	3	945.039	894.158	825.662	81.9348	83.8694	86.2552	83.2246	83.82	888.29
6	9	4	936.426	934.839	874.018	90.2532	87.545	106.406	96.8952	95.27	915.09
6	9	5	927.484	884.276	822.439	71.1338	76.7762	75.6798	90.8336	78.61	878.07
6	9	6	889.233	899.959	867.975	95.8634	85.3848	119.11	107.535	101.97	885.72
6	10	1	No ignition								
6	10	2	892.107	879.3	874.766	71.1338	82.902	109.018	91.3818	88.61	882.06
6	10	3	959.174	908.092	952.675	92.091	91.672	129.75	107.051	105.14	939.98
6	10	4	927.267	873.625	863.699	65.3948	72.359	67.168	77.7112	70.66	888.20
6	10	5	944.788	941.118	900.355	74.0356	82.5796	94.7994	97.7334	87.29	928.75
6	10	6	909.236	853.707	864.111	72.5524	81.5802	86.4164	90.9304	82.87	875.68
6	11	1	778.72	760.692	784.17	47.8228	54.6904	61.7514	47.1458	52.85	774.53
6	11	2	904.841	879.803	883.405	79.2588	92.4134	114.209	96.9918	95.72	889.35
6	11	3	885.569	884.192	932.777	85.4814	90.6402	103.118	90.3822	92.41	900.85
6	11	4	954.621	900.014	892.591	78.2592	76.8406	74.906	80.9676	77.74	915.74
6	11	5	907.29	869.272	882.764	66.491	73.7776	93.8966	81.7092	78.97	886.44
6	11	6	933.461	1298.53	716.418	117.627	102.247	162.056	112.855	123.70	982.80
6	12	1	764.864	751.042	726.194	39.1498	45.9528	49.2738	49.9186	46.07	747.37
6	12	2	822.447	808.399	812.847	50.37	65.9428	63.9438	64.234	61.12	814.56
6	12	3	864.966	853.445	841.169	58.7206	68.361	87.5126	79.0008	73.40	853.19
6	12	4	881.689	850.012	816.851	63.1056	66.1362	80.3228	81.3222	72.72	849.52
6	12	5	935.595	692.042	1214.21	88.6734	84.611	131.845	119.045	106.04	947.28
6	12	6	780.686	755.393	778.761	43.2768	55.0128	60.5262	56.915	53.93	771.61
6	13	1	777.953	734.959	758.717	42.9866	47.307	54.5936	56.4638	50.34	757.21
6	13	2	879.249	869.495	889.674	64.0406	85.0624	95.7022	95.2186	85.01	879.47
6	13	3	899.492	852.789	869.942	71.6818	77.421	83.9016	84.8688	79.47	874.07
6	13	4	897.732	923.634	883.201	97.153	120.174	117.691	113.403	112.11	901.52
6	13	5	918.966	1727.74	597.484	88.9636	94.477	118.626	105.923	102.00	1081.40
6	13	6	908.795	862.199	887.385	76.5826	89.1248	103.537	100.345	92.40	886.13

6	14	1	846.586	831.362	796.893	51.6918	63.6858	57.1408	61.042	58.39	824.95
6	14	2	888.201	814.32	877.532	87.029	78.7106	89.8986	98.7652	88.60	860.02
6	14	3	895.032	862.669	898.346	63.1378	78.3238	87.7706	83.7082	78.24	885.35
6	14	4	896.876	810.33	824.758	72.23	96.218	84.7398	94.8962	87.02	843.99
6	14	5	923.015	824.137	921.645	83.9984	86.6422	102.505	91.5106	91.16	889.60
6	14	6	915.271	837.062	843.138	73.2296	87.9318	94.5414	82.9344	84.66	865.16
6	15	1	788.287	764.89	758.356	42.1482	52.5946	52.9494	49.9508	49.41	770.51
6	15	2	880.987	863.273	843.734	68.4578	84.7398	82.9988	81.2256	79.36	862.66
6	15	3	875.809	843.598	842.439	62.0738	74.6482	73.9066	83.3858	73.50	853.95
6	15	4	903.962	856.866	860.066	72.23	85.9006	107.18	103.472	92.20	873.63
6	15	5	894.125	836.2	857.61	66.3942	86.3842	84.9978	94.477	83.06	862.65
6	15	6	901.398	898.181	882.027	89.3182	99.9904	118.755	105.923	103.50	893.87
6	16	1	830.679	813.626	805.174	59.7524	60.0104	51.8532	57.6888	57.33	816.49
6	16	2	893.271	799.146	877.351	92.5746	90.7046	102.441	98.1204	95.96	856.59
6	16	3	856.098	860.057	775.268	69.167	78.0658	85.2558	95.8956	82.10	830.47
6	16	4	953.083	938.178	938.687	84.9978	106.471	100.216	109.566	100.31	943.32
6	16	5	864.326	880.159	863.522	80.9354	79.7424	96.605	100.409	89.42	869.34
6	16	6	843.323	988.598	732.905	85.6426	80.7742	77.6788	87.029	82.78	854.94
6	17	1	773.455	729.78	737.246	40.3428	43.8894	48.3388	53.8198	46.60	746.83
6	17	2	901.662	1645.33	599.48	119.239	117.917	156.575	117.046	127.69	1048.82
6	17	3	855.614	873.548	812.108	77.3564	73.9066	83.4502	88.3188	80.76	847.09
6	17	4	862.213	803.536	818.702	65.8462	77.2276	76.8728	84.8688	76.20	828.15
6	17	5	912.853	794.562	938.864	94.9284	85.3524	103.666	109.469	98.35	882.09
6	17	6	903.392	821.607	851.683	73.0684	66.8134	80.0648	80.7096	75.16	858.89
7	1	1	780.311	768.419	760.864	48.2098	56.4314	59.7202	59.2366	55.90	769.86
7	1	2	851.567	858.978	869.176	59.301	72.6492	81.677	69.167	70.70	859.91
7	1	3	884.981	895.414	866.189	74.229	75.4542	69.4572	83.031	75.54	882.19
7	1	4	988.781	992.237	975.819	90.7692	107.664	91.8654	100.377	97.67	985.61
7	1	5	883.385	845.82	862.777	64.5886	71.4884	67.3938	70.5856	68.51	863.99
7	1	6	893.281	861.77	867.379	70.6502	71.0048	66.1362	67.1358	68.73	874.14
7	2	1	788.37	765.34	777.271	47.3392	56.238	61.1066	59.9458	56.16	776.99
7	2	2	861.567	886.87	857.833	55.6898	78.2914	81.161	67.9096	70.76	868.76
7	2	3	887.039	858.925	893.748	64.911	74.1968	74.8738	86.2552	75.06	879.90
7	2	4	847.711	836.514	881.04	61.1066	72.7136	61.9126	67.555	65.82	855.09
7	2	5	866.039	880.035	880.628	65.9428	76.1636	76.2602	67.5872	71.49	875.57
7	2	6	863.88	856.99	864.308	63.299	71.2628	59.6556	63.299	64.38	861.73
7	3	1	786.837	766.146	788.083	51.9498	61.6224	76.4538	62.364	63.10	780.36
7	3	2	857.636	890.888	857.079	60.9454	85.3202	65.9428	80.9998	73.30	868.53
7	3	3	884.804	870.021	865.717	64.9756	72.8748	67.5226	73.3584	69.68	873.51
7	3	4	889.534	859.232	864.649	73.036	69.7152	64.7176	73.4552	70.23	871.14
7	3	5	904.842	869.858	861.313	67.8452	75.0674	66.2008	70.9726	70.02	878.67

7	3	6	880.92	845.278	862.223	70.908	74.1322	73.552	67.9096	71.63	862.81
7	4	1	797.004	750.635	777.837	52.8204	64.234	55.3674	55.1096	56.88	775.16
7	4	2	865.987	885.862	858.536	60.9776	79.0654	82.2572	76.8406	74.79	870.13
7	4	3	870.068	854.946	881.438	63.2668	74.0034	86.4488	75.1962	74.73	868.82
7	4	4	906.824	898.861	896.195	63.8472	81.5156	71.166	85.965	75.62	900.63
7	4	5	858.572	843.126	836.96	65.7494	65.8462	66.9424	64.911	65.86	846.22
7	4	6	916.542	887.514	881.796	74.906	77.2276	74.7772	75.9378	75.71	895.28
7	5	1	781.187	767.482	784.784	51.4662	64.621	58.6884	54.916	57.42	777.82
7	5	2	893.881	874.454	851.413	66.4588	78.5494	70.7146	81.1932	74.23	873.25
7	5	3	870.499	875.343	864.018	64.492	77.8402	64.363	70.4568	69.29	869.95
7	5	4	881.732	847.066	868.812	69.1348	72.617	72.5846	74.0356	72.09	865.87
7	5	5	884.717	839.487	875.905	67.1358	74.3902	65.7816	68.232	68.88	866.70
7	5	6	883.58	879.578	837.457	62.5252	73.1972	69.1992	73.971	69.72	866.87
7	6	1	776.952	755.081	760.799	49.4028	61.2032	56.0124	54.6582	55.32	764.28
7	6	2	896.241	873.628	877.765	66.0074	72.8426	69.554	78.3238	71.68	882.54
7	6	3	907.419	891.973	867.522	66.7812	74.5836	63.17	69.973	68.63	888.97
7	6	4	865.748	850.842	846.182	69.9086	72.2622	65.3624	63.3312	67.72	854.26
7	6	5	885.504	865.931	886.375	58.624	69.7474	63.2668	74.0678	66.43	879.27
7	6	6	970.224	993.679	996.97	88.8346	95.1862	102.183	97.6044	95.95	986.96
7	7	1	783.322	767.907	750.839	50.4022	56.7862	54.9484	56.4638	54.65	767.36
7	7	2	855.542	840.665	855.796	66.2652	66.8778	63.8148	84.224	70.30	850.67
7	7	3	875.608	896.625	847.958	65.1046	74.487	73.3584	70.231	70.80	873.40
7	7	4	978.15	982.07	985.313	83.418	97.2176	99.3132	91.2206	92.79	981.84
7	7	5	1004.4	1016.44	988.623	92.8004	107.954	105.504	87.3192	98.39	1003.15
7	7	6	899.061	865.623	856.889	69.296	71.295	76.4214	70.1666	71.79	873.86
7	8	1	794.963	755.928	774.609	53.2718	59.4944	52.6592	59.172	56.15	775.17
7	8	2	868.733	872.232	860.16	68.619	72.0044	74.2934	76.5504	72.87	867.04
7	8	3	882.316	853.223	863.295	56.1412	78.4528	62.1382	64.3952	65.28	866.28
7	8	4	881.47	846.377	831.511	60.913	69.0702	60.4294	67.1036	64.38	853.12
7	8	5	893.013	856.383	878.851	65.3302	73.2296	71.5852	72.1656	70.58	876.08
7	8	6	954.266	998.286	974.98	84.1918	100.861	111.694	94.0256	97.69	975.84
7	9	1	789.922	754.821	780.027	46.7266	56.109	58.0436	59.3654	55.06	774.92
7	9	2	879.559	853.132	833.254	57.2376	68.1352	62.8798	64.7176	63.24	855.32
7	9	3	879.559	866.378	877.01	64.105	73.8098	68.5866	74.7772	70.32	874.32
7	9	4	878.741	830.293	875.997	67.8452	69.7152	74.1646	67.2326	69.74	861.68
7	9	5	862.623	841.008	857.137	67.7806	67.039	59.5912	68.619	65.76	853.59
7	9	6	868.273	853.128	859.861	64.5886	69.7474	62.0416	65.8784	65.56	860.42
7	10	1	790.847	763.439	764.053	52.2078	54.1746	49.5316	61.7836	54.42	772.78
7	10	2	857.354	870.38	850.476	65.427	73.4874	61.558	65.169	66.41	859.40
7	10	3	857.354	870.38	850.476	65.427	73.4874	61.558	65.169	66.41	859.40
7	10	4	863.8	879.056	858.675	64.1372	72.3912	64.3308	69.6184	67.62	867.18

7	10	5	883.502	850.619	850.269	69.9408	70.1342	67.3614	66.8134	68.56	861.46
7	10	6	802.431	839.117	840.164	54.916	72.5846	65.2658	62.5896	63.84	827.24
7	11	1	780.458	760.505	741.625	52.5624	55.5932	49.9508	53.175	52.82	760.86
7	11	2	867.121	830.973	860.549	63.7826	70.4244	70.9726	72.7136	69.47	852.88
7	11	3	864.715	854.513	865.776	59.3332	68.0708	67.0068	65.5236	64.98	861.67
7	11	4	844.12	854.447	866.873	55.6898	73.2618	66.4588	66.6522	65.52	855.15
7	11	5	872.833	882.66	873.599	56.367	71.1016	72.0044	71.295	67.69	876.36
7	11	6	872.162	877.871	861.494	68.103	72.907	63.8472	63.6536	67.13	870.51
7	12	1	769.177	759.148	745.745	51.6274	52.8848	49.435	55.6254	52.39	758.02
7	12	2	834.351	855.925	826.699	57.0118	74.4548	61.8158	67.974	65.31	838.99
7	12	3	872.107	870.304	850	63.7504	70.3922	65.298	68.4578	66.97	864.14
7	12	4	866.619	844.729	839.465	65.3624	69.8764	67.8774	69.0058	68.03	850.27
7	12	5	835.307	839.031	854.524	70.1666	73.4874	75.5832	82.5796	75.45	842.95
7	12	6	872.377	872.008	845.652	56.496	69.296	74.0678	70.908	67.69	863.35
7	13	1	789.051	754.687	744.919	46.7266	52.917	50.8858	57.6888	52.05	762.89
7	13	2	866.539	870.414	854.927	57.5276	69.8442	62.7508	68.361	64.62	863.96
7	13	3	878.057	884.513	851.208	68.8124	73.6808	71.6496	67.6838	70.46	871.26
7	13	4	863.653	850.15	852.471	56.5282	68.8446	63.3634	63.0732	62.95	855.42
7	13	5	853.42	848.096	850.691	58.7528	67.2648	62.0416	61.8482	62.48	850.74
7	13	6	953.68	983.555	926.123	82.1282	98.8942	74.6804	88.9958	86.17	954.45
7	14	1	782.006	745.128	742.461	46.5654	50.6924	47.0814	52.627	49.24	756.53
7	14	2	854.392	834.088	847.285	56.3992	69.6184	61.3644	66.2974	63.42	845.26
7	14	3	855.796	838.312	858.743	57.7534	70.9726	69.1348	66.4264	66.07	850.95
7	14	4	868.994	882.071	852.6	61.6868	70.102	68.5544	65.3302	66.42	867.89
7	14	5	875.348	870.074	840.266	66.7488	71.6174	65.7494	71.1338	68.81	861.90
7	14	6	873.764	886.598	855.58	63.5892	71.6174	65.6204	68.103	67.23	871.98
7	15	1	776.944	764.082	758.982	42.922	52.4658	52.0466	51.7886	49.81	766.67
7	15	2	846.758	853.878	830.961	61.8158	65.2012	56.367	64.0084	61.85	843.87
7	15	3	843.369	849.61	857.407	51.982	69.1026	66.8778	64.7822	63.19	850.13
7	15	4	826.735	843.837	845.888	49.435	68.49	56.9796	69.6828	61.15	838.82
7	15	5	832.37	824.201	823.224	54.3358	66.9424	63.976	61.6224	61.72	826.60
7	15	6	851.986	851.047	868.361	52.627	67.8452	59.301	68.8768	62.16	857.13
7	16	1	783.769	762.91	755.978	42.922	54.0134	50.499	53.3362	50.19	767.55
7	16	2	843.022	815.726	850.201	55.0128	70.7468	63.3312	70.0054	64.77	836.32
7	16	3	844.249	857.532	848.776	55.5286	67.297	57.8502	64.6532	61.33	850.19
7	16	4	864.69	886.283	853.583	67.0068	74.358	69.3282	64.4598	68.79	868.19
7	16	5	854.163	847.065	843.733	60.236	64.7498	58.6884	62.1382	61.45	848.32
7	16	6	853.576	856.301	853.658	65.1046	67.2326	62.5574	65.8784	65.19	854.51
7	17	1	777.476	781.339	751.178	43.986	53.175	50.499	56.5926	51.06	770.00
7	17	2	832.318	786.453	834.207	55.7866	60.913	61.7836	63.8794	60.59	817.66
7	17	3	869.479	860.369	858.539	64.3308	69.1026	60.0426	61.2678	63.69	862.80

7	17	4	856.78	816.439	844.011	57.3664	62.7186	57.0764	66.5554	60.93	839.08
7	17	5	873.75	827.825	844.495	66.491	66.5554	66.1686	62.2028	65.35	848.69
7	17	6	853.801	843.929	844.422	57.302	67.3938	58.108	62.493	61.32	847.38
8	1	1	No ignition								
8	1	2	987.621	1006.73	955.012	77.8724	103.73	86.9646	96.089	91.16	983.12
8	1	3	1265.39	4793.49	621.789	165.055	151.191	181.272	131.297	157.20	1265.39
8	1	4	1107.79	3567.35	623.507	104.536	102.183	127.267	101.731	108.93	1107.79
8	1	5	1086.13	1007.33	929.193	118.626	97.024	112.661	106.793	108.78	1007.55
8	1	6	1165.02	972.694	1080.1	163.636	128.009	134.135	141.421	141.80	1072.60
8	2	1									
8	2	2	1002.95	1002.86	1013.25	98.0236	101.957	87.8996	107.696	98.89	1006.35
8	2	3	1113.21	2498.01	701.07	126.3	136.134	135.876	157.575	138.97	1113.21
8	2	4	1096.29	3092.73	593.571	147.225	109.534	122.302	119.464	124.63	1096.29
8	2	5	1098.44	996.86	1023.93	103.634	100.023	113.306	94.9606	102.98	1039.74
8	2	6	1052.4	1051.4	972.128	101.248	102.828	114.016	100.377	104.62	1025.31
8	3	1									
8	3	2	1035	1436.29	783.04	94.4124	100.861	83.5146	106.987	96.44	1084.78
8	3	3	1255.45	1092.19	1071.65	236.729	122.173	116.047	109.824	146.19	1139.76
8	3	4	1126.64	1351.62	1072.27	136.488	318.753	155.414	130.588	185.31	1183.51
8	3	5	1025.3	963.826	983.142	95.2508	85.3524	80.5484	101.473	90.66	990.76
8	3	6	1123.86	1444.25	1006.35	118.626	259.427	162.282	115.209	163.89	1191.49
8	4	1	No ignition								
8	4	2	980.778	1606.79	722.595	85.3524	97.3142	90.1888	106.632	94.87	1103.39
8	4	3	1107.26	1407.14	1009.11	115.305	274.807	144.936	126.429	165.37	1174.50
8	4	4	1276.3	1077.73	1042.04	165.474	134.07	125.558	113.339	134.61	1132.02
8	4	5	1179.87	1527.75	832.428	134.489	149.611	193.46	136.778	153.58	1180.02
8	4	6	1144.61	1155.25	1161.68	145.806	160.831	268.939	135.908	177.87	1153.85
8	5	1	No ignition								
8	5	2	1275.86	1152.31	1050.13	187.785	135.424	159.058	147.16	157.36	1159.43
8	5	3	1278.09	1100.74	1090.51	163.572	162.959	178.306	176.888	170.43	1156.45
8	5	4	1094.1	1026.11	980.108	99.41	102.054	112.081	90.2856	100.96	1033.44
8	5	5	1148.43	2362.8	650.967	138.648	136.972	169.472	130.62	143.93	1148.43
8	5	6	1068.35	1424.11	967.054	130.814	138.648	176.017	147.966	148.36	1153.17
8	6	1	No ignition								
8	6	2	978.37	1662.72	685.239	92.478	100.377	94.8638	100.829	97.14	978.37
8	6	3	1041.8	1026.37	1008.29	88.609	102.924	105.891	93.7032	97.78	1025.49
8	6	4	1106.72	2286.25	657.762	121.85	107.406	117.756	125.204	118.05	1106.72
8	6	5	1318.3	1316.95	985.912	230.571	186.625	209.001	120.432	186.66	1207.05
8	6	6	1044.09	1025.97	1213.17	127.525	121.109	196.072	124.559	142.32	1094.41
8	7	1	No ignition								
8	7	2	1085.18	1586.14	748.731	100.474	125.977	102.247	106.406	108.78	1140.02

8	7	3	1133.77	998.4	1226.54	139.97	134.65	153.157	156.188	145.99	1119.57
8	7	4	1076.98	1234.23	1094.37	115.241	171.213	128.75	117.433	133.16	1135.19
8	7	5	1116.04	1156.38	1069.44	128.202	178.209	120.948	110.598	134.49	1113.95
8	7	6	1291.6	102196	518.174	209.484	142.195	149.095	123.463	156.06	1291.60
8	8	1	No ignition								
8	8	2	1034.11	990.942	999.313	81.967	102.505	79.033	98.1848	90.42	1008.12
8	8	3	1188.25	1378.37	1151.13	139.68	384.334	178.951	137.23	210.05	1239.25
8	8	4	1151.23	1481.82	909.728	136.198	130.62	136.295	171.374	143.62	1180.93
8	8	5	1097.08	4566.95	567.224	113.21	95.412	117.594	100.7	106.73	1097.08
8	8	6	1289.13	3197.83	751.615	172.341	331.295	176.436	145.065	206.28	1289.13
9	1	1	786.019	744.595	745.269	51.434	52.0466	54.0778	55.6898	53.31	758.63
9	1	2	1011.01	908.959	942.089	93.3484	84.7076	84.1596	94.9606	89.29	954.02
9	1	3	1016.32	916.236	958.275	101.893	78.8718	77.9368	90.4468	87.29	963.61
9	1	4	1043.45	1052.24	969.972	101.925	99.3778	123.527	104.375	107.30	1021.89
9	1	5	1018.23	1090.91	979.706	109.308	99.0554	110.34	110.695	107.35	1029.62
9	1	6	1040.21	953.089	975.96	97.6366	92.478	113.081	107.503	102.67	989.75
9	2	1	786.526	747.663	747.201	49.8864	49.6284	53.1428	54.8194	51.87	760.46
9	2	2	945.841	884.945	876.82	85.1268	84.7398	98.8942	83.7404	88.13	902.54
9	2	3	1037.61	996.192	992.502	91.2528	108.341	97.9914	118.465	104.01	1008.77
9	2	4	982.333	1005.03	866.598	75.293	84.8688	92.8326	93.542	86.63	951.32
9	2	5	1045.05	1245.51	817.683	104.794	105.762	93.3808	110.404	103.59	1036.08
9	2	6	977.167	905.228	976.362	85.6426	81.29	78.8074	93.8644	84.90	952.92
9	3	1	810.764	771.214	780.763	49.2416	54.1422	53.0784	53.3362	52.45	787.58
9	3	2	1054.95	979.785	1009.62	101.506	95.3798	88.5444	110.082	98.88	1014.79
9	3	3	1091.78	1017.37	1017.28	97.0886	92.2522	112.919	101.409	100.92	1042.14
9	3	4	1052.64	1055.36	987.929	96.1536	100.055	107.696	118.336	105.56	1031.98
9	3	5	1057.5	1056.75	1017.32	93.6386	102.247	127.074	100.184	105.79	1043.86
9	3	6	1055.01	1054.88	995.221	103.505	102.312	125.623	105.343	109.20	1035.04
9	4	1	820.239	754.744	768.29	53.9488	57.6566	62.9766	71.4562	61.51	781.09
9	4	2	1024.83	991.061	964.217	82.4508	86.9968	80.0004	90.0276	84.87	993.37
9	4	3	1109.33	1059.03	1029.55	103.086	95.9278	113.854	102.344	103.80	1065.97
9	4	4	1059.63	1046.54	991.765	96.5726	94.7348	108.244	113.016	103.14	1032.65
9	4	5	1098.42	1011.85	966.527	107.438	94.5092	103.344	106.922	103.05	1025.60
9	4	6	1051.04	1057.74	937.069	97.669	95.154	103.44	95.541	97.95	1015.28
9	5	1	758.354	756.05	751.577	40.6006	52.498	56.4638	56.7216	51.57	755.33
9	5	2	952.822	914.21	897.25	72.8104	76.0346	78.4204	88.9958	79.07	921.43
9	5	3	961.85	914.036	913.843	85.2236	78.7106	73.7454	89.8664	81.89	929.91
9	5	4	954	858.749	931.663	70.7468	82.5796	71.6496	93.413	79.60	914.80
9	5	5	979.985	902.2	887.706	71.424	90.4468	87.1902	89.544	84.65	923.30
9	5	6	1020.24	957.39	1021.41	92.1232	105.343	103.698	113.693	103.71	999.68
9	6	1	779.538	752.963	772.808	53.562	55.2708	55.6898	62.912	56.86	768.44

9	6	2	877.693	841.593	839.846	68.0386	72.8748	83.9016	76.099	75.23	853.04
9	6	3	1012.65	1030.14	951.504	91.8976	93.7676	96.5404	106.245	97.11	998.10
9	6	4	1001.75	920.371	935.831	93.2196	81.8058	96.9918	86.3842	89.60	952.65
9	6	5	1042.05	997.025	980.697	98.5716	100.764	101.957	108.663	102.49	1006.59
9	6	6	1017.8	1011.28	965.27	96.9918	96.218	101.57	100.506	98.82	998.12
9	7	1	839.959	833.507	841.329	52.498	61.2032	65.975	61.6224	60.32	838.27
9	7	2	1045.7	1007.93	976.196	92.4458	92.0266	102.795	100.829	97.02	1009.94
9	7	3	1102.43	1135.67	997.344	104.859	101.022	126.945	100.345	108.29	1078.48
9	7	4	1054.73	993.068	999.913	95.7022	93.6064	92.2846	105.214	96.70	1015.90
9	7	5	1049.53	1050.94	1035.99	100.764	93.284	135.424	96.1212	106.40	1045.49
9	7	6	1107.96	1059.82	1042.15	103.601	102.892	131.491	117.014	113.75	1069.98
9	8	1	942.593	961.25	917.853	67.5872	86.1908	78.3882	77.0018	77.29	940.57
9	8	2	1035.68	1000.38	969.13	87.8352	87.4804	79.8392	100.055	88.80	1001.73
9	8	3	1056.22	1004.24	992.22	92.2522	89.544	103.988	95.7344	95.38	1017.56
9	8	4	1098.64	1058.84	1003.53	99.7968	101.957	116.176	98.1526	104.02	1053.67
9	8	5	1106.36	1089.93	996.345	115.724	102.892	109.695	103.472	107.95	1064.21
9	8	6	1098	1015.46	1012.71	102.795	95.025	125.784	105.697	107.33	1042.06
10	1	1	723.496	696.429	733.518	37.9246	53.7876	55.174	50.3378	49.31	717.81
10	1	2	784.818	812.857	802.68	51.4018	61.7836	59.559	86.4164	64.79	800.12
10	1	3	835.636	814.665	821.667	67.2326	71.972	101.764	88.4154	82.35	823.99
10	1	4	828.884	822.765	819.266	87.7062	82.3218	89.4794	93.0906	88.15	823.64
10	1	5	898.937	881.788	810.257	65.7816	78.904	79.162	96.8306	80.17	863.66
10	1	6	925.936	882.876	815.135	69.2316	85.4814	102.828	153.641	102.80	874.65
10	2	1	736.123	710.13	703.784	41.3744	47.6294	46.1786	50.241	46.36	716.68
10	2	2	785.439	810.374	798.696	59.3978	78.227	93.0584	108.405	84.77	798.17
10	2	3	829.665	826.14	808.214	65.6204	73.6164	84.4174	88.7378	78.10	821.34
10	2	4	845.636	826.957	820.072	84.6432	94.0256	84.6754	104.794	92.03	830.89
10	2	5	905.593	864.235	835.047	71.8432	79.5166	89.4472	92.7036	83.38	868.29
10	2	6	914.644	875.424	827.276	69.973	77.1952	86.7712	100.893	83.71	872.45
10	3	1	736.324	720.772	732.739	37.6344	59.6878	46.7266	54.3034	49.59	729.95
10	3	2	797.967	795.237	812.474	60.5906	71.1982	66.1686	73.6808	67.91	801.89
10	3	3	823.388	822.073	823.781	107.986	95.541	90.3178	96.7338	97.64	823.08
10	3	4	803.347	802.772	813.077	68.2964	68.7156	82.902	88.2542	77.04	806.40
10	3	5	838.362	825.246	836.811	102.666	97.7012	83.9984	94.7348	94.78	833.47
10	3	6	897.68	873.736	821.074	61.042	74.0034	88.0286	87.6094	77.67	864.16
10	4	1	735.09	744.79	747.268	44.115	52.2078	49.8542	54.4324	50.15	742.38
10	4	2	792.218	833.227	809.388	60.3004	60.0426	64.8144	84.7076	67.47	811.61
10	4	3	797.194	798.944	807.962	61.3644	78.9364	97.0886	86.223	80.90	801.37
10	4	4	934.612	858.618	816.476	79.6134	85.1268	89.673	90.5112	86.23	869.90
10	4	5	807.727	809.322	792.923	52.917	60.4618	67.6838	72.488	63.39	803.32
10	4	6	892.166	881.013	815.143	62.1706	72.617	77.7756	81.2578	73.46	862.77

10	5	1	737.887	724.62	706.436	40.117	44.3086	43.9216	47.8874	44.06	722.98
10	5	2	780.532	812.082	809.081	63.4602	71.1016	68.0708	87.1258	72.44	800.57
10	5	3	882.629	861.429	809.623	63.041	81.2256	77.2276	91.5752	78.27	851.23
10	5	4	873.26	855.282	791.623	58.5272	70.2954	75.2608	68.8446	68.23	840.06
10	5	5	907.848	862.103	801.984	69.6506	84.0306	90.5756	97.6366	85.47	857.31
10	5	6	862.495	874.11	810.878	56.8828	71.7786	70.5534	77.8724	69.27	849.16
10	6	1	717.259	696.166	695.469	39.182	50.9504	57.2052	48.7902	49.03	702.96
10	6	2	769.947	779.546	783.865	50.628	61.7192	58.0114	57.8178	57.04	777.79
10	6	3	821.455	835.07	811.457	76.9696	81.677	109.373	101.57	92.40	822.66
10	6	4	836.546	843.811	809.704	71.4884	94.477	84.2562	84.3852	83.65	830.02
10	6	5	887.748	879.988	819.337	62.235	73.6164	94.6382	83.7404	78.56	862.36
10	6	6	834.193	817.102	824.539	57.5922	63.17	81.967	83.0634	71.45	825.28
10	7	1	730.257	704.478	687.927	42.3418	43.1478	50.8214	47.0814	45.85	707.55
10	7	2	779.467	811.506	779.472	56.4314	60.4294	67.7162	71.553	64.03	790.15
10	7	3	831.493	823.119	811.609	128.944	111.726	94.8316	100.345	108.96	822.07
10	7	4	846.996	859.265	820.247	74.906	90.5112	101.86	93.284	90.14	842.17
10	7	5	882.927	863.83	812.871	57.5922	68.1998	80.7742	74.1968	70.19	853.21
10	7	6	893.065	857.063	812.237	90.9626	107.857	121.27	118.014	109.53	854.12
10	8	1	714.878	750.253	698.015	36.2802	48.6612	53.8844	48.2742	46.78	721.05
10	8	2	766.829	792.709	803.232	48.3064	58.9464	61.2678	75.6154	61.03	787.59
10	8	3	882.021	842.441	815.989	54.7872	69.5862	89.3828	81.8382	73.90	846.82
10	8	4	818.688	820.996	783.269	77.2276	78.8074	84.6432	86.1262	81.70	807.65
10	8	5	875.135	857.627	812.266	56.5282	69.3928	63.557	68.5866	64.52	848.34
10	8	6	866.492	870.192	803.402	66.3942	72.9716	86.5454	80.484	76.60	846.70
11	1	1	No ignition								
11	1	2	852.162	808.906	771.717	53.4008	70.2954	83.7082	81.7736	72.29	810.93
11	1	3	1002.85	966.184	955.688	89.5762	96.2502	89.963	84.482	90.07	974.91
11	1	4	983.478	932.458	924.072	88.222	99.3454	75.4864	83.2246	86.57	946.67
11	1	5	1044.76	1050.82	943.564	116.595	108.341	110.501	99.4422	108.72	1013.05
11	1	6	1099.15	943.111	896.92	107.922	94.3802	113.725	106.342	105.59	979.73
11	2	1	781.366	788.763	769.475	54.11	56.0124	63.976	66.2008	60.07	779.87
11	2	2	832.095	808.017	800.633	73.3908	70.618	91.8332	76.1958	78.01	813.58
11	2	3	1131.36			120.077	114.564	122.624	110.179	116.86	1131.36
11	2	4	1018.1	953.001	928.343	100.087	92.1232	76.6794	94.0578	90.74	966.48
11	2	5	977.559	1051.44	896.217	92.8326	104.343	97.9268	83.6436	94.69	975.07
11	2	6	1006.52			83.7082	108.986	94.6382	87.8996	93.81	1006.52
11	3	1	No ignition								
11	3	2	833.365	802.643	779.571	64.5564	92.5424	91.414	97.5722	86.52	805.19
11	3	3	1040.11	988.727	957.651	114.725	97.1208	100.506	92.7036	101.26	995.50
11	3	4	1062.34	1042.97	937.261	112.919	102.795	95.2508	104.988	103.99	1014.19
11	3	5	1027.1			118.626	105.439	99.0876	121.915	111.27	1027.10

11	3	6	No ignition								
11	4	1	No ignition								
11	4	2	828.686	829.141	811.054	70.4568	87.287	88.1576	70.7792	79.17	822.96
11	4	3	1039.24	1369.12	791.348	100.7	107.47	88.351	100.764	99.32	1066.57
11	4	4	1020.83	1003.6	922.891	86.8678	92.3168	89.3828	92.4458	90.25	982.44
11	4	5	1033.37			95.4442	101.248	85.03	93.1872	93.73	1033.37
11	4	6	1083.09	1441.83	766.595	110.243	105.826	99.8292	106.342	105.56	1097.17
11	5	1	792.675	773.495	753.975	49.5316	66.104	50.37	59.0108	56.25	773.38
11	5	2	807.377	817.676	780.317	51.3694	58.8174	55.3998	67.7484	58.33	801.79
11	5	3	1096.22	1011.87	984.813	116.659	101.216	96.476	112.403	106.69	1030.97
11	5	4	1170.54			125.913	107.922	108.986	94.0256	109.21	1170.54
11	5	5	983.097			95.9278	100.571	93.284	105.052	98.71	983.10
11	5	6	1035.72			99.281	90.2856	98.604	92.5424	95.18	1035.72
11	6	1	No ignition								
11	6	2	827.308	803.409	798.374	67.2648	82.3862	71.7142	66.6844	72.01	809.70
11	6	3	1041.33	997.841	965.179	110.824	91.4462	105.729	99.2166	101.80	1001.45
11	6	4	1020.35	971.787	1014.43	90.1566	99.6034	95.7022	84.9656	92.61	1002.19
11	6	5	1072.94	1377.74	781.372	106.632	107.696	97.669	102.602	103.65	1077.35
11	6	6	990.078			123.591	116.337	89.7374	94.7348	106.10	990.08
11	7	1	No ignition								
11	7	2	838.156	785.021	799.8	73.8744	79.968	88.8024	67.7484	77.60	807.66
11	7	3	996.157	1002.29	905.226	92.5746	103.44	98.5394	101.054	98.90	967.89
11	7	4	1079.49			115.692	88.093	118.11	103.44	106.33	1079.49
11	7	5	968.472	1049.11	989.959	96.1858	123.011	110.437	95.2186	106.21	1002.51
11	7	6	1045.17			98.7652	102.989	110.953	85.3848	99.52	1045.17
11	8	1	794.215	783.583	767.592	54.1746	59.3654	61.8158	65.6204	60.24	781.80
11	8	2	1039.38	1001.74	955.546	112.113	101.312	85.5782	96.6372	98.91	998.89
11	8	3	1056.24			104.246	92.5424	86.0618	91.285	93.53	1056.24
11	8	4	944.543	982.563	937.725	102.602	86.6744	99.023	87.0614	93.84	954.94
11	8	5	1089.16			138.616	133.103	125.881	119.658	129.31	1089.16
11	8	6	1045.54	899.954	850.944	90.8658	106.793	82.9344	101.667	95.57	932.15
12	1	1	806.295	848.493	796.34	54.0456	62.3962	57.2376	55.5932	57.32	817.04
12	1	2	1341.96	1139.87	1230.9	160.831	180.692	225.444	134.844	175.45	1237.58
12	1	3	997.304	989.62	930.477	80.8064	96.6694	79.5812	94.9606	88.00	972.47
12	1	4	1204.1	1207.37	1074.81	154.028	131.845	195.814	197.942	169.91	1162.09
12	1	5	1388.28	1170.96	984.947	244.757	167.408	134.36	112.403	164.73	1181.40
12	1	6	1153.03	1446.62	917.674	137.875	127.396	133.038	180.08	144.60	1172.44
12	2	1	869.777	839.068	819.777	56.3024	63.7826	57.3342	57.2052	58.66	842.87
12	2	2	903.49	893.165	835.548	77.2598	84.9334	74.3902	97.7656	83.59	877.40
12	2	3	1272.58	1046.84	987.873	135.166	145.355	119.98	127.912	132.10	1102.43
12	2	4	1181.59	1524.14	808.726	146.129	148.353	144.097	172.019	152.65	1171.49

12	2	5	1047.58	992.751	944.557	96.7016	87.545	85.5136	86.2876	89.01	994.96
12	2	6	1283.25	1080.87	1065.64	247.014	140.39	156.865	126.203	167.62	1143.25
12	3	1	852.395	826.985	799.715	51.0148	58.2692	55.432	61.5256	56.56	826.37
12	3	2	1023.08	992.486	940.256	77.7756	91.5752	88.6412	94.3802	88.09	985.27
12	3	3	1224.77	1187.58	1088.6	160.638	170.891	131.845	131.394	148.69	1166.98
12	3	4	1404.24	1126.64	998.818	205.519	145.806	169.472	196.168	179.24	1176.57
12	3	5	1472.77	1144.02	962.365	276.613	138.52	124.107	120.335	164.89	1193.05
12	3	6	1321.52	1227.24	985.635	243.177	141.131	118.658	113.822	154.20	1178.13
12	4	1	849.353	837.045	811.069	49.5962	67.7806	61.7514	61.977	60.28	832.49
12	4	2	950.599	924.944	874.921	69.8764	83.16	81.7092	96.7338	82.87	916.82
12	4	3	1042.19	969.416	944.197	81.967	84.7722	86.7712	89.6406	85.79	985.27
12	4	4	1388.69	1120.97	1032.66	174.856	150.352	107.535	144.71	144.36	1180.77
12	4	5	1377.9	1121.55	1159.37	127.912	135.263	146.935	129.943	135.01	1219.61
12	4	6	1342.5	1151.59	1018.62	215.449	187.012	116.95	126.493	161.48	1170.90
12	5	1	852.814	850.427	806.166	54.5292	68.7802	64.3952	69.6184	64.33	836.47
12	5	2	1000.79	994.891	900.484	76.1312	94.219	90.6402	96.9918	89.50	965.39
12	5	3	959.488	929.229	914.594	72.0366	82.354	93.3808	100.152	86.98	934.44
12	5	4	1548.87	1192.59	1183.88	320.526	143.839	146.193	142.872	188.36	1308.45
12	5	5	1134.62	1182.42	1054.34	102.699	136.649	140.067	142.421	130.46	1123.79
12	5	6	1342.94	1105.34	1057.99	179.886	127.041	145.806	202.971	163.93	1168.76
12	6	1	No ignition								
12	6	2	935.535	898.707	866.094	88.8668	81.5802	97.3142	97.2498	91.25	900.11
12	6	3	1086.9	1038.95	921.899	115.144	98.8296	87.1902	85.4492	96.65	1015.92
12	6	4	1032.01	1252.59	821.154	120.851	106.89	105.052	109.341	110.53	1035.25
12	6	5	1095.58			131.91	106.89	99.6356	105.471	110.98	1095.58
12	6	6	1042.04	963.688	944.427	89.8664	98.8942	92.349	87.9964	92.28	983.39
12	7	1	802.901	771.159	774.419	54.6582	52.7558	54.6582	63.7182	56.45	782.83
12	7	2	1552.05	1132.46	1100.23	384.173	147.966	134.36	155.705	205.55	1261.58
12	7	3	1048.29			95.6376	106.858	113.177	88.8024	101.12	1048.29
12	7	4	951.482	1078.84	932.749	87.6416	116.047	86.9968	104.407	98.77	987.69
12	7	5	1128.79			110.404	119.561	203.842	101.57	133.84	1128.79
12	7	6	1064.59			102.634	97.9268	119.368	88.7378	102.17	1064.59
12	8	1	844.154	835.316	827.695	55.98	66.2974	61.1066	62.5252	61.48	835.72
12	8	2	965.087	948.306	880.635	89.8986	93.7676	89.5762	90.7692	91.00	931.34
12	8	3	1004.44			82.7408	105.729	127.815	91.2206	101.88	1004.44
12	8	4	1338.51	1270.88	1472.45	183.207	228.281	346.546	201.553	239.90	1360.61
12	8	5	1014.15	973.385	930.658	92.0588	94.6382	76.2602	84.2562	86.80	972.73
12	8	6	1049.5	1043.5	928.406	96.4114	110.437	92.8326	91.027	97.68	1007.14
13	1	1									
13	1	2	865.135	846.956	828.601	57.979	75.035	79.968	77.1952	72.54	846.90
13	1	3	1255.49	2624.88	785.958	159.251	200.682	121.915	123.753	151.40	1255.49

13	1	4	1211.4	1338.35	1083.47	186.689	340.71	118.497	144.259	197.54	1211.07
13	1	5	903.287	912.844	890.578	65.975	75.6154	86.4488	87.8674	78.98	902.24
13	1	6	878.369	868.717	858.982	64.1372	81.032	102.151	97.024	86.09	868.69
13	2	1	No ignition								
13	2	2	888.135	868.857	844.659	65.9106	94.4124	98.1848	82.902	85.35	867.22
13	2	3	873.087	851.005	871.887	59.6878	79.0008	79.42	90.221	77.08	865.33
13	2	4	901.981	912.342	880.307	68.232	81.1932	77.3564	86.61	78.35	898.21
13	2	5	919.427	883.112	863.883	72.5202	66.8456	68.5544	75.5832	70.88	888.81
13	2	6	886.586	877.405	902.767	70.0376	93.0584	84.3852	76.5504	81.01	888.92
13	3	1	No ignition								
13	3	2	870.488	858.569	864.039	75.6798	95.3474	86.61	90.479	87.03	864.37
13	3	3	1284.74	1259.38	1175.98	186.947	183.884	166.344	128.686	166.47	1240.03
13	3	4	882.877	863.206	928.684	66.4264	78.904	71.2306	77.3242	73.47	891.59
13	3	5	898.783	900.872	870.969	69.5862	83.3534	73.8098	85.2236	77.99	890.21
13	3	6	874.833	877.7	877.089	68.619	89.9954	88.6734	88.1576	83.86	876.54
13	4	1	No ignition								
13	4	2	909.892	934.585	904.457	70.618	85.9328	79.5166	86.1586	80.56	916.31
13	4	3	923.552	940.944	935.461	71.4884	84.9334	73.0038	80.4518	77.47	933.32
13	4	4	1473.83	1206.01	1015.39	187.624	165.474	123.656	132.813	152.39	1231.74
13	4	5	1480.13	1425.76	923.345	242.049	171.181	127.976	148.45	172.41	1276.41
13	4	6	1123.92	970.367	1132.75	156.511	105.729	108.663	124.172	123.77	1075.68
13	5	1	No ignition								
13	5	2	1248.36	1035.96	1158.97	150.61	129.621	130.975	134.135	136.34	1147.76
13	5	3	1239.39	1324.07	1075.26	164.41	177.21	126.751	157.317	156.42	1212.91
13	5	4	1158.63	998.748	1184.28	103.118	113.79	128.17	111.372	114.11	1113.89
13	5	5	1499.31	1043.04	1120.95	375.21	123.011	158.896	131.91	197.26	1221.10
13	5	6	1272.55	1067.8	1087.91	153.19	122.882	115.982	116.015	127.02	1142.75
13	6	1	No ignition								
13	6	2	977.5	918.225	946.962	74.616	84.2884	83.6436	92.1556	83.68	947.56
13	6	3	1233.93	1208.66	1092.96	127.461	211.451	111.63	110.05	140.15	1178.52
13	6	4	1199.22	1672.08	812.733	138.1	149.643	136.972	104.762	132.37	1228.01
13	6	5	1262.45	1097.77	1199.13	169.311	116.982	126.912	152.255	141.37	1186.45
13	6	6	1364.97	1197	953.971	149.74	171.826	123.398	109.889	138.71	1171.98
13	7	1	No ignition								
13	7	2	901.906	922.599	945.85	66.8778	85.417	72.6492	87.674	78.15	923.45
13	7	3	1267.6	1208.86	1024.98	164.861	165.119	143.485	122.205	148.92	1167.15
13	7	4	1167.28	1170.7	1011.25	119.11	185.077	120.4	115.821	135.10	1116.41
13	7	5	1347.03	1068.12	1333.78	168.279	165.055	257.332	148.869	184.88	1249.64
13	7	6	1156.13			146.935	142.711	285.318	125.397	175.09	1156.13
13	8	1	No ignition								
13	8	2	942.921	943.907	908.903	63.9438	86.223	90.3822	110.437	87.75	931.91

13	8	3	1294.77	1094.99	1130.2	183.207	134.328	125.171	110.888	138.40	1173.32
13	8	4	1218.74	1220.57	990.343	147.547	237.277	109.405	125.977	155.05	1143.22
13	8	5	1282.02	1290.64	995.306	169.923	196.781	164.894	113.371	161.24	1189.32
13	8	6	1318.61	1216.52	1045.17	144.871	219.963	126.139	121.463	153.11	1193.43

Firing Cycle 2 Data

Case	Run	V12	V23	V34	P1_max	P2_max	P3_max	P4_max	Pmax Avg	V avg
1	1	2033.725	5540.555	3351.728	792.175	423.638	241.759	308.178	441.4375	3642.003
1	2	2665.983	1505.307	2498.503	168.795	199.747	152.674	150.191	167.8518	2223.264
1	3	3038.928	1941.152	2132.009	305.598	319.624	248.046	269.132	285.6	2370.696
1	4	9567.637	1400.644	2045.158	591.751	411.676	308.274	252.753	391.1135	4337.813
1	5	1639.868	2121.637	2311.199	309.306	305.792	271.712	355.574	310.596	2024.235
1	6	1237.726	1309.913	1306.214	126.816	160.928	143.904	144.097	143.9363	1284.617
1	7	2283.233	1411.257	1626.305	292.637	257.235	255.913	241.759	261.886	1773.598
1	8	2372.266	1754.169	1586.958	322.654	279.805	295.152	233.311	282.7305	1904.464
1	9	1340.175	1358.862	1329.21	183.239	174.953	174.018	161.766	173.494	1342.749
1	10	2325.657	1927.546	1746.76	346.901	385.914	313.659	217.577	316.0128	1999.987
1	11	2301.742	2104.962	1889.791	415.674	427.7	342.258	566.15	437.9455	2098.832
1	12	2179.327	1977.838	1718.022	316.464	385.43	292.863	300.504	323.8153	1958.396
1	13	2356.188	2076.747	1924.33	308.597	339.034	437.599	285.802	342.758	2119.088
1	14	2219.263	1578.622	1608.908	369.728	252.27	205.583	305.115	283.174	1802.265
1	15	1234.692	1385.921	1326.2	156.156	165.925	157.704	141.711	155.374	1315.604
1	16	1409.126	1427.311	1441.709	94.2836	108.696	109.824	160.799	118.4007	1426.049
1	17	1393.916	1388.451	1418.745	81.9026	95.4442	102.183	117.079	99.1522	1400.371
1	18	1371.102	1352.118	1419.581	94.2836	92.0266	108.341	92.7682	96.85485	1380.934
1	19	1580.61	1794.181	1593.46	167.795	175.179	180.37	157.51	170.2135	1656.084
1	20	1670.526	1689.827	1708.645	225.122	158.477	173.76	153.286	177.6613	1689.666
2	1	1771.69	1535.5	1892.48	218.641	308.565	404.421	300.569	308.049	1733.223
2	2	1972.79	1791.85	1596.59	366.698	207.098	194.911	299.053	266.94	1787.077
2	3	1967.97	1597.57	1790	372.985	245.724	277.999	280.288	294.249	1785.18
2	4	802.605	786.645	821.529	48.3064	55.3352	58.9786	56.3348	54.73875	803.593
2	5	814.02	807.376	812.252	58.3014	64.621	62.6864	66.7488	63.0894	811.216
2	6	2167.76	1716.52	1732.34	728.688	243.081	249.4	283.416	376.1463	1872.207
2	7	1979.45	1713.9	1653.41	377.015	210.806	220.543	265.553	268.4793	1782.253
2	8	1435.72	1637.49	2015.43	230.506	272.647	456.364	274.001	308.3795	1696.213
2	9	2022.81	1695.41	1319.3	629.734	259.331	380.078	763.156	508.0748	1679.173
2	10	1858.63	1497.49	1840.43	341.71	307.888	471.131	320.623	360.338	1732.183
2	11	1989.05	1418.95	1876.72	281.481	233.956	321.3	289.155	281.473	1761.573
2	12	2230.41	1607.61	1490.77	518.85	261.265	224.09	414.094	354.5748	1776.263
2	13	1944.41	1379.29	1966.99	375.693	243.532	312.659	327.588	314.868	1763.563
2	14	2219.86	1726.53	1623.04	616.675	274.968	196.62	295.249	345.878	1856.477
2	15	1925.64	1280.01	2255.46	312.885	196.072	489.38	290.122	322.1148	1820.37
2	16	1950.7	1283	1969.9	326.459	267.101	436.728	311.724	335.503	1734.533
2	17	1775.34	1882.29	1428.59	255.139	233.924	208.904	398.456	274.1058	1695.407
2	18	2003.51	1439.88	1538.95	504.889	228.572	301.89	642.599	419.4875	1660.78
2	19	2012.32	1620.41	1377.4	397.296	284.996	194.137	588.398	366.2068	1670.043

2	20	1805.92	1602.7	1492.31	420.51	252.657	280.127	360.604	328.4745	1633.643
3	1	964.736	953.2976	911.554	53.93203	65.2942	65.97803	71.90615	64.2776	943.1959
3	2	983.57	964.2633	934.1725	61.49416	79.05012	70.46213	78.97421	72.49516	960.6686
3	3	952.1976	951.1443	892.9007	60.29912	69.2005	62.5059	76.00738	67.00322	932.0809
3	4	938.9806	946.1633	908.0236	62.35626	69.27543	60.56105	75.74568	66.98461	931.0558
3	5	965.4355	941.7947	901.8466	61.6083	67.81685	62.73025	67.21829	64.84342	936.359
3	6	953.4827	955.2082	911.1721	63.24203	69.74012	76.27616	75.02213	71.07011	939.9543
3	7	964.7371	979.6205	907.4642	57.80797	67.95407	73.88219	76.73228	69.09413	950.6073
3	8	854.9751	849.2925	817.844	52.27908	64.83897	63.34944	66.19305	61.66514	840.7039
3	9	860.2167	872.7936	793.5039	50.6541	62.36769	57.22185	63.65415	58.47445	842.1714
3	10	864.3758	863.1966	831.5633	52.65141	58.67757	54.98745	65.4822	57.94966	853.0452
3	11	881.1642	870.1497	820.6485	53.66718	67.7166	62.36769	64.19574	61.9868	857.3208
3	12	1003.248	968.7632	918.4865	57.1621	68.41019	68.2961	83.07834	69.23668	963.4992
3	13	910.967	957.6266	870.6365	51.38602	67.61204	63.85018	86.68839	67.38416	913.0767
3	14	916.7856	923.4867	868.7315	58.84532	63.74841	52.86863	63.13991	59.65057	903.0013
3	15	865.4282	857.9712	833.8231	44.99518	62.88949	61.77994	63.10417	58.19219	852.4075
3	16	908.6749	910.7017	864.6389	54.12116	59.66849	60.52741	68.61554	60.73315	894.6718
3	17	937.5848	937.5171	861.0936	62.88949	71.12081	73.51863	68.11448	68.91085	912.0652
3	18	963.6776	943.8135	918.2732	53.47591	63.35611	73.23608	70.91825	65.24659	941.9214
3	19	976.2815	955.5688	913.4115	57.04801	70.38623	78.44219	75.78209	70.41463	948.4206
3	20	953.6654	942.7044	915.012	64.15403	69.36014	86.08023	77.15021	74.18615	937.1273
4	1	818.544	808.839	773.421	45.7594	55.3998	55.98	61.0098	54.53725	800.268
4	2	834.524	818.143	792.612	52.1756	67.0712	59.7846	67.0068	61.50955	815.093
4	3	820.86	819.952	769.742	51.982	59.6556	53.8844	65.5236	57.7614	803.518
4	4	809.466	815.658	782.779	53.7554	59.7202	52.2078	65.298	57.74535	802.6343
4	5	832.272	811.892	777.454	53.1106	58.4628	54.0778	57.9468	55.8995	807.206
4	6	808.996	810.46	773.097	53.6586	59.172	64.7176	63.6536	60.30045	797.5177
4	7	818.545	831.173	769.951	49.048	57.6566	62.6864	65.1046	58.6239	806.5563
4	8	814.262	808.85	778.899	49.7896	61.7514	60.3328	63.041	58.7287	800.6703
4	9	819.254	831.232	755.718	48.242	59.3978	54.497	60.623	55.68995	802.068
4	10	823.215	822.092	791.965	50.1442	55.8834	52.369	62.364	55.19015	812.424
4	11	839.204	828.714	781.57	51.1116	64.492	59.3978	61.1388	59.03505	816.496
4	12	851.22	821.961	779.303	48.5	58.0436	57.9468	70.489	58.74485	817.4947
4	13	772.923	812.512	738.704	43.5992	57.3664	54.1746	73.552	57.17305	774.713
4	14	825.933	831.97	782.641	53.0138	57.431	47.6294	56.8828	53.73925	813.5147
4	15	779.665	772.947	751.192	40.5362	56.6572	55.6576	56.8506	52.4254	767.9347
4	16	818.626	820.452	778.954	48.7578	53.7554	54.5292	61.8158	54.71455	806.0107
4	17	844.671	844.61	775.76	56.6572	64.0728	66.233	61.3644	62.08185	821.6803
4	18	817.646	800.792	779.122	45.3724	53.7554	62.1382	60.1716	55.3594	799.1867
4	19	828.34	810.766	774.997	48.4032	59.7202	66.5554	64.2984	59.7443	804.701
4	20	809.151	799.851	776.355	54.4324	58.8496	73.036	65.4592	62.9443	795.119

5	1	1773.96	1784.46	1976.42	226.831	236.568	232.537	286.446	245.5955	1844.947
5	2	1487.85	1996.52	2100.27	225.896	446.53	354.865	248.465	318.939	1861.547
5	3	2070.23	2199.8	1779.1	968.163	373.726	233.956	285.705	465.3875	2016.377
5	4	1511.62	1951.93	1811.26	271.486	410.741	293.314	549.771	381.328	1758.27
5	5	1993.3	1777.66	1989.6	364.086	268.165	230.796	294.958	289.5013	1920.187
5	6	1858.66	1791.17	1788.37	296.603	294.765	257.622	329.296	294.5715	1812.733
5	7	1774.39	1616.43	2253.47	245.08	248.401	531.328	298.118	330.7318	1881.43
5	8	1628.63	1982.58	1975.13	262.652	293.25	361.893	280.482	299.5693	1862.113
5	9	1985.67	1601.3	1995.33	240.662	300.44	297.989	328.684	291.9438	1860.767
5	10	1613.89	1973.41	1971.25	224.09	317.173	224.928	272.776	259.7418	1852.85
5	11	1549.91	2195.45	1795.31	290.799	537.906	286.317	280.804	348.9565	1846.89
5	12	1786.22	1771.91	2116.73	211.677	311.886	303.116	259.46	271.5348	1891.62
5	13	1507.6	1900.7	2008.63	256.655	337.002	336.293	272.518	300.617	1805.643
5	14	1606.59	1792.14	2201.95	188.237	245.596	341.839	277.515	263.2968	1866.893
5	15	1595	2011.33	1978.03	249.658	433.472	226.895	295.829	301.4635	1861.453
5	16	1491.77	1961.96	2214.52	206.357	639.987	282.384	256.268	346.249	1889.417
5	17	1247.63	1001.07	1989.04	156.446	151.61	429.538	299.924	259.3795	1412.58
5	18	1480.6	1952.21	1992.47	215.675	248.368	341.355	284.383	272.4453	1808.427
5	19	1602.44	2032.69	1896.59	313.143	267.714	310.789	260.008	287.9135	1843.907
5	20	1514.64	2521.75	1769.39	334.971	534.424	240.63	312.788	355.7033	1935.26
6	1	1781.65	1932.18	1793.82	229.99	234.311	269.036	259.331	248.167	1835.883
6	2	1981.04	1793.71	1467.51	249.465	302.568	260.072	370.889	295.7485	1747.42
6	3	990.487	990.553	968.709	73.1328	94.8962	80.8064	77.9046	81.685	983.2497
6	4	1098.97	1008.3	979.386	101.119	89.2216	130.201	105.407	106.4872	1028.885
6	5	2048.79	1758.18	1623.93	308.919	253.43	230.119	324.654	279.2805	1810.3
6	6	2198.82	1785.65	1874.78	699.766	276.516	245.66	311.466	383.352	1953.083
6	7	1968.49	1780.7	1615.82	708.794	198.006	280.03	302.019	372.2123	1788.337
6	8	1989.38	1620.54	1775.03	290.251	245.434	226.992	317.238	269.9788	1794.983
6	9	1819.64	1785.87	1950.35	552.931	394.329	301.923	285.286	383.6173	1851.953
6	10	1774.12	1936.67	1817.69	266.327	226.573	293.604	235.923	255.6068	1842.827
6	11	1968.11	1468.69	2021.41	341.065	266.94	352.672	292.024	313.1753	1819.403
6	12	1756.93	1602.39	1786.69	264.425	312.563	265.167	405.969	312.031	1715.337
6	13	1001.58	1175.72	843.915	80.226	93.0906	97.153	93.4452	90.9787	1007.072
6	14	989.188	994.09	971.548	78.5494	85.3202	89.963	85.9974	84.9575	984.942
6	15	1814.23	1762.55	1953.91	251.302	419.414	302.987	247.046	305.1873	1843.563
6	16	1000.18	1007.24	958.093	77.0664	93.026	102.763	85.6104	89.61645	988.5043
6	17	1757.36	1623.39	2004.92	201.875	314.981	251.109	247.627	253.898	1795.223
6	18	1967.16	1802.93	1478.37	467.52	317.044	260.878	547.998	398.36	1749.487
6	19	993.232	1026.69	987.653	76.0668	96.9274	84.4498	92.1232	87.3918	1002.525
6	20	1603.59	1983.82	1781.99	288.349	394.329	228.088	308.726	304.873	1789.8
7	1	1979.9	1983.31	1965.75	359.153	358.089	287.801	382.529	346.893	1976.32

7	2	1981.85	1970.04	1964.64	291.089	294.894	311.144	319.978	304.2763	1972.177
7	3	1966.2	1961.79	1794.33	351.931	346.03	291.025	353.381	335.5918	1907.44
7	4	1982.53	1959.18	1975.34	297.248	384.786	305.856	303.019	322.7273	1972.35
7	5	1964.91	1915.68	1907.51	322.719	341.162	247.981	271.196	295.7645	1929.367
7	6	1962.9	1902.25	1850.25	349.609	312.24	251.851	344.805	314.6263	1905.133
7	7	1982.87	1964.55	1921.98	294.604	327.007	274.775	301.955	299.5853	1956.467
7	8	1972.31	1911.34	1842.19	222.607	294.636	284.802	310.886	278.2328	1908.613
7	9	2210.92	1974.7	1969.83	443.757	284.415	286.414	315.174	332.44	2051.817
7	10	2074.11	1795.37	1960.81	318.56	324.17	298.892	265.424	301.7615	1943.43
7	11	1945.07	1969.47	1787.53	297.57	299.859	259.718	378.627	308.9435	1900.69
7	12	1797.6	1973.85	1972.68	245.531	338.357	258.589	314.014	289.1228	1914.71
7	13	1986.49	1976.33	1782.44	290.412	337.647	262.265	270.035	290.0898	1915.087
7	14	1970.27	1969.45	1786.68	419.962	364.763	234.633	367.729	346.7718	1908.8
7	15	1943.59	1965.81	1963.18	302.6	307.372	326.653	270.744	301.8423	1957.527
7	16	1991.16	1769	1990.92	352.769	298.344	283.641	356.735	322.8723	1917.027
7	17	1762.6	1783.04	2193.51	247.724	392.782	408.484	308.661	339.4128	1913.05
7	18	1950.99	1943.89	1802.19	250.496	443.08	254.849	312.466	315.2228	1899.023
7	19	1551.08	2395.4	1991.03	427.829	456.977	336.357	318.366	384.8823	1979.17
7	20	2211.31	1780.45	1974.76	515.368	245.531	292.572	326.62	345.0228	1988.84
8	1	1517.73	1994.74	2134.19	221.704	329.425	349.093	283.416	295.9095	1882.22
8	2	1824.27	1787.75	1959.69	287.027	401.358	323.59	284.222	324.0493	1857.237
8	3	1623.32	2220.72	1763.77	286.511	336.583	244.37	287.543	288.7518	1869.27
8	4	1924.89	1500.9	2028.59	327.136	242.887	398.65	322.139	322.703	1818.127
8	5	1278.53	1988.11	1981.31	344.096	393.362	349.093	325.975	353.1315	1749.317
8	6	1258.92	2263.39	1783.58	197.136	860.339	229.378	257.299	386.038	1768.63
8	7	1790.18	1795.23	1975.16	238.244	317.625	185.593	292.83	258.573	1853.523
8	8	1733.09	1924.12	1871.66	387.913	335.132	286.801	320.462	332.577	1842.957
8	9	1496.94	1994.95	1959.14	329.812	796.303	323.428	394.362	460.9763	1817.01
8	10	1388.99	1812.1	1797.45	421.381	542.903	238.857	433.117	409.0645	1666.18
8	11	1593.6	1796.2	1995.54	251.367	318.656	330.489	306.243	301.6888	1795.113
8	12	1490.78	1986.47	1991.7	262.781	591.784	290.67	315.787	365.2555	1822.983
8	13	1789.26	1736.64	2078.16	250.335	368.471	443.37	332.682	348.7145	1868.02
8	14	1640.92	1462.92	2260.92	220.866	211.387	778.021	333.069	385.8358	1788.253
8	15	1487.99	1968.98	1968.57	195.846	343.676	257.17	246.434	260.7815	1808.513
8	16	1379.13	1767.2	1987.73	279.643	510.048	307.468	339.034	359.0483	1711.353
8	17	1701.22	1540.29	2093.56	291.928	260.685	399.811	332.392	321.204	1778.357
8	18	2213.34	1910.34	1666.26	563.732	344.934	210.258	290.799	352.4308	1929.98
8	19	1608.94	1988.88	1705.01	280.546	461.619	209.42	358.863	327.612	1767.61
8	20	1396.98	2015.88	1980.37	216.062	667.136	278.934	273.356	358.872	1797.743
9	1	1478.43	1963.9	1866.97	259.331	593.912	298.279	343.064	373.6465	1769.767
9	2	1962.43	1942.28	1591.36	756.966	360.023	213.547	292.282	405.7045	1832.023

9	3	2066.58	1792.66	1612.16	507.662	377.563	400.165	415.19	425.145	1823.8
9	4	1629.47	2198.27	1938.92	292.508	728.591	239.308	290.735	387.7855	1922.22
9	5	1616.76	2170.26	1796.86	323.751	509.693	247.53	226.927	326.9753	1861.293
9	6	1977.89	1773.3	1783.43	346.675	289.284	205.551	279.031	280.1353	1844.873
9	7	1900.16	1776.38	1949.86	388.01	293.411	505.05	294.185	370.164	1875.467
9	8	1582.89	1813.75	1931.9	368.471	504.857	329.619	265.715	367.1655	1776.18
9	9	2252.94	1779.17	1840.47	666.039	307.791	245.176	298.602	379.402	1957.527
9	10	1786.38	1807.82	1819.17	292.089	323.17	314.304	341.323	317.7215	1804.457
9	11	1463.27	2020.79	2192.26	228.539	312.466	323.557	273.163	284.4313	1892.107
9	12	1637.43	1777.09	2084.23	253.108	222.22	341.71	329.651	286.6723	1832.917
9	13	1792.69	1837.09	2007.34	205.486	240.243	249.336	303.664	249.6823	1879.04
9	14	1972.49	1767.24	1796.39	309.822	242.275	248.949	305.405	276.6128	1845.373
9	15	1581.83	1815.82	1978.18	359.088	291.928	332.843	309.919	323.4445	1791.943
9	16	1776.52	1632.55	1984.41	285.35	244.403	308.597	289.735	282.0213	1797.827
9	17	1650.23	1967.67	1980.25	148.515	382.174	286.479	249.368	266.634	1866.05
9	18	1608.94	2002.76	1906.73	259.879	417.995	279.031	320.72	319.4063	1839.477
9	19	1805.63	2045.22	1849.68	314.884	299.376	234.053	230.055	269.592	1900.177
9	20	1982.94	1900.73	1845.56	455.945	221.382	242.984	271.97	298.0703	1909.743
10	1	968.413	902.049	844.076	85.2558	94.606	94.6382	93.0906	91.89765	904.846
10	2	938.05	862.808	870.154	85.8362	80.5806	89.3828	91.1882	86.74695	890.3373
10	3	957.637	901.844	852.481	97.0564	97.282	106.342	122.076	105.6891	903.9873
10	4	980.333	876.709	868.147	90.092	85.6104	80.7096	96.4438	88.21395	908.3963
10	5	998.618	898.957	842.769	95.541	103.086	79.2588	91.0916	92.24435	913.448
10	6	925.927		299.555	95.9278	94.2512	99.7324	109.824	99.93385	612.741
10	7	979.134	856.184	889.75	80.5806	73.552	85.3848	84.3208	80.95955	908.356
10	8	973.665	914.396	821.444	81.5156	83.1922	84.4174	94.5092	85.9086	903.1683
10	9	1841.93	1982.2	1962.35	287.736	301.246	283.125	267.81	284.9793	1928.827
10	10	948.721	871.43	874.572	84.0628	82.612	87.5772	85.8362	85.02205	898.241
10	11	2214.79	1783.68	1967.93	375.758	247.53	349.383	344.16	329.2078	1988.8
10	12	973.092	894.387	843.664	79.7102	85.3524	98.7006	96.1858	89.98725	903.7143
10	13	973.541	870.688	863.539	76.486	77.034	93.7354	94.09	85.33635	902.5893
10	14	1984.27	1773.69	1975.08	296.699	258.976	332.424	341.162	307.3153	1911.013
10	15	941.709	912.309	819.189	70.0376	98.3138	76.357	91.0916	83.95	891.069
10	16	943.765	881.26	842.419	71.3594	83.2568	81.5156	111.726	86.96445	889.148
10	17	897.109	908.828	829.194	73.5842	87.4482	82.7408	88.9636	83.1842	878.377
10	18	1776.65	1796.2	1984.1	283.77	247.111	377.595	258.525	291.7503	1852.317
10	19	923.818	898.392	853.563	76.8406	86.223	93.5742	93.961	87.6497	891.9243
10	20	1720.13	9951.2	1112.55	355.058	322.687	293.959	319.237	322.7353	4261.293
11	1	1151.92		478.459	140.841	169.149	155.35	136.327	150.4168	815.1895
11	2	1158.93	949.254	883.571	126.3	164.99	175.727	132.458	149.8688	997.2517
11	3	1030.22	876.291	863.015	87.7062	108.728	116.95	117.111	107.6238	923.1753

11	4	2213.5	1938.71	1936.08	458.395	301.407	246.531	301.923	327.064	2029.43
11	5	1166.37	7496.52	537.046	125.397	149.03	129.492	118.175	130.5235	3066.645
11	6	1757.8	2003.18	1910.38	211.612	281.771	227.733	257.428	244.636	1890.453
11	7	1214.11	1144.56	981.539	129.492	133.006	123.205	128.847	128.6375	1113.403
11	8	1185.74	3181.96	605.628	190.945	124.784	176.275	156.607	162.1528	1657.776
11	9	2132.15	1671.89	2082.94	366.762	260.62	281.255	367.858	319.1238	1962.327
11	10	1187.42	5960.29	546.266	132.845	147.225	131.426	118.401	132.4743	2564.659
11	11	1620.73	1996.39	1979.82	270.648	264.296	280.256	368.826	296.0065	1865.647
11	12	1188.76	3755.63	587.128	132.394	126.171	112.629	114.338	121.383	1843.839
11	13	1948.47	1780.66	1971.84	224.67	306.566	253.043	262.136	261.6038	1900.323
11	14	1174.03	988.716	960.496	135.65	137.907	99.8936	125.075	124.6314	1041.081
11	15	2019.98	1966.03	1875.04	408.871	353.059	238.889	313.885	328.676	1953.683
11	16	1239.95	3350.85	642.344	148.74	170.729	154.77	125.687	149.9815	1744.381
11	17	1147.9	952.852	983.733	111.501	171.826	117.337	152.287	138.2378	1028.162
11	18	1771.08	1772.25	2152.2	252.108	284.06	311.853	314.271	290.573	1898.51
11	19	2085.34	1889.68	1950.9	577.5	296.957	267.552	315.529	364.3845	1975.307
11	20	1760.99	1774.7	1946.67	239.05	331.263	307.888	286.414	291.1538	1827.453
12	1	924.41	894.295	906.582	73.0684	79.5812	85.675	96.5082	83.7082	908.429
12	2	1822.04	1945.48	3768.64	315.432	265.908	246.595	265.296	273.3078	2512.053
12	3	1735.08	1851.86	1960.7	228.894	303.083	250.915	238.309	255.3003	1849.213
12	4	2234.51	1766.92	1978.98	406.839	288.123	218.738	316.464	307.541	1993.47
12	5	2210.31	1775.28	1977.67	544.354	304.986	333.294	274.356	364.2475	1987.753
12	6	1774.61	1858.6	1987.65	226.863	248.143	286.156	287.285	262.1118	1873.62
12	7	1595.13	1962.01	1957.96	293.475	250.109	320.913	231.925	274.1055	1838.367
12	8	1795.72	1991.63	1919.54	220.027	290.477	238.534	268.423	254.3653	1902.297
12	9	1954.79	1955.12	1825.37	281.417	311.95	280.901	247.466	280.4335	1911.76
12	10	2100.53	1838.46	1900.9	266.875	248.626	243.242	245.724	251.1168	1946.63
12	11	1773.09	1883.66	2065.91	217.835	288.349	348.19	240.759	273.7833	1907.553
12	12	1617.32	1990.73	1951.86	232.086	376.306	356.993	283.577	312.2405	1853.303
12	13	923.807	898.738	882.142	69.296	83.9984	79.6134	79.7102	78.1545	901.5623
12	14	974.126	945.722	922.031	83.2568	92.7682	112.371	104.472	98.217	947.293
12	15	1903.12	1835.52	1976.85	273.969	243.758	334.101	289.509	285.3343	1905.163
12	16	1787.69	1781.11	1955.2	285.963	291.541	300.859	260.782	284.7863	1841.333
12	17	2040.72	1961.84	1790.98	638.568	265.102	328.103	248.336	370.0273	1931.18
12	18	1977.12	1748.18	1915.28	334.391	300.117	303.374	300.053	309.4838	1880.193
12	19	2238.02	1964.41	1777.27	453.398	364.021	356.025	377.467	387.7278	1993.233
12	20	1656.52	1993.6	1970.35	251.367	426.572	239.695	264.457	295.5228	1873.49
13	1	932.089	940.219	929.964	63.1056	79.5166	96.7662	69.8118	77.30005	934.0907
13	2	2234.39	1875.23	1880.45	344.257	320.043	273.84	247.143	296.3208	1996.69
13	3	1988.09	1784.23	1959.02	288.155	316.013	243.177	456.138	325.8708	1910.447
13	4	894.29	911.49	869.623	61.6224	74.9706	78.7106	86.6744	75.4945	891.801

13	5	915.452	902.809	893.069	72.7136	80.9676	92.5102	78.9364	81.28195	903.7767
13	6	899.01	897.869	873.941	78.614	83.8694	89.2216	95.96	86.91625	890.2733
13	7	1967.89	1778.41	1987.5	271.518	268.616	298.086	298.376	284.149	1911.267
13	8	1790.12	1824.4	1981.8	228.056	292.959	295.732	304.953	280.425	1865.44
13	9	2010.38	1987.68	1795.63	237.599	274.13	261.62	360.668	283.5043	1931.23
13	10	1771.33	2210.23	1786.62	255.849	300.44	244.628	348.19	287.2768	1922.727
13	11	1895.84	1925.29	1806.07	495.345	347.03	347.578	299.569	372.3805	1875.733
13	12	1945.5	1796.08	1984.31	296.442	257.944	271.454	287.317	278.2893	1908.63
13	13	934.323	973.186	911.733	63.428	86.1262	84.9978	87.8996	80.6129	939.7473
13	14	2469.33	1999.55	1815.83	908.189	302.987	268.165	308.597	446.9845	2094.903
13	15	2217.38	1989.94	1760.47	389.299	274.549	301.761	299.408	316.2543	1989.263
13	16	1982.4	1887.86	1862.67	227.669	258.654	214.643	264.715	241.4203	1910.977
13	17	906.264	913.944	891.903	61.6224	73.0038	77.0986	78.7106	72.60885	904.037
13	18	1978.36	1977.22	1789.98	342.226	225.509	280.804	256.364	276.2258	1915.187
13	19	1790.84	1918.75	2017.19	314.078	346.32	285.608	243.306	297.328	1908.927
13	20	1634.07	2173.24	1806.19	276.709	456.686	254.398	255.784	310.8943	1871.167